US Army Corps
of Engineers
Construction Engineering
Research Laboratories

USACERL Technical Report 97/89
June 1997

CONSTRUCTION PRODUCTIVITY ADVANCEMENT RESEARCH (CPAR) PROGRAM

Development of an Innovative Post-Tensioning System for Prestressed Clay Brick Masonry Walls

by

Ravi K. Devalapura, Gary L. Krause, Steven C. Sweeney, Don Littler,
Ervall Staab, and Maher K. Tadros

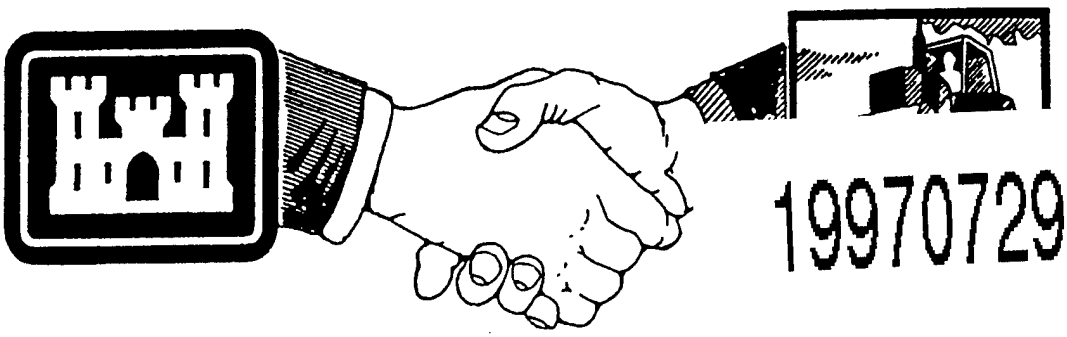

**A Corps/Industry Partnership To Advance
Construction Productivity and Reduce Costs**

USER EVALUATION OF REPORT

REFERENCE: USACERL Technical Report 97/89, *Development of an Innovative Post-Tensioning System for Prestressed Clay Brick Masonry Walls*

Please take a few minutes to answer the questions below, tear out this sheet, and return it to USACERL. As user of this report, your customer comments will provide USACERL with information essential for improving future reports.

1. Does this report satisfy a need? (Comment on purpose, related project, or other area of interest for which report will be used.)

_____

_____

_____

2. How, specifically, is the report being used? (Information source, design data or procedure, management procedure, source of ideas, etc.)

_____

_____

3. Has the information in this report led to any quantitative savings as far as manhours/contract dollars saved, operating costs avoided, efficiencies achieved, etc.? If so, please elaborate.

_____

_____

4. What is your evaluation of this report in the following areas?

   a. Presentation: _____

   b. Completeness: _____

   c. Easy to Understand: _____

   d. Easy to Implement: _____

   e. Adequate Reference Material: _____

   f. Relates to Area of Interest: _____

   g. Did the report meet your expectations? _____

   h. Does the report raise unanswered questions? _____

i. General Comments. (Indicate what you think should be changed to make this report and future reports of this type more responsive to your needs, more usable, improve readability, etc.)

_____

_____

_____

_____

_____

_____

5. If you would like to be contacted by the personnel who prepared this report to raise specific questions or discuss the topic, please fill in the following information.

Name: _____

Telephone Number: _____

Organization Address: _____

_____

_____

6. Please mail the completed form to:

Department of the Army
CONSTRUCTION ENGINEERING RESEARCH LABORATORIES
ATTN: CECER-TR-I
P.O. Box 9005
Champaign, IL 61826-9005

REPORT DOCUMENTATION PAGE

Form Approved
OMB No. 0704-0188

1. AGENCY USE ONLY *(Leave Blank)*	2. REPORT DATE	3. REPORT TYPE AND DATES COVERED
	June 1997	Final

4. TITLE AND SUBTITLE
Development of an Innovative Post-Tensioning System for Prestressed Clay Brick Masonry Walls

5. FUNDING NUMBERS
CPAR
FAD 91-080352, dated 8 July 1991

6. AUTHOR(S)
Ravi K. Devalapura, Gary L. Krause, Steven C. Sweeney, Don Littler, Ervall Staab, and Maher K. Tadros

7. PERFORMING ORGANIZATION NAME(S) AND ADDRESS(ES)
U.S. Army Construction Engineering Research Laboratories (USACERL)
P.O. Box 9005
Champaign, IL 61826-9005

8. PERFORMING ORGANIZATION REPORT NUMBER
TR 97/89

9. SPONSORING / MONITORING AGENCY NAME(S) AND ADDRESS(ES)
Headquarters, U.S. Army Corps of Engineers
ATTN: CEMP-ET
20 Massachusetts Ave. NW
Washington, DC 20314-1000

10. SPONSORING / MONITORING AGENCY REPORT NUMBER

11. SUPPLEMENTARY NOTES
Copies are available from the National Technical Information Service, 5285 Port Royal Road, Springfield, VA 22161.

12a. DISTRIBUTION / AVAILABILITY STATEMENT
Approved for public release; distribution is unlimited.

12b. DISTRIBUTION CODE

13. ABSTRACT (Maximum 200 words)

Clay brick masonry veneer systems, widely used throughout the United States, typically are subject to cracking, water infiltration, thermal inefficiencies, and other problems. These problems could be overcome with the development of an effective post-tensioning system for prestressing clay brick veneer walls. Such a prestressing system also could offer significant benefits in ease of construction, structural performance, and reduced life-cycle costs.

In this research a simple, economical post-tensioning system was developed to improve the structural performance of clay brick veneers and load-bearing walls. The results of this study indicate that prestressed clay brick masonry walls perform much better than standard clay brick construction. The system documented here employs a special two-cored clay brick designed to accommodate the insertion of prestressing tendons. This customized brick varies in shape only, and can be manufactured by most modern brick-producing plants. All other components are standard, commercially available materials. The system is documented and ready for adoption by construction specifiers and engineers. If used appropriately and within the guidelines and limitations stated in this report, the system will provide overall construction and performance benefits over standard brick masonry configurations.

14. SUBJECT TERMS
Construction Productivity Advancement Research (CPAR)
masonry
prestressing
compressive strengths
bricks

15. NUMBER OF PAGES
152

16. PRICE CODE

17. SECURITY CLASSIFICATION OF REPORT	18. SECURITY CLASSIFICATION OF THIS PAGE	19. SECURITY CLASSIFICATION OF ABSTRACT	20. LIMITATION OF ABSTRACT
Unclassified	Unclassified	Unclassified	SAR

Foreword

This study was conducted for Headquarters, U.S. Army Corps of Engineers under Construction Productivity Advancement Research (CPAR) Work Unit LRI, "Prestressed Clay Brick Walls," under Funding Authorization Document (FAD) 91-080352, dated 8 July 1991. The technical monitor was Charles Gutberlet, CEMP-ET.

The work was performed by the Engineering Division (FL-E) of the Facilities Technology Laboratory (FL), U.S. Army Construction Engineering Research Laboratories (USACERL). The USACERL Principal Investigator was Steven C. Sweeney. Larry M. Windingland is Acting Chief, CECER-FL-E and Donald F. Fournier is Acting Operations Chief, CECER-FL. The USACERL technical editor was Gordon L. Cohen, Technical Information Team.

Dr. Michael J. O'Connor is Director of USACERL.

Contents

List of Figures and Tables

Figures

Tables

1 Introduction

1.1 Background

Masonry has been in use for centuries in building construction throughout the world. Its popularity arises from its simple method of construction, pleasing aesthetic appearance, and durability. Brick masonry has been favored for non-structural applications such as building claddings (veneers), partitions, infilled walls, etc., and limited structural applications. However, brick seldom has been used in load bearing and flexural applications due to its low tensile strength. Clay bricks are very strong, with compression strength normally exceeding 10,000 psi (69 MPa). Clay bricks produce a fairly strong masonry assemblage even when used with the lowest grade mortar. Brick masonry in non-load bearing applications tends not to exploit the full potential of the engineering properties of the brick. If the engineering properties of brick masonry were more fully utilized, a number of benefits would result, including better durability, improved efficiency, and greater resistance to impact or accidental loads.

Currently, the most extensive application of clay brick masonry in the United States is in the construction of veneers. A veneer is defined as "a wall having a facing of masonry units, or other weather-resisting, noncombustible materials, securely attached to the backing, but not so bonded as to intentionally exert common action under load" [Brick 1987]. The primary functions of a veneer are to transfer wind and externally applied loads to structural components and to provide an aesthetically pleasing appearance. Veneers also provide support to the thermal insulation barriers attached to the exterior walls of a building. A veneer is considered to be a nonstructural element that supports no loads other than its own weight. Anchored veneer consists of a single masonry wythe as the exterior finish separated from a backing by an air space. Concrete masonry, steel studs, timber, or light structural steel members are commonly used as the backing. Wind load is transferred from the veneer to the backing by the ties that connect it to the backing at regular spacing. Brochelt [1988] describes the history of anchored masonry veneer and its structural design requirements.

Cracking and related water infiltration is a significant problem for masonry veneer systems. Water can severely damage the interior of the structure when weep holes are missing or blocked. Metal wall ties function as thermal bridges that reduce the

effectiveness of insulation, and make the installation of insulation difficult. These problems could be overcome with the development of an effective post-tensioning system for prestressing clay brick veneer walls. Prestressing could significantly reduce the amount of cracking in brick walls and could provide enough strength to resist lateral loads without the need for wall ties between story levels. A post-tensioning system offers significant potential benefits in ease of construction, structural performance, and reduced life-cycle costs.

Under the Army Corps of Engineers Construction Productivity Advancement Program (CPAR), the U.S. Army Construction Engineering Research Laboratories (USACERL) initiated a Cooperative Research and Development Agreement (CPAR-CRDA) with the University of Nebraska (Omaha) Center for Infrastructure Research to develop and test a post-tensioning system for prestressing clay brick walls.

1.2 Objective

The objective of the research work was to develop a post-tensioning system for prestressing clay brick masonry walls that will (1) improve the structural performance of clay brick veneer structures, (2) improve the structural performance of clay brick masonry load-bearing (structural) walls, and (3) be simple and economical to install.

1.3 Approach

Previous efforts to develop post-tensioning techniques for clay brick veneers were studied and evaluated. A new, two-cored brick design was developed to better accommodate post-tensioning hardware. Bricks were fabricated according to the design and tested to confirm structural and material properties. The post-tensioning system developed for the two-cored bricks was based on a field-installable threaded rod-and-nut assembly incorporating direct tension indicating (DTI) washers. Sample prestressed panels were assembled and tested in the laboratory to determine the system's structural properties. Other panels were assembled and montored over time to determine prestress losses in the system. Analytical models were developed and compared to the test results. The models were subsequently used in the development of design guidelines and construction details for the prestressed clay brick wall system.

1.4 Scope

This report summarizes the research program to develop a prestressed clay brick wall system. The results and conclusions were based on testing and analysis of a single system that was developed after careful study and consideration of many tensioning systems and unit configurations. However, the proposed system is not the only possible solution. Other systems should be evaluated for potential benefit and possibly compared to the proposed system for optimization. The proposed design procedures and details should be applicable to other systems as well.

1.5 Units of Weight and Measure

U.S. standard units of weight and measure are used throughout this report. Conversion factors for standard international (SI) units are given below.

Metric conversion factors

1 in.	=	25.4 mm
1 ft	=	0.305 m
1 sq ft	=	0.093 m^2
1 cu ft	=	0.028 m^3
1 lb	=	0.453 kg
1 gal	=	3.78 L
1 psi	=	6.89 kPa
°F	=	(°C × 1.8) +32

1.6 Mathematical Notation Used in This Report

a = depth of equivalent compression zone at nominal strength

A_m = cross-sectional area of masonry

A_n = net cross-sectional area of masonry

A_{ps} = area of prestressing tendon

b = width of section

c = distance from the neutral axis to extreme compression fiber

C = total compression force acting in the section

d = distance from the compression face of a flexural member to the centroid of longitudinal tensile reinforcement

ΔM_s = incremental service load moment

E_m = modulus of elasticity of masonry

E_{ps} = modulus of elasticity of prestressing tendon

f_b = stress in the bottom fiber of masonry at cracking stage

f_{mi} = stress in masonry in the bottom fiber at initial prestress transfer

f'_m = specified compressive strength of masonry

$f_{m\,(bot)}$ = stress in masonry in the bottom fiber

$f_{m\,(top)}$ = stress in masonry in the top fiber

f_{me} = stress in masonry due to effective prestress

f_{ps} = stress in prestressing tendon at nominal strength

f_{pu} = specified tensile strength of prestressing tendon

f_{py} = specified yield strength of prestressing tendon

f_r = modulus of rupture of masonry

f_s = stress in tendon due to prestress and applied loads

f_{se} = effective prestress in the tendon

f_{si} = stress in tendon due to initial prestress

F_a = allowable average axial compressive stress for concentric applied load

F_{br} = allowable bearing stress

h = overall depth of the member cross section

I_g, I_{cr} = gross, cracked moment of inertia of the wall cross section

k = ratio of depth of the compressive stress in a flexural member to the depth, d

l = span length between the supports

L = clear span length between the supports

M = moment at midspan due to uniformly distributed load

M_a = applied moment in the member

M_{add} = additional moment acting in the member

M_{cr} = nominal cracking moment strength

M_d = moment due to dead load of the member

M_n = nominal moment strength

M_s, M_{ser} = service moment at the mid height of the panel

M_u = ultimate moment strength of the member

M_y = nominal moment strength at yield strength

n = modular ratio (= E_{ps}/E_m)

P_e = effective force in prestressing tendon

Q = applied factored load

r = radius of gyration

R = strength enhancement factor

R_4 = interpolation coefficient

s = spacing of reinforcement

S = section modulus

T = total tensile force acting in the cross section

w = uniformly distributed load per unit length of the member

$(1-\alpha)$ = coefficient to account for the variation in member stiffness due to cracking

δ_c = midspan deflection of the member

Δ_{cr} = midspan deflection of the member at cracking moment strength, M_{cr}

Δ_s = midspan deflection of the member at service load

$\varepsilon_{m\,(top)}$ = strain in masonry in the extreme top fiber

$\varepsilon_{m\,(bot)}$ = strain in masonry in the extreme bottom fiber

ε_{me} = strain in masonry due to effective prestress

ε_{mu} = strain in masonry at nominal strength

ε_{ps} = strain in prestressing tendon at nominal strength

ε_{pu} = strain at specified tensile strength in prestressing tendon

ε_{py} = strain at specified yield strength of prestressing tendon

ε_s = strain in the steel due to prestress and applied loads

ε_{se} = strain in prestressing tendon due to effective prestress

ϕ = curvature of the section

ρ = ratio of the area of flexural tensile reinforcement, A_s, to the area bd

2 Overview of Prestressing Research, Techniques, and Applications

2.1 Brick Masonry Veneer Walls

2.1.1 *Current System of Construction*

In the current system of construction, the veneer is attached to the backup system using metal ties at regular intervals. These ties are embedded in the form of a grid behind the wall, and they are permanently secured to both the veneer wythe and the metal stud backup system. The Uniform Building Code [UBC 1994] Section 1403 gives the height limitation, and design requirements for backing, anchor ties, and metal studs used in the construction of anchored veneers. The Brick Institute of America [BIA 1987] also addresses the considerations and recommendations for the design, detailing, materials selection, and construction of brick veneer/steel stud panel walls. Typical brick veneer/steel stud wall construction is shown in Figure 2.1*.

2.1.2 *Problems Observed*

Brick veneers are normally exposed to outdoor temperatures and humidity. The metal stud gridwork is much more flexible than the rigid brick wall, which leads to differential movements resulting in the development of internal stresses in the connectors. A study showed that because of low tensile strength of the masonry, cracking of the brick veneer will occur when steel stud backing is used [Papanikolas et al. 1989]. Once the metal ties are exposed to moisture over a period of time, corrosion of the ties takes place which can lead to premature failure of the wall [Shiv Kumar and Heidersbach 1986]. Numerous wall failures due to corrosion of metal ties have been reported in the past [Grimm 1992, 1984; Cowie 1990]. A number of masonry organizations have cautioned designers regarding the potential problems experienced with the current system of stud/veneer construction [NCMA 1981] and [PCA 1983]. Recent tests conducted on 16 full-sized brick veneer and steel stud curtain walls concluded that the current design methods ignore important structural interactions which can result in inadequate performance [McGinley et

* Figures and tables are presented at the end of the chapter in which they are first discussed.

al. 1986]. The existence of differential movement due to incompatible stiffness between masonry veneer and the building frame is a known problem [Differential 1991; Grimm 1975; Wyatt 1978; Goyal et al. 1992]. Another problem of the current system is that the ties which attach the brick wall to the metal studs act as a thermal bridge from the exterior wall to the interior of the building, thus reducing the insulation capacity of the wall [Brick 1982].

2.2 Prestressed Masonry Walls

Prestressing of masonry walls can help to reduce or eliminate all the above mentioned problems. The introduction of prestress in a masonry wall greatly increases the out-of-plane load resistance of the wall. Also the amount of load needed to cause cracking of the wall is increased, reducing the chances of cracking occurring due to severe loads or environmental effects. These benefits are produced primarily by the large strength capacity of clay bricks in compression compared to their strength in bending or tension. The elimination of cracks in a wall will help to reduce water penetration in the wall and its associated problems. The prestressing will also improve the shear capacity of the wall. It changes the brittle failure mechanism of unreinforced masonry to a more favorable ductile one.

Similar to prestressed concrete, both pretensioning and post-tensioning techniques can be used for masonry. Pretensioning is generally suitable for plant application as it requires the prestressing tendons to be externally held until the masonry member is completed, grouted, and the grout cured. Post-tensioning is the process by which the prestressing tendon is stressed against the end of the completed masonry member. Post-tensioning is favored for masonry applications due to its simplicity, and elimination of prestress loss due to elastic compression of masonry. Also, post-tensioning does not require grouting to transfer the prestress to the element. Grouting is required primarily for the protection of the steel from corrosion. Two-way prestressing is also possible, but since the largest compressive strength of masonry is oriented vertically and the loads are applied perpendicular to the bed joints, vertical prestressing has received the most attention.

2.3 Advantages of Prestressed Wall

With the post-tensioning applied, the clay brick wall will have the strength required to span between the structural elements (floors) of the building. This will allow the metal stud system to be detached from the clay brick wall (see Figure 2.2) and help to virtually eliminate the need for metal ties. Cracks will be effectively minimized or eliminated by maintaining the prestress in the cross section. Clay bricks tend

to expand from moisture absorption, which may be advantageous in offsetting the prestress losses due to relaxation in the post-tensioning steel. The problem of thermal bridging from the metal ties is also eliminated, resulting in a more effective insulation.

2.4 Development of Prestressed Masonry

Though prestressing can be applied to both concrete or brick masonry in a similar way, most research has focused on concrete block work. This may be attributed to the advantage of concrete units having larger cores which makes it easier for post-tensioning. Standard bricks in the United States have a three core configuration which does not index when used in running bond pattern. Post-tensioning is favored over pretensioning due to its simplicity where steel bars are introduced through the masonry units and tensioned. In contrast to pretensioning, it does not require grouting for stress transfer, and does not induce elastic deformation losses.

Extensive applications of prestressed masonry were started in the second half of the 20th century. Prestressed masonry is commonly used in the United Kingdom for pier or wall sections. First attempts at prestressing masonry in the United States were reported by P.H. Jackson in 1886, in which metal rods with nuts were used in girder application. Anderegg and Dalzell [1935] conducted tests on masonry floor systems. A series of masonry beams and columns were tested by applying loads at various points, and failures in compression and diagonal shear or tension were noticed. Samuely [1953] applied prestressing technique to masonry brick piers up to 30 ft (10 m) high in a school building in the United Kingdom. He discovered an increase in cracking moment capacity in the piers to resist flexural loads. At the same time, stone blockwork was post-tensioned in India by Ramaswamy [1953]. Taylor [1961] from the United States also applied post-tensioning to stone masonry retaining walls which later led to some practical applications. Hinkley [1966] conducted tests on one-story high prestressed brick shear walls. Two tests were made on plain walls and five on prestressed walls. He also tried to prestress a six-story concrete block building based on his earlier experience with single story walls. He found that the post-tensioning was economical for reinforced construction, and strength and reliability can be increased by vertically prestressing the wall.

The ultimate strength of square walls was predicted by simple beam theory. Foster [1970] built a prestressed brick masonry water tank for a brick plant in the United Kingdom. The tank was 16 ft (4.8 m) in diameter and 40 ft (12 m) high with cavity walls on a sliding joint. Prestressing was applied both longitudinally and circumferencially. Cavity walls were grouted after the construction of the tank. A very

small creep loss was noticed and this work was considered as a major achievement in prestressed brick masonry.

In Australia, Rosenhaupt et al. [1967] found that the cracking capacity of prestressed walls (box beams) was improved significantly upon prestressing. A test on full sized (8 x 33 ft) post-tensioned concrete masonry wall was conducted. The results of the test were compared with the truss analogy analysis. Results showed a good agreement between experimental results and both the truss and lattice analogy. The tests indicated that the problems associated with masonry houses built on moving soils could be overcome by using post-tensioning methods. Gero [1969] proposed post-tensioned walls to support reinforced concrete floors anchored with the post-tensioning tendons of the walls. These ideas did not seem to have any practical applications.

Hanlon [1970] described several church steeples that were rehabilitated using post-tensioning. He also used ducts for post-tensioning and grout for corrosion protection of the hardware. Hanlon provided some information on shake table tests of post-tensioned concrete masonry cavity walls from New Zealand. It was also learned that prestressed masonry is more resistant to lateral forces from earthquakes.

Mehta and Fincher [1970] from Texas Tech University, showed that the prestressed brick beams are an alternative to concrete or steel members. U shaped brick beams were pretensioned. The steel wires were tensioned in the cavity of the beams and then filled with grout. Bond between the brick masonry and the grout was adequate to develop 80 percent of the predicted values. They reported that cracking patterns usually originated at mortar joints and propagated through the masonry. A considerably greater deflections than expected were also noticed.

Thomas [1969] tested masonry beams with bricks laid in different patterns and in both directions. High levels of prestress were used in the members and hence compressive failures were typically noticed. They suggested that a reduction in the number of mortar joints by making longer and deeper masonry units would reduce the tendency to failure.

2.5 Recent Research and Applications

After a slow development, prestressed masonry has recently gained more popularity around the world. Researchers have started applying prestressed masonry to different structures and many research and experimental studies have also been published. Theoretical analysis of prestressed masonry has been based on pre-

stressed concrete behavior. Studies have shown the superiority of prestressed masonry over plain reinforcing.

Curtin published several papers based on his research and applications from 1975 to 1986. He is considered one of the engineers from the United Kingdom who has pioneered the modern development and use of post-tensioned masonry. Curtin et al. [1975] described a system of construction for a school building using post-tensioned brick panels. Panels were shorter and the level of prestress was low. Later, tall diaphragm (cavity) walls with transverse masonry ribs were post-tensioned. This led to the development of 'fin walls' in which fins (pockets) are spaced at regular intervals along the length of the wall. Fins are deep pilasters that are normally thicker than the wall. These were shown to have 15 times the bending resistance of a cavity wall, and upon post-tensioning the resistance increased to 150 times that of the original cavity wall [Curtin et al. 1982]. Two successful applications of diaphragm walls included a building located in an area of severe mining settlement; it showed no cracks in the brickwork after post-tensioning [Shaw 1982] and a hall for the Salvation Army where post-tensioned walls were built as free cantilevers [Curtin et al. 1982]. Curtin and Beck [1986] described the construction of a 10 ft (3 m) high concrete block retaining wall. In this case, a single post-tensioning tendon was used at each pocket (fin) of the diaphragm wall. Curtin recognized the advantage of using eccentricity for unidirectional lateral loading [Curtin 1987], and it resulted in a significant reduction of material costs. Eccentricity in prestressed sections gives higher flexural strength, greater stiffness, and results in slender walls [Curtin et al. 1987]. The technique used in post-tensioning was simple. High-strength steel rods were secured in a concrete footing. The cavity wall was constructed around the bars to the desired height. The corrosion protection was applied to the bars as the wall was being built. The wall was capped at the top and the bar was tensioned using a torque wrench after the masonry had cured. Care was needed to accurately measure the prestress force, and in the detailing of the cross ribs of the diaphragm wall [Curtin 1986]. Curtin and Beck estimated that the post-tensioned concrete block wall was 25 percent cheaper than the equivalent reinforced concrete wall [Curtin and Beck 1986].

In the early and middle 1980s, Phipps and other investigators conducted several studies on different geometric beam shapes such as box, I and T cross-sections. Montague and Phipps [1984, 1985] and Phipps and Montague [1987] tested concrete block beams which represented portions of cantilever diaphragm walls. Roumani and Phipps [1985, 1986] experimented with clay brick beams constructed with different configurations. Various longitudinal and cross-rib bond and tie arrangements were examined. Beams with both restrained and unrestrained steel were compared. Four different shear failures were identified depending on the cross sectional shape and shear span-to-depth ratio. Restrained tendons provided greater

strength and higher ductility compared to unrestrained tendons, which resulted in a change in effective depth as the beams deform under loads. The studies indicated that elastic theory can be used to analyze the cracking of flexural strengths accurately. Also it is concluded that various types of shear failure relevant to the type of section should be checked in addition to bending failure. Garrity and Phipps [1987, 1988] verified a substantial increase in the horizontal flexural strength of clay brick masonry under vertical precompression. This increased resistance was due to the increase in friction in the bed joints. Ductile failure was noticed for solid brickwork subjected to lateral loads.

Sinha and his co-investigators in the United Kingdom worked on prestressed brick elements using variables such as brick type, mortar, steel area, and prestressing force in the cross section [Pedreschi and Sinha 1982; Sinha and Pedreschi 1984; Pedreschi and Sinha 1985]. They proposed load-deflection relationships based on two methods of analysis: (1) stress-strain behavior of materials, and (2) the 'stress block' method. The nonlinearity in the brickwork behavior was taken into account in the proposed theoretical methods. They were found to be accurate and to reflect the general behavior of prestressed concrete members. The studies showed that beams with larger steel ratio failed through the influence of shear, but beams with low levels of steel experienced ductile behavior [Pedreschi and Sinha 1986; Sinha 1983; Sinha and Udehi 1986; Sinha and Walker 1986]. The shear strength of beams decreased with increase in ratio of the shear span/depth as predicted.

Mallagh [1982] used external post-tensioning to prestress a concrete blockwork for grain storage tanks in Ireland. He adopted an ingenious technique by pulling individual wires alternatively. A lever tool was used to pull the wires together at *stragged* points. The force in the circumferential wires was measured by the pull in the lever tool. A protective coating of gunite was applied on the silos following the post-tensioning. Thus the problem of shrinkage in the case of normal reinforcing was taken care off by the prestressing technique.

Bradshaw et al. [1982] described the use of post-tensioned brick masonry to build a retaining wall for a farm building in the United Kingdom. It was designed very similar to diaphragm walls. Drinkwater and Bradshaw [1982] employed a torque wrench for tensioning the steel, and used a cap plate and precast concrete beam for capping at the top of the wall.

Suter et al. [1983] showed the increased resistance of prestressed walls to lateral loads, analyzed on the basis of a finite element model. A two-dimensional analysis was used to investigate the stress distribution in the masonry walls subjected to concentrated amounts of prestressing at a few selected locations. Hendry [1988] presented a series of tests in which concentrated loading was applied to brickwork

specimens subjected to uniform precompression. Based on these tests, he proposed a formula to calculate the enhancement factor, R (ratio of bearing strength to uniaxial strength). It was clear that the experimental value of the enhancement factor for centrally loaded walls is considerably higher.

Page and Huizer [1988] compared the results of test specimens loaded monotonically with a horizontal racking force on reinforced and post-tensioned hollow masonry shear walls. It was shown that post-tensioning is potentially an extremely effective method of increasing the shear capacity of the wall. The ungrouted post-tensioned wall demonstrated more strength than the wall which was reinforced and grouted with the same type and amount of unstressed reinforcement. The potential benefits appeared to be even more substantial, if the horizontal as well as the vertical prestressing was used to suppress the formation of diagonal tensile cracks in the central region of the wall.

Huizer and Shrive [1986] in Canada tested a wall in shear with a window opening. The specimen was constructed with a hollow masonry wall containing unbonded tendons in both the vertical and horizontal directions. The horizontal post-tensioning was added as a substitute for the bond beams at top and bottom of the wall and opening [Huizer and Loov 1985; Huizer and Shrive 1985]. The tests showed that the walls deformed under lateral loads, and the magnitude of the forces in the vertical tendons changed during those deflections. Considerable improvement in structural performance was observed in those tests.

In Switzerland, Ganz [1989] applied a post-tensioning technique to a kindergarten and a factory building in Switzerland. The school building extension walls were up to 4 m high and had large window openings. A cast-in-place concrete slab provided dead-anchorage and prefabricated stressing anchors were placed in prefabricated concrete elements. The factory building walls were 10 in. (250 mm) thick fireproof single-leaf walls. These masonry walls were 7.7 m high and prestressed with tendons spaced 2.0 m apart. The cantilever wall was designed to withstand a wind velocity of 21m/sec. Ganz [1993] described the innovative methods used for the strengthening of lateral load resisting frames and walls of structures using the post-tensioning technique. VSL International's proprietary system was used in the above applications. In light of these successful applications of prestressed masonry in actual buildings, it can be concluded that post-tensioning is a very effective method for the strengthening of structures, since it provides improved strength, improved cracking behavior, and makes optimum use of the existing structure.

2.5.1 Previous Studies on Lateral Loading

Several studies have been reported on masonry walls subjected to lateral loads, comprising both concrete and brick masonry. Most of the research in the United States concentrated on concrete block masonry, in contrast with the United Kingdom, where brick masonry is more popular. The literature review included both types of masonry, and no distinctions were made between the two in this section.

Sakr and Neis [1994] tested six full scale cavity masonry walls along with three reference walls (single wythe) under a uniformly distributed out-of-plane lateral loading. The cavity width was varied from 3 in. (76 mm) to 4.5 in. (114 mm). The ties were made of metal steel strips. The loaded wythe in all walls was reinforced with 10 mm bars both vertically and horizontally. The walls were 1.6 x 2.79 m in size, including a bottom reinforced concrete beam. The results showed that the ultimate capacity varied from 200 percent to 167 percent of the single wall capacity. Both wythes experienced the same lateral deflection and failed by flexural bond failure mechanism. It was concluded that the cavity wall can be satisfactorily analyzed by assuming that the total applied moment is distributed between the two wythes according to their ratios of flexural rigidity.

Another study recently conducted by Sinha and Liang Ng [1994] in the United Kingdom showed that clay brick masonry possesses both strength and stiffness orthotropies and cannot be idealized as rigid-plastic. The aim of the study was to investigate the yield-line method adopted in the BS 5628 Code for the design of masonry subjected to lateral loads. Two different sized wallettes were tested under four point loading and using an air bag. Flexural tensile stresses were developed both parallel and perpendicular to the bed-joints and all specimens were tested until failure. The failure pressure of the walls was compared with the yield line analysis and it was found that the yield-line analysis consistently overestimated the failure pressure of the walls.

Liaw and Drysdale [1992] from Canada proposed a reinforced masonry veneer wall system which is built as an independent veneer wall and overcomes some of the flaws involved with the steel/stud backup wall system. They conducted wind loading using an air pressure chamber on a full scale (8.9 x 17 ft) wall. Load-displacement test results were analyzed to assess the effectiveness of this form of construction. The loading sequences included the effects of cavity pressurization, cracking of the veneer, cyclic tests of the interior wall, and loading to failure. The proposed reinforced masonry veneer wall with an independent interior wall proved to be feasible and to result in a wall system with ample strength and stiffness

characteristics. They also identified several improvements necessary to improve the durability and field constructibility.

As a part of the US-Japan Program on Masonry Building Research, tests were conducted at Drexel University to study the elastic and inelastic behavior of vertically spanned reinforced concrete block masonry walls under monotonic and cyclic out-of-plane lateral loads [Hamid, June 1989]. Four walls of 32 x 104 in. were studied using parameters such as percentage of steel reinforcement, and extent of grouting. The walls were tested as simply supported elements loaded equally at middle third points. The results indicated an increase in moment capacity with an increase in the vertical reinforcement and with grouting. The comparison between the theoretical and experimental results demonstrated reasonable predictions of flexural strength of fully and partially grouted masonry walls using the method contained in the 1985 Uniform Building Code.

Three facade wall panels of perforated clay brick were built and tested by Plauk [1989] in Berlin, Germany. The wall panels were 250 x 350 x 11.5 cm and connected to a structural steel frame. Two vertical studs along with ties were connected to the specimen to represent actual building construction. A steel bar 6 mm in diameter was embedded in each second vertical and horizontal joints which were approximately 25 cm apart. Air bags were used to simulate the wind loading and panels were loaded gradually up to failure. Pressure-load curves were presented. The failure load of all three panels was found to be approximately 4.5 to 4.6 kN/m^2. The study concluded that the facade had the strength required to resist wind loading, and a mid-span deflection due to wind loads of 1 mm was acceptable.

Hamid and Harris [1984] published a comprehensive compilation of research studies conducted on the nonlinear behavior of reinforced masonry walls under out-of-plane loading. The authors identified the areas which require additional studies to develop a sophisticated design methodology based on nonlinear response. It is also concluded that more research is required on material properties in the inelastic range, safety factors, bond type, grouting, and the validity of the yield line method for masonry elements.

Similarly, Essawy, and Drysdale [1983] described the need for additional investigation of the out-of-plane bending of walls. The paper reviewed the current design procedures and provisions in British, Australian, and North American masonry codes. A wall specimen for auxiliary test was built with concrete blocks to determine flexural tensile strength normal and parallel to the bed joints, and was 6.0 x 2.8 m. Lateral load was applied in increments of 0.2 kN/m^2. For flexural tension parallel to the bed joint, twenty test specimens of 400 x 1,590 mm were tested which gave an average value of 1.32 MPa. Test results were compared with

various methods of design. The main conclusions from the research were that (1) plastic theory should not be used for unreinforced masonry since it is brittle and (2) ultimate load predictions may not be generalized to untested wall configurations and therefore, the yield-line theory does not fulfill the requirements of a general design method.

Amrehein et al. [1983] from California reported an extensive testing program based on a research project on masonry walls using both concrete and brick masonry. Thirty-two walls, including twelve concrete tilt-up walls were tested with both lateral and vertical load on them to determine their performance. The panels were 24 ft-8 in. high and 4 ft-0 in. wide. The thickness of the walls varied from 6 in. to 10 in. Panels were loaded with an eccentric vertical load applied to a steel angle ledger to simulate a typical roof load. Lateral pressure was applied through an air bag for the full height and width of the panels. Load-deflection curves for all tests were plotted. Based on the performance of the walls, design techniques were developed and recommended for code adoption.

Rodriguez et al. [1994] at Drexel University conducted tests on post-tensioned masonry walls subjected to out-of-plane loads. The parameters introduced in the tests included the level of prestress, reinforcement ratio, and the fixity of the tendon inside the cell. The full scale wall specimen was built using hollow concrete blocks composed of one and a half blocks wide and eight blocks in height. A high-strength threaded bar was placed at the center and was anchored in a concrete beam. The specimen was tested in flexure applying loads at middle third points. The panel showed ductile behavior with a maximum deflection of 1.6 in. (42 mm). The ultimate load was two times the cracking load, and the panel behaved linearly up to cracking stage. The study concluded that more research is necessary to understand the behavior in the post-cracking stage.

Graham and Page [1994] conducted tests on fifteen lightly prestressed masonry walls of hollow clay blocks to study the flexural behavior. The walls were constructed from hollow clay units of 12 x 3 x 6 in. (310 x 76 x 150 mm) with 1:1:6 mortar in running bond. The overall dimensions of the walls were 67 x 32 in. (1700 x 800 mm). A single prestressing rod was introduced at the center, and different levels of prestress were introduced. Other parameters such as grouted, ungrouted and guided bars were also investigated. The level of prestress had a direct influence on the serviceability behavior, in particular to the cracking moment. The degree of restraint of the prestressing rod in the core had a marked influence on the ultimate behavior. When the rod was free to move in the cavity, the geometric effects were significant, the load carrying capacity of the wall was reduced, and the failure mode changed from under-reinforced to an undesirable over-reinforced feature.

Dawe and Aridru [1992] investigated two series of post-tensioned concrete masonry walls subjected to uniform lateral loading. The aim of the testing was to determine the load-deflection curves, initial cracking loads, wall stiffness, crack patterns, and the ultimate loads. The results for two traditionally reinforced concrete masonry walls were also presented for comparison purposes. All specimens measured 4 x 8 ft (1.2 x 3 m) and 6 or 8 in. thick. The walls were built in running bond with Type S mortar, and two No. 15 high-strength steel plain bars were spaced 23.6 in. (600 mm) apart. Post-tensioning was applied after 21 days of moist and air curing, and the level of post-tension force applied to each series of walls varied from 3.4 kips/ft (50 kN) to 6.7 kips/ft (100 kN). The specimens were positioned vertically and subjected to incremental lateral positive pressures of 6.3 psf (0.3 kPa). All the post-tensioned concrete masonry walls behaved elastically up to the cracking load, at which point the load-deflection curves began to deviate. Results showed that for a particular wall thickness, increasing the post-tensioning forces in a wall increased the initial cracking load, the initial wall stiffness, and the ultimate failure loads. The results of the tests showed the reliability of the behavior of post-tensioned concrete masonry walls.

Curtin et al. [1991] tested a 6.0 m high fin wall with air bag lateral loading. Several tests were carried out using varying magnitudes of prestress; including zero prestress as in a plain masonry fin wall. The loaded height varied from 4.2 m to 6.0 m. After each test the load was removed and the wall recovery noted. The lateral cracks due to overloading closed completely after the removal of the load. The paper describes the effects of slenderness ratio, bending compression, shear strength, and bending resistance in both directions. The results confirmed the massive increase in both vertical and lateral load bearing strengths of prestressed geometric sections and the enhancement of bending and horizontal shear strengths.

Ungstad et al. [1990] from the University of Alberta conducted similar experimental tests to assess the utility of prestress applied to slender concrete masonry walls. A total of nine walls were tested, of which six were post-tensioned and the remaining three conventionally reinforced. Three of the post-tensioned walls were restrained with 'guide blocks', and the other three were left ungrouted. Standard 8 in. high lightweight blocks were laid in running bond with Type S mortar applied to face shells only. Two 15 mm Dywidag threaded bars were used as prestressing tendons. The prestress was applied 4 months after they were built by jacking the tendons to 70 percent of their ultimate load. The specimens were monitored for approximately 6 months to observe prestress losses, then tested in flexure by applying out-of-plane loads. The specimen was supported on a specially designed pin joint and loaded by jacks at two points. Deflections were recorded at several points and surface strains were recorded. At ultimate load, the prestressed panels deflected only 17 mm whereas the reinforced walls deflected about 160 mm. The

tests clearly demonstrated that prestressed concrete block masonry walls can be constructed using standard blocks and construction techniques, and that they offer improved serviceability and reliability over conventionally reinforced walls.

Geschwindner and Ostag [1990] and Ostag [1986] investigated fully grouted post-tensioned wall panels constructed of conventional concrete masonry units and mortar. Their testing included three groups of wall panels with different amounts of post-tensioning force for each group and a reinforced masonry wall panel as a reference panel. The specimens were made of 8 in. concrete masonry units and Type S mortar, constructed in stack bond with eight units high. One 5/8 in. continuously threaded prestressing rod was used for post-tensioning. Prestress was transferred through a 7 x 7 x 1 in. thick plate. The panels were tested in flexure to study the cracking and ultimate behavior. Deformation of the masonry caused by the grouting, shrinkage and creep was monitored for a period of 90 days in order to assess its impact on prestress loss. Loads were applied up to the cracking load and then released to complete the first cycle. The procedure was repeated for the second cycle which was intended to examine the behavior of the cracked section. Five of the panels were reloaded to produce a bending moment close to the calculated ultimate moment. Test data showed that during the first loading cycle for each post-tensioned panel, the response was elastic until the cracking moment. The study concluded that post-tensioned walls constructed of conventional masonry were feasible, stronger than reinforced masonry, and can be constructed using commonly available masonry materials.

Curtin and Howard [1988] from the United Kingdom experimented with prestressed brick diaphragm walls which demonstrated a large increase in lateral loading resistance. The research was carried out on 6 m x 3.375 m walls acting as free-standing cantilever walls. The magnitude of the prestress, loaded heights, and magnitude of lateral loading were varied. The compressive force was in excess of 6,000 kN. Lateral load was applied using six air-bags inflated with maximum pressure in the bottom bag and to a minimum pressure at the top bag to simulate triangular distributed loading of earth or water pressure. Six loading tests were carried out on two walls and one on the third. Issues such as slenderness ratio, horizontal and vertical shear strengths, ductility, loss of prestress due to creep, and flexural strength were discussed. The analysis and results showed a large increase in lateral load resistance when prestressed. No evidence of shear lag effect was found.

Al-Manaseer and Neis [1987] conducted experiments on four unbonded post-tensioned concrete masonry wall panels and two reinforced wall panels to study their flexural strength. The 4 x 8 ft (1.2 x 2.4 m) panels were built using 8 in. (190 mm) masonry blocks and Type M mortar, and 3/8 in. strands were used as prestressing steel. The panels were post-tensioned and after 24 days the grouting

operation was completed. The panels were simply supported and laterally loaded at midpoint with a monotonically increasing static load. The load versus midpoint deflection curves were recorded up to failure and comparisons were carried out under elastic, service, and ultimate loading conditions. The results indicated that the load capacity of the wall panels can be increased by post-tensioning. Panels experienced a ductile behavior independent of the configuration of the steel. Both prestressed and reinforced panels deflected less than 0.04 in. (1.1 mm) in the elastic range, which is considerably less than code requirements.

Curtin [1986] published another investigation on the structural behavior of post-tensioned brick diaphragm walls. Tests were carried out on two tall, narrow diaphragm walls under varying loads of prestress and subjected to varying magnitudes of lateral loading. Creep, elastic contraction, principal tensile strength and shear lag were also examined. The walls were 7.415 x 7.60 m and were designed based on simple working stress theory. One 40 mm diameter Macalloy high-tensile steel rod per cell was used. The walls acted as propped cantilevers, tied at the top and partially restrained at the base because of their own weight. The test results showed a very close correlation between the predictions and experimental results. Elastic contraction loss of prestress was recovered by restressing, after a period of time. The prestress loss due to creep in the brickwork was about 15 percent.

Dikkers and Yokel [1970] tested unreinforced brick wall panels, 4 x 8 ft, by applying uniform transverse loads, uniform axial compressive loads, or a combination of both types of loading. Test results were used to develop analytical procedures for predicting the strength of the walls subjected to axial compression and bending. The 8 ft brick walls behaved as slender walls with reduced moment capacity due to slenderness effects. The load capacity of the brick walls tested was closely predicted by the moment magnifier method and theoretical slenderness effects.

2.5.2 Previous Studies on Prestress Losses

Prestress losses occur due to natural material properties such as creep, shrinkage, and elastic deformation of the materials being stressed. In addition, prestress losses can occur during the prestressing operation itself. Creep and shrinkage are time dependent phenomena and are classified as long-term effects. Short-term losses occur due to elastic shortening, anchorage, and friction. The magnitude of the prestress losses depends on the initial and effective prestressing forces, the strength of individual materials, and environmental factors. Short-term losses are dictated by the prestressing technique and are somewhat controllable in comparison with the long-term effects.

The determination of prestress losses is important in understanding the behavior of prestressed masonry elements. Unlike concrete masonry, clay bricks tend to expand due to the absorption of moisture, which can cause a permanent gain in steel stresses in prestressed masonry. This unique phenomenon of clay brick masonry expansion is an irreversible and permanent effect, and its impact on prestressing is not yet fully understood.

The proposed system eliminates the elastic deformation losses of masonry because the elastic deformation of masonry occurs simultaneously with torque application, hence no loss occurs. The literature survey revealed that there are very few research or experimental studies published on prestress losses in masonry.

Levy and Spira [1973] conducted a theoretical analysis of prestressed masonry based on a finite difference technique. The theoretical results were compared with experimental results which included a prestress loss study on two masonry piers and a composite gable wall. The masonry walls were built using ordinary and special hollow concrete blocks through which the prestressing wires were placed and post-tensioned. Strains in the masonry and steel and deflections in the top beam were measured at regular intervals over a period of seven months. Laboratory experiments and follow-up on an actual construction site showed good agreement between measured values and those predicted by analysis. Investigation showed the loss to be in the range of 12 to 15 percent, of which a large measure was attributed to the shrinkage of masonry and reinforced concrete elements. Prestressed walls showed a distinct structural advantage over conventional walls due to their increased resistance against tension and shear.

Tatsa et al. [1973] published another experimental study on the loss of steel stresses in post-tensioned concrete block masonry walls. Two different concrete blocks were investigated (hollow and aerated). Three different series of tests were conducted with different hygrometric conditions. Test results of this study concluded that the prestress losses for masonry walls are of the same order of magnitude as in conventional prestressed concrete (up to 20 percent). It also suggested that the early application of prestress before the mortar has hardened is unacceptable, and that aerated concrete elements are suitable for prestressing.

Wyatt [1978] conducted tests on sixteen types of brick samples to study their moisture expansion and contraction properties. The samples were monitored for a period of 5 years. The author noticed a potential expansion range from 0.002 percent to 0.12 percent for pressed bricks and 0.132 percent for extruded bricks. The total movements in brick masonry due to thermal expansion, reversible moisture expansion, and long-term moisture expansion were shown to be 0.02 percent, 0.01 percent and 0.12-0.2 percent respectively. The most important factor

in masonry construction is long-term permanent moisture expansion since it causes a larger strain. The paper also made general recommendations for control joint spacing to accommodate dimensional changes in masonry.

Warren and Lenczner [1982] reported a study on two brick walls subjected to axial loading at the top and a free-standing wall as control panel for comparison of moisture and temperature movements. The walls were single wythe and were 28 courses high and four bricks wide. Highly sensitive acoustic vibrating wire gages were instrumented on the bricks and across the mortar joints in vertical and horizontal directions to measure the strains in both directions. Based on the results recorded continuously for 400 days, the authors have drawn creep strain curves at different locations of the wall in both horizontal and vertical directions. Most of the creep strain was developed in the first 60 days from load application. Test results showed that the bricks towards the center of the wall were more highly compressed than those towards the edge of the wall in the lateral direction. The largest tensile strains in the mortar joints were at the top. The horizontal and vertical joints were subjected to tension at the top and bottom of the wall, with only very small stresses being recorded near the center of the wall. The Poisson's ratio for the brickwork after 400 days was found to be 0.197 and for the bricks it was 0.087. The total creep deformation due to the bricks was three times that due to the mortar.

A second series of tests were conducted by Lenczner and Davis [1984] on losses of prestress in post-tensioned brickwork. Two post tensioned walls and two columns were tested under axial loading to predict the loss of prestress theoretically. Each wall had two single unconnected wythes with 1.535 m x 0.9 m. Five Macalloy bars 25 mm in diameter were placed between the leaves of the walls and post-tensioned with spreader plates at the top. The column specimens were 0.33 x 1.53 m, and post-tensioned using a single 32 mm diameter rod. The percentage loss in prestress in the tested specimens for the bricks ranged between 8 to 17 percent. Parameters such as effect of brick strength, type of the brick, geometry of the specimen, and the effect of initial prestress were also considered in the study. The loss of prestress in the walls ceased after 175 days, and the bars which were stressed to a lower level experienced larger losses. Fifty percent of the loss of prestress in the walls occurred during the first 25 days. In the columns, the loss of prestress continued much longer than the walls, but ceased after one year. Fifty percent of the loss of prestress in columns occurred during the first 35–40 days.

Huizer and Shrive [1984] reported a study on a wall post-tensioned both horizontally and vertically. A unique hollow concrete masonry block wall was built with units which were at least three years old and were not expected to exhibit much creep or shrinkage. No grouting was used in the wall. The wall was 1.8 x 2.6 m with an opening of 0.6 x 0.8 m. Four 7 mm diameter high-strength steel wires were

used for post-tensioning in both directions. The loss of prestress after 200 days in relatively short tendons was less than 20 percent. It was concluded that the two way prestressing is advantageous, and the long-term losses were expected to be within the acceptable limits for design purposes.

Taneja et al. [1986] conducted a three-dimensional finite element analysis to calculate the long-term loss of prestress in post-tensioned hollow masonry walls. Creep and shrinkage of the masonry units as well as the mortar bed, and relaxation of the prestressing steel were taken into consideration. The mathematical expressions of short-term experimental creep and shrinkage data were extrapolated to long-term values. Upper and lower limits on loss of prestress, which corresponded respectively to the most and the least creep and shrinkage in mortar and block units, were calculated. Based on the results, graphs are plotted for a period of 500 days. The computed results had a good correlation with the short-term experimental values. It was concluded that 50 percent of the ultimate prestress loss may occur during the first 50 days. In the case of concrete masonry, 24–31 percent of loss was expected and 17–22 percent in the case of hollow brick wall specimens. In the analysis, an average compressive stress of 25 percent of the ultimate strength of masonry was assumed. The authors also concluded that the upper bound of prestress loss reflects the worst case of creep and shrinkage in concrete block units and mortar whereas lower bound represents the best case of creep and shrinkage strains.

The most extensive work on creep of brick masonry and its effect on prestress losses was published by Lenczner [1986], which was based on two decades of research. The results in the paper were based on various specimens comprising brick-work walls, columns, and beams—with different types of brick and mortar—which were subjected to a sustained loads at different stress levels. The measurement of creep strain in an actual building was performed in a highly stressed wall, at the basement level of a 10-story load bearing brickwork tower. The measurements were recorded at different stages of construction and over a period of 3 years. Comparisons made with the theoretically developed values showed higher predicted strains than measured strain at early time periods, and very close correlation at a period of 1,200 days. A set of guidelines was presented that related the elastic modulus of brickwork and creep in walls and columns with the square root of the brick strength as well as the characteristic compressive strength of the masonry. A creep-time function was derived for brickwork, and the experimental results showed closer correlation to the proposed methods than relations given in BS 5628: Part 2 [Code 1985].

Lenczner and Harvey [1991] conducted more tests on walls and column specimens to determine the creep behavior and associated phenomena in concrete block

masonry. The column specimens included four half story columns and two half story control columns. One double leaf wall and one single leaf control wall of one story high were also built. For the creep tests, axial loads were applied at 28 days. The duration of the creep test was 346 days. Graphs were plotted for creep strain and moisture strain with respect to time. In post-tensioned tests, five 25 mm diameter Macalloy steel bars were used in the wall specimen, and one 32 mm bar was used in the column specimen. All of the experimental results were compared with different predicted results. The comparison showed that the guide lines were accurate for block work columns but not for walls. Alternative theories were presented to calculate the loss of prestress in post-tensioned masonry due to creep and shrinkage.

Schultz and Scolforo [1992] summarized the design provisions in codes and research performed to date on prestressed masonry including prestress loss determination. Individual factors affecting the prestress loss in masonry are outlined in the paper. A comparison study between the British and North American codes was given. A large discrepancy can be noticed between the codes, and the paper identifies the areas in need of further research.

Recently, Brooks and Bingel [1994] published a paper on stress relaxation due to creep and moisture movement in masonry walls. The work included experimental tests on concrete block and brick masonry walls, and the results were assessed with other analytical methods developed from concrete. Three identical wall specimens were 13 courses high and 2 bricks wide, and 5 blocks high by 1 block wide for brick and concrete masonry, respectively. Strain measurements were taken using Demec points attached on both sides of the wall over a gage length of 750 mm. Loading was applied at the age of 34 days for concrete masonry and 28 days for brick walls. Creep and stress relaxation curves were plotted and compared with other theoretical predictions. The results showed that total relaxation in clay masonry can be estimated using other methods developed for concrete with an accuracy of $\pm$30 percent. When account is taken of the nonlinear stress-strain relationship of the block work the accuracy of prediction is improved.

The Masonry Standards Joint Committee (MSJC) is working currently to develop code specifications for prestressed masonry in North America [Prestressed 1995]. Provisions were included to calculate the effective prestress after considering seven different effects which can change the prestress. The commentary addressed individual specific considerations that should be given to calculate the prestress loss. It suggested to ignore the changes in prestress due to thermal fluctuations if masonry is prestressed with high-strength prestressing steels.

2.6 Pertinent Codes, Standards, and Specifications

At present there is no code or standard methodology available in North America for the analysis and design of prestressed masonry. Most of the applications in the United States are in the experimental stages. Schultz and Scolforo [1992] compared the code practices of the United States and the United Kingdom for the design of prestressed masonry elements. The proposed provisions for the adoption to North American Code were based on prestressed concrete theory. The MSJC [Prestressed 1995] is currently developing code and specification criteria for prestressed masonry to be incorporated into the ACI 530/ASCE 5/TMS 402 Standard [Building 1992], which currently addresses only plain and reinforced masonry. Some of the MSJC [Prestressed 1995] proposed recommendations are used in this research study. Provisions for reinforced masonry are covered in the UBC [1994]. The reinforced masonry provisions in the United States are based on working stress methods. Allowable stresses for individual materials are given and the members are designed for service loads. The British Code, BS 5628 [Code 1985] has included prestressed masonry since the 1970s. It uses a limit state design criteria in serviceability limit state and ultimate limit state are recognized. The fundamental design equation is:

$$f/\gamma = Q \qquad \text{[Eq 2-1]}$$

Where f is the strength of the masonry, γ is the partial safety factor and Q is the applied factored load. Partial safety and load factors depend on the limit state and quality of construction and inspection. Phipps [1992] outlined the principles and codification of prestressed masonry design in the BS 5628: Part 2. He described efficient sections through stress block diagrams for various geometric cross sections. Design methods for bending, shear, axial load and prestress loss estimation were also given. Phipps [1993] proposed the design clauses for prestressed masonry for inclusion in Eurocode No. 6 (EC 6) and the revisions for the British Masonry Code BS 5628: Part 2. These guides were based on the development and testing of post-tensioned masonry walls in the United Kingdom along with major differences between the two codes. Haseltine [1982] briefly discussed the development of reinforced and prestressed masonry criteria in the Code BS 5628: Part 2. Based on some of the research he conducted, limited state guidelines have been developed for reinforced and prestressed brick work [Haseltine 1978]. He emphasized the need for further research because the guidelines are derived from the well known behavior of reinforced and prestressed concrete.

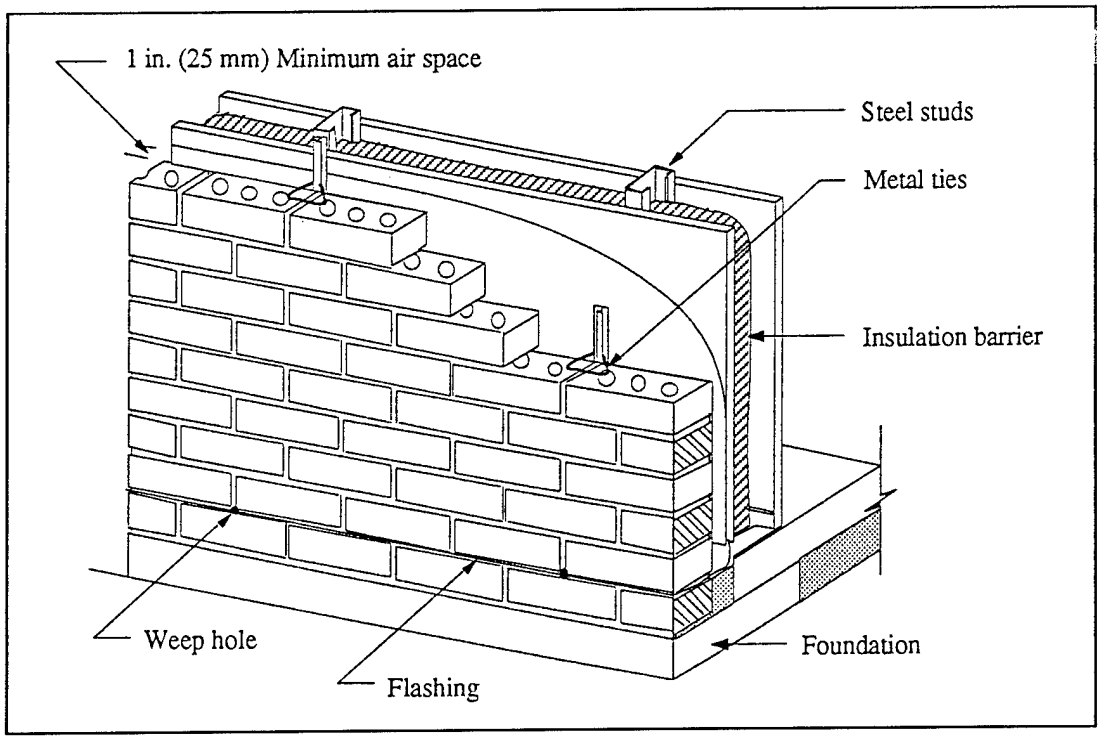

Figure 2.1. Typical brick veneer/metal stud system.

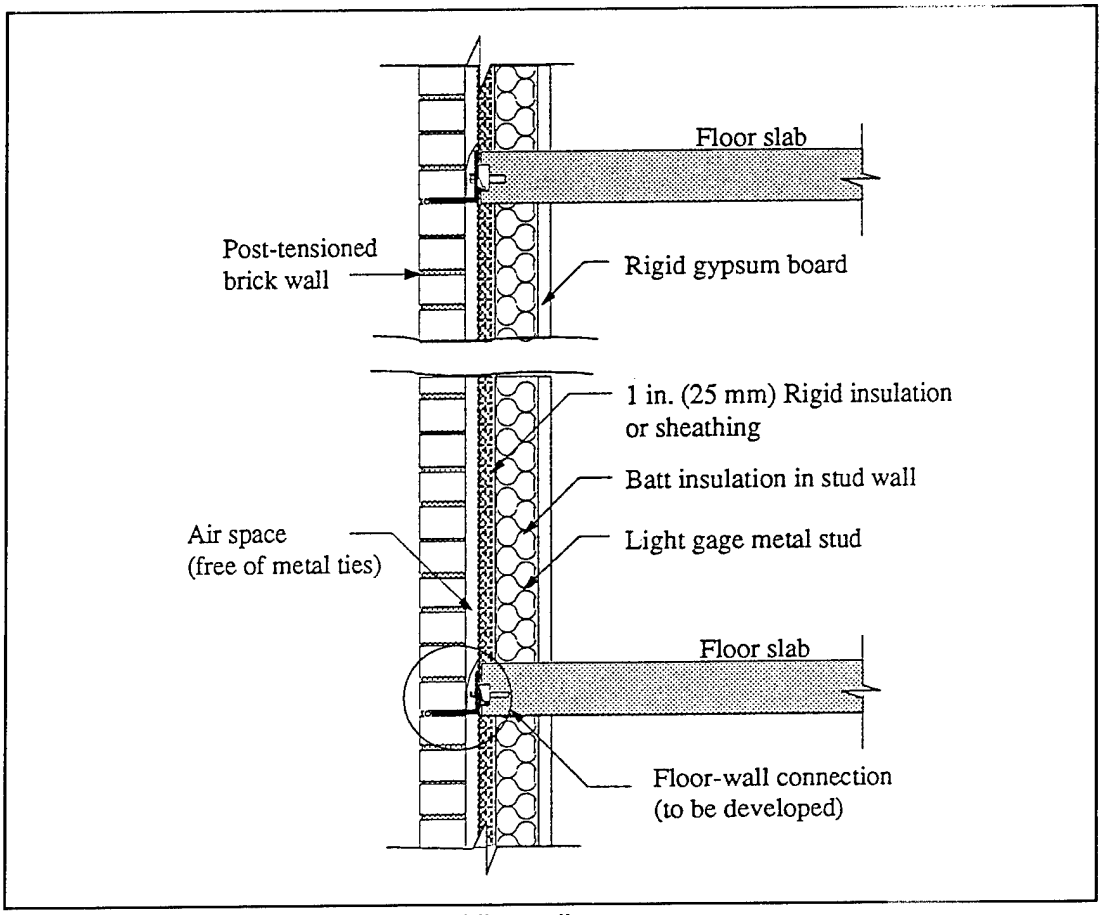

Figure 2.2. Post-tensioned masonry cladding wall.

3 Analytical Modeling

Load-deflection relationships for the post-tensioned grouted masonry panels have been developed to compare with the experimental results. The relations were derived with assumptions based on well established theories of prestressed concrete member behavior and material properties [Lin and Burns 1981]. The measured material properties are used in the analysis. The moment and curvature relation at various stages of loading are derived first and then they are converted to load and deflections using the relations from structural mechanics. The UBC [1994] method of calculating deflection is also included in Section 3.3. This chapter gives only the theoretical analysis expressed in terms of stress and strain values in masonry and steel. Detailed calculations for all three methods are given in Appendix A.

3.1 Moment-Curvature Analysis

The general assumptions used in the moment-curvature analysis were as follows:

1. The strain was distributed linearly over the cross section of the member. This assumption simplified the variation of strain along the cross-section using similar triangles. Masonry compression strains were assumed at various stages of loading, and hence the strain in the steel was calculated by linear interpolation.
2. The effective compressive strain, ϵ_{me}, and the post-tensioning bar tensile strain, ϵ_{se}, corresponded to the effective stress, f_{se}, existed before any lateral load applications. The strains in masonry and steel were different depending on their modulus of elasticity before the load application.
3. The actual measured stress and strain curves from the material tests were used in the analysis. Stress values were found from the stress-strain curves after determining the theoretical strain values.
4. The steel was assumed fully bonded to the surrounding grout. Therefore, changes in strain were equal to the masonry strain. This assumption also guaranteed a constant effective depth, d, in the cross-section.
5. Tension and compression forces acting on the cross section must be in equilibrium with flexural loads applied on the member. Neutral axis depths were calculated based on this condition. After satisfying equilibrium, the

moment was calculated by algebraically summing the moments at the level of compression force.

6. The compressive block depth was assumed to be 0.85 times the depth of neutral axis. This was an approximation, since the masonry stress-strain curve was not complete.

3.1.1 Material and Section Properties

At the initial prestressing stage, the gross masonry cross-sectional area is used as the effective area (b x h), as the bricks were to be considered to be solid according to ASTM C 216-87 [1987] classification. Thus the moment of inertia, I_g, and section modulus, S, were calculated based on these values. The UBC [UBC 1994] specifies a value of $2.5\sqrt{f'_m}$ as the modulus of rupture for solid brick masonry. The actual measured modulus of rupture of $2.66\sqrt{f'_m}$ was used. Actual measured modulus of elasticity values for masonry and steel were used in the analysis. The modulus of elasticity of the high-strength steel threaded bars was 26,500 ksi (182,760 MPa) which is less than the manufacturer suggested value of 29,000 ksi (200,000 MPa).

Section properties were calculated as follows:

Cross sectional area of masonry (gross), $A_m = b \times h$

Section modulus, $s = \frac{bh^2}{6}$

Gross moment of Inertia, $I_g = \frac{bd^3}{12}$

Modulus of rupture of masonry, $f_r = 2.66\sqrt{f'_m}$

Effective area of prestressing bar = A_{ps}

Effective prestress = f_{se}

Modulus of elasticity of masonry = E_m

Modulus of elasticity of prestressing steel = E_{ps}

3.1.2 Moment-Curvature Relations at Various Stages

In the following stress and strain diagrams, compressive stresses are considered as positive and tensile stresses as negative. Table 3.1 shows equations used in the theoretical analysis at various loading stages. Figure 3.1 shows the moment-curvature relation developed from the analysis.

3.2 Bilinear Behavior Method

The midheight deflection equations given in the UBC [UBC 1994] are based on bilinear relationship (consists of two linear portions, see Figure 3.2). The deflection before the member has cracked is calculated using the gross moment of inertia, I_g, and further deflections beyond cracking stage are calculated using the cracked moment of inertia, I_g.

$$\Delta = \frac{5M_s h^2}{48E_m I_g} \quad for\ M_{ser} \le M_{cr}$$

$$\Delta = \frac{5M_s h^2}{48E_m I_g} + \frac{5(M_{ser} - M_{cr})h^2}{48E_m I_{cr}} \quad for\ M_{cr} < M_{ser} < M_n$$

The cracking moment strength of the wall shall be determined from the formula:

$$M_{cr} = Sfr$$

where f_r is the modulus of rupture of masonry. The modulus of rupture from Section 3.1 was used. The cracked moment of inertia was calculated from the equation:

$$I_{cr} = \frac{b(kd)^3}{3} + nA_{ps}(d - kd)^2$$

where kd is the neutral axis depth.

3.3 Horton and Tadros Method

Horton and Tadros [1990] proposed a method to calculate a load-deflection relation that includes the effect of tension stiffening. The paper also compared the results of their study with five other methods. The proposed method showed a good agreement with the test data. The method includes an interpolation range between uncracked and fully cracked equations to calculate deflections and is graphically represented in Figure 3.3.

The equation for deflection in its general form is:

$$\Delta = \Delta_1 R_4 + \Delta_{cr}(1 - R_4)$$

The interpolation coefficient is a function of cracking moment, M_{cr}, and the applied moment, M_a. For simply supported members, it is given by the following equation:

$$R_4 = 1 - \left(1 - \frac{M_{cr}}{M_a}\right)^2$$

Combining the above two equations,

$$\Delta = \Delta_{cr}(1 - \alpha)$$

$$\text{where, } \alpha = \left(\frac{M_{cr}}{M_a}\right)^2 \left(2 - \frac{M_{cr}}{M_a}\right)\left(1 - \frac{I_{cr}}{I_g}\right) \text{ when } M_{cr} \le M_a \le M_y$$

$$\alpha = \left(1 - \frac{I_{cr}}{I_g}\right) \text{ when } M_{cr} > M_a$$

Figure 3.4 shows the comparison of all three methods with the experimental load-deflection curves. Detailed calculations of these are given in Appendix A. The moment-curvature relation developed based on the actual material properties predicts a behavior that is close to the experimental curves. The method from Harton and Tadros [1990] resulted in higher deflection values compared to the UBC's bilinear relation. From the figure, it can be seen that both UBC and Horton and Tadros methods were conservative in predicting deflection compared to the actual deflection behavior of the masonry. All these methods were very close to the actual test data at the ultimate strength level.

Table 3.1. Moment and curvature equations at various stages.

Loading Stage	Moment	Curvature
(a) Initial post-tensioning	0	0
(b) Self weight +	M_d	$\frac{\varepsilon_m(top) - \varepsilon_m(bot)}{h}$
(c) Cracking	$M_d + M_{add}$	$\frac{\varepsilon_m(top) + \varepsilon_m(bot)}{h}$
(d) After cracking	$M_d + M_{add} + \Delta M_s$	$\frac{\varepsilon_m(top) + \varepsilon_s}{d}$
(e) At ultimate	M_u	$\frac{\varepsilon_m(top) + \varepsilon_s}{d}$

(a) Initial post-tensioning of masonry:

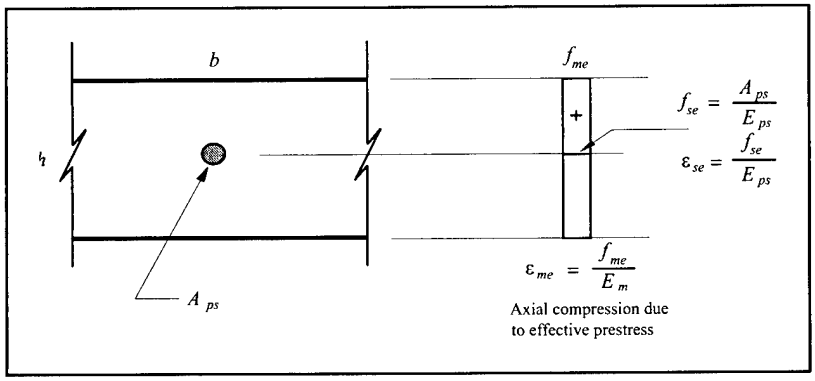

(b) Self-weight and superimposed dead load (SIDL):

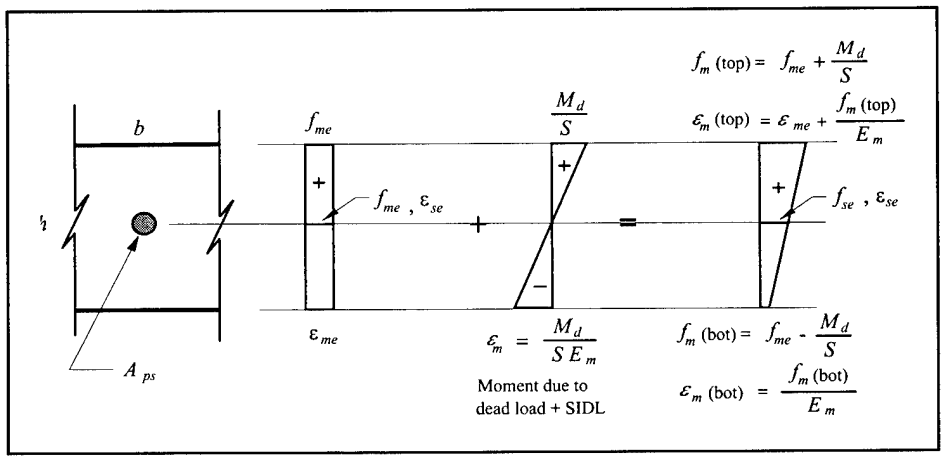

(c) At the cracking moment stage:

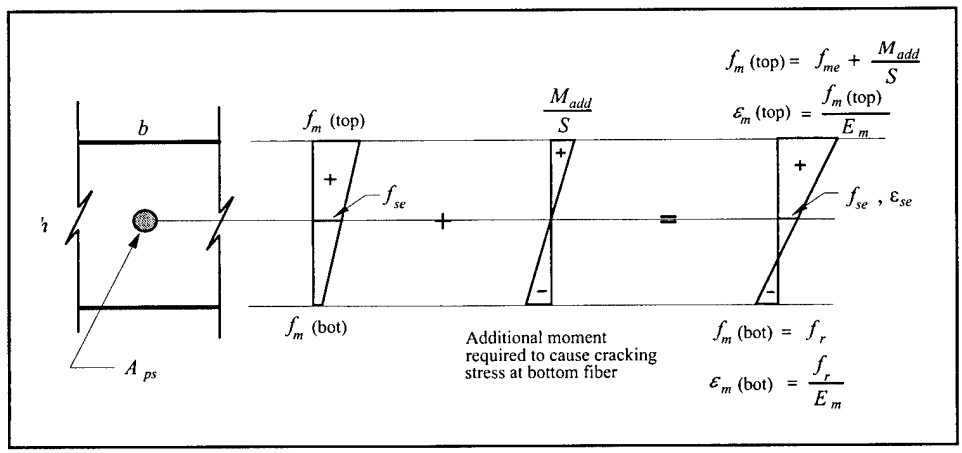

Figure 3.1. Theoretical moment-curvature relationship.

(d) At different strain increments of top fiber of masonry after cracking:

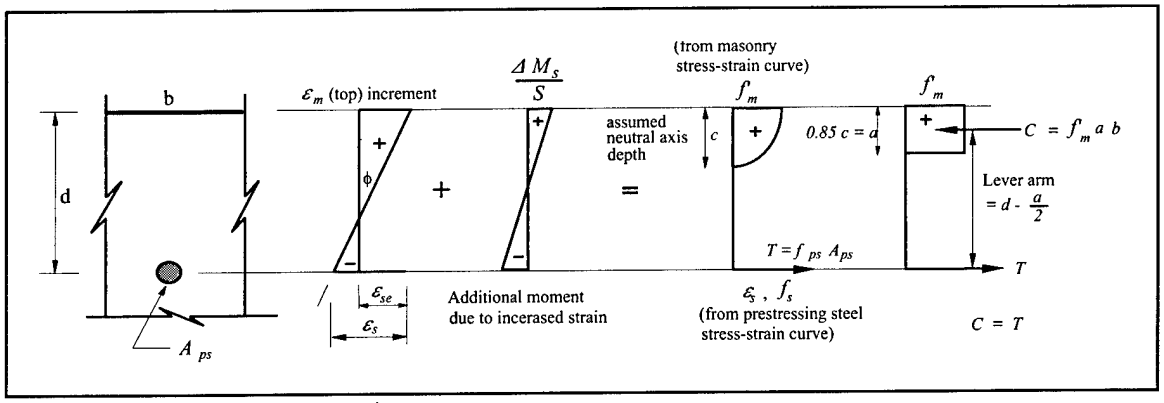

(e) At ultimate moment capacity:

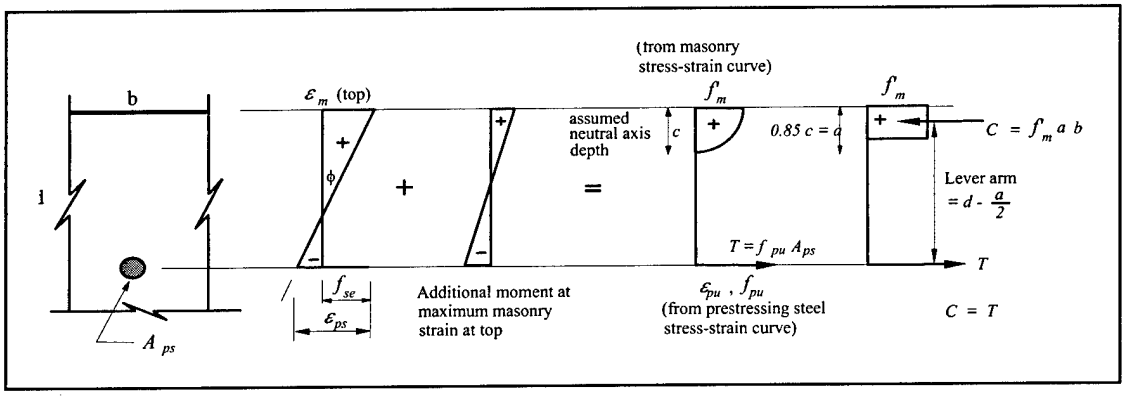

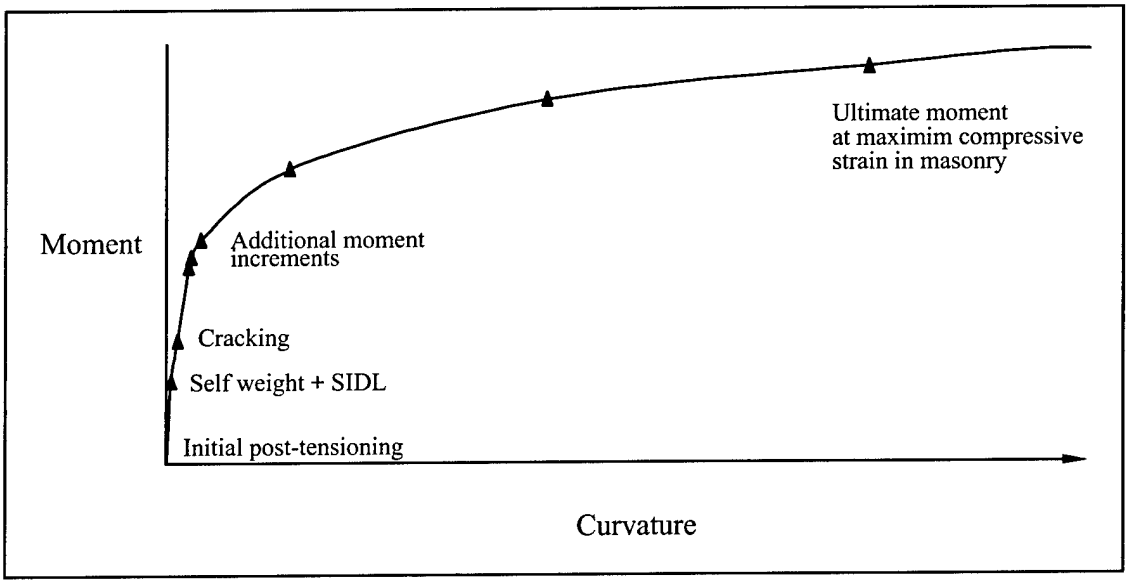

Figure 3.1. Cont'd.

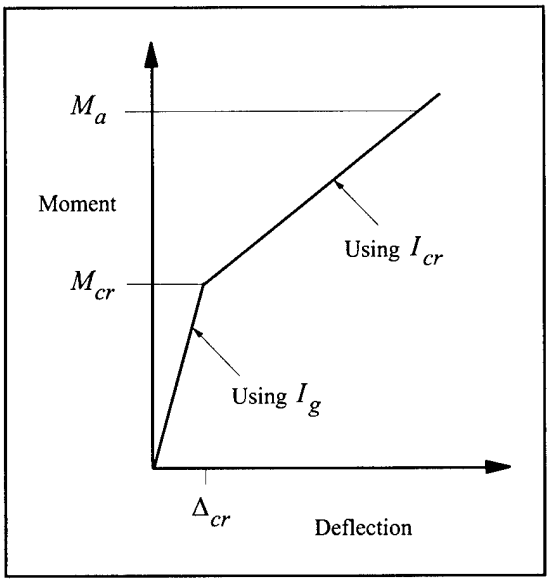

Figure 3.2. Bilinear moment-deflection relationship.

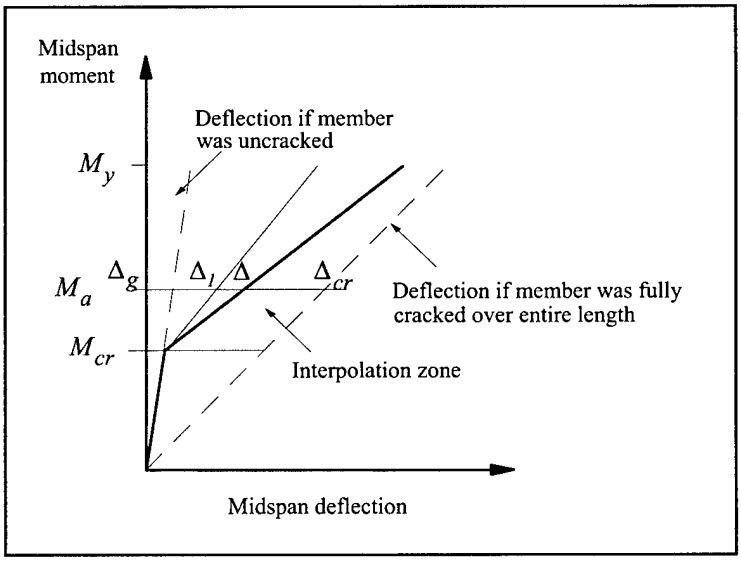

Figure 3.3. Graphical representation of interpolation equation.

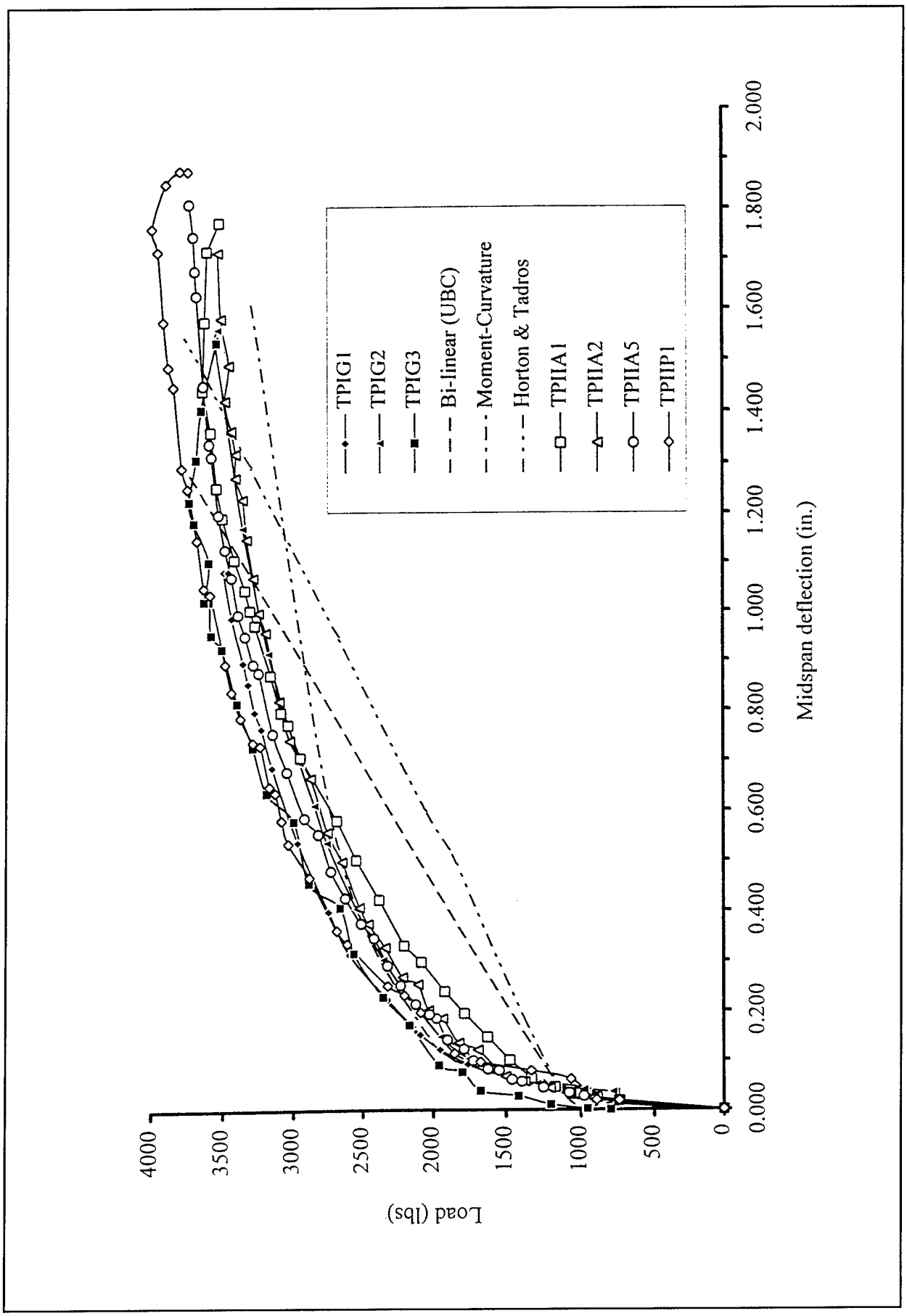

Figure 3.4. Comparison between experimental and theoretical results.

4 Experimental Work

4.1 Innovative Features of the Proposed System

A new brick shape was designed for use in this research. The new bricks were manufactured at a brick plant and shipped to the laboratory. They have the same properties as standard modular clay bricks satisfying ASTM specification Grade SW, and Type FBS [Standard 1987]. The number of cores was reduced to two (standard modular brick has three cores) and made larger to accommodate prestressing bars and grout with the minimum face shell thickness of 3/4 in. (19 mm). The cores were designed to index in running bond pattern with a standard mortar joint of 3/8 in. (10 mm). The bricks were classified as solid with a coring area of 25 percent of the gross cross-sectional area, and its overall dimensions were maintained the same as the standard brick with 3 3/5 x 7 3/5 x 2 ¼ in. (92 x 194 x 57 mm). Figure 4.1 shows both the standard and new two-cored bricks with dimensions.

The proposed prestressing technique involved using high-strength bars as the prestressing steel inserted into the wall at the required spacing. The bars were continuously threaded which helped in developing bond between the steel and surrounding masonry. Standard hexagonal nuts were used on both sides of the rod, and tensioned from the top of the wall (one side only). Bar diameters up to 1 in. (25 mm) may be accommodated in the wall using this system, which had a core diameter of 2 1/8 in. (54 mm). Grouting of the cores was done immediately before the post-tensioning operation. Commercially available or hand-mixed grout with a flowable consistency can be used.

The initial prestressing force in the bar was measured using a direct tension indicator (DTI) washer inserted between the nut and the bearing plate/angle. DTI washers are manufactured according to ASTM F-959 specifications [Standard 1993] and are available to use with different sized bars. The use of DTIs is new and gaining popularity in structural steel "slip critical" connections. A standard torque wrench was employed to apply torque (prestressing force) in the bar. Figure 4.2 shows all hardware components of the proposed post-tensioning system.

The following sections describe the experimental work conducted during this research, including materials, components, and panels tests. The results of the material tests are presented in Section 4.2. The material properties obtained in

each stage of testing were used in the analysis of that particular stage of panel tests. Section 4.3 gives the methods adopted to estimate the prestressing force applied to the specimens and during testing. Section 4.4 describes the flexural testing of post-tensioned panels during Stage I and II, and the prestress loss study is described in Section 4.5.

4.2 Evaluation of Material Properties

The constituent materials were tested in accordance with ASTM specifications to evaluate their properties. This included the testing of the prestressing bars, brick, mortar, and masonry prisms. The following sections summarize the tests conducted on materials and the results obtained under each section. The tests on bricks, prestressing steel, and DTI washers were carried out at the beginning of the project instead of at each stage of testing program.

4.2.1 Brick

Compressive strength, water absorption (both cold and boiling), and modulus of rupture tests were conducted in the laboratory as per ASTM C 67 [1987] specifications, and the results obtained are tabulated in Table 4.1. It can be noticed from the table that the bricks satisfy the ASTM requirements. Plant certified values provided by the manufacturer are also given in the table. Figure 4.3 shows a brick unit being tested in compression.

4.2.2 Mortar

Mortar cubes were tested according to ASTM C 270 [Standard 1987] proportion specifications. Twelve mortar cubes of 2 in. (50 mm) side length were molded from the mortar mix produced by the masons during the construction of Stage I panels. The proportions of the mix used were 1:1:6, Portland cement : lime : aggregates, which is categorized as Type N mortar. Type N mortar was selected for the wall specimens since it has lower strength than types M and S mortars, and it is the most workable (and popular) of all these types. The specimens were removed from the molds after 48 hours and further cured with burlap and plastic covers to maintain a constant humidity. These cubes were tested at different time intervals beginning from the day of post-tensioning to the day of specimen testing, to determine the strength of the masonry accurately. The test results obtained are shown in Table 4.2. The table also includes tests conducted on the mortar used in Stage II and prestress loss panels. The results show a variation of 9 percent between the three batches of testing. ASTM requires a minimum strength of 750 psi (5.17 MPa) at the age of 28 days for Type N mortar when the mortar is specified

based on its properties. All of the mortar specimens satisfied the minimum requirements.

4.2.3 Masonry Prisms

Masonry prisms were built by the construction crew during panel construction using the same bricks and mortar as used for the wall specimens. They were used for both compression and modulus of elasticity tests. Figure 4.4 shows the dimensions of a typical masonry prism. These prisms were made of five course of bricks with four mortar joints in stacked bond. The average height to thickness ratio of the specimens was 3.56. They were tooled on one side to represent the actual wall specimens. The thickness of the mortar joint was 3/8 in. The strength results of all of the specimens tested for modulus of elasticity were included with the compression test results.

4.2.3.1 Compressive Strength. The prism compression tests were conducted according to ASTM E 447 [1984]. Roof tiles were used as capping materials which were shown to be accurate and easy to use. Figure 4.5 shows a prism specimen failed in compression. The specimens normally experienced cracking first along the least face shell thickness of 3/4 in. (19 mm). It was observed during the test that after the first crack, the prisms withstood a significant amount of additional load before failure. Tables 4.3, 4.4, and 4.5 show the test results.

The results of the 28–33 day tests varied from a minimum of 2,290 psi (15.8 MPa) to a maximum of 3,610 psi (24.9 MPa), an average value 2,845 psi (19.6 MPa) with a standard deviation of 427.9. This average value was eight percent lower than the 3,100 psi (21.4 MPa), given in Table 21-D of the UBC [1994] for the materials used.

Seventeen prisms were built by the masons during the Stage II panel construction. They were tested beginning from post-tensioning day to the end of panel testing. The procedure was similar to Stage I tests. Table 4.4 gives the details of the test results. The average strength of the prisms at the beginning of panel testing (30 days) was 3,430 psi (23.7 MPa). The value ranged from 2,785 psi (19.2 MPa) to 3,235 psi (22.3 MPa) with a standard deviation of 180.5. This is 10 percent higher compared to the UBC [1994] specified value of 3,100 psi (21.4 MPa).

Nineteen more prisms were built during construction of the prestress loss panels. They were tested at regular intervals starting from the age of three days to study the strength development. Table 4.5 shows the test results. The average 28 day strength was 3,600 psi (24.8 MPa), which is 26 percent higher than the Stage I panel strength. The results had a standard deviation of 247.1. The results are 16 percent higher than the UBC [1994] value of 3,100 psi (21.4 MPa).

The compressive strength of masonry varied largely in each stage of testing, though the same materials were used. The use of Table 1.6.2.1 of ACI 530/ASCE 5/TMS 402 Standard [Building 1992] results in compressive strength of 2,270 psi (15.7 MPa) based on the compressive strength of brick units and Type N mortar.

4.2.3.2 ***Modulus of Elasticity.*** During the 28 day and 33 day prism compression tests of Stage I, four of the specimens were instrumented with a Demec gage to monitor the strain experienced by the specimens. The process of measuring strain using the Demec gage consists of gluing two locator pins at approximately 8 in. (203 mm) apart on the test prisms. The strain is measured between these two pins at desired load intervals during the course of the test. The Demec gage had an accuracy of measuring 0.8×10^{-5} strain. The Demec gage was firmly secured on the pins. The readings were taken up to the first cracking, and then removed to avoid any possible damage to the equipment. Figure 4.6 shows a test specimen fitted with the Demec gage. Stress-strain curves were plotted and are shown in Figures 4.7 through 4.9 for all three stages. The modulus values were determined on the secant modulus of elasticity taken between $0.05\,f'_m$ and $0.33\,f'_m$.

The modulus of elasticity of masonry of the Stage I prisms (see Figure 4.7) was found to be 2,160,000 psi (14,900 MPa), which is equivalent to $760\,f'_m$ with a prism strength of 2,845 psi (19.6 MPa). Six prisms used in Stage II were tested to determine the modulus of elasticity of the panels. The modulus of elasticity was found to be equal to 2,401,000 psi (16,560 MPa) or $700\,f'_m$ with a prism strength of 3,430 psi (23.7 MPa). The stress strain curves were plotted and shown in Figure 4.8. The third batch of prisms was tested to determine the modulus of elasticity for the prestress loss panels. Three specimens were tested and the procedure was very similar to the first time. The modulus of elasticity was found to be equal to 2,486,000 psi (17,145 MPa) or $690\,f'_m$ with a prism strength of 3,600 psi (24.8 MPa). The stress-strain curves for prestress loss panels are shown in Figure 4.9.

Table 4.6 summarizes modulus of elasticity values for all three stages. The UBC [1994], Section 2106 specifies a value of $750\,f'_m$ which is close to the values from the tests. The ACI 530/ASCE 5/TMS 402 standard [Building 1992], Table 5.5.1.2, yields a value of 2.272×10^6 psi (15,670 MPa) for the brick and mortar properties used. Previous tests conducted on similar materials gave lower values for the modulus of elasticity compared to the code value [Devalapura et al. 1994].

4.2.4 Prestressing Steel

The prestressing bars used for Stage I testing and prestress loss panels were 120 ksi (828 MPa), 5/8 in. (16 mm) high-strength continuously threaded steel bars. They were manufactured by Williams Form Engineering Corp., Grand Rapids, MI.

Two groups of bars were tested in the laboratory to find the actual properties of the material. The first group of specimens was tested to find the ultimate tensile strength of bars. A Tinius Olsen testing machine with a capacity of 120 kips (534 kN) was used for the testing. The test results are shown in Table 4.7.

The second group of test specimens were tested to obtain actual stress-strain behavior of the bars. Each specimen was instrumented with a strain gage at the center of the gage length and the readings were recorded by a data acquisition system. An MTS testing machine was used for loading the bar specimens. The bars were loaded up to failure. Figure 4.10 shows the stress-strain curve plotted from the test results. From the figure, it can be noticed that the steel does not have any significant yielding point. The yield strength was determined using the 0.2 percent offset method. Table 4.7 summarizes the test results.

4.2.5 Direct Tension Indicator (DTI) Washer

The direct tension indicator (DTI) washers were checked for their accuracy before their use on the test panels. The DTI washers were manufactured in compliance with ASTM F 959 [Standard 1993] specifications and were supplied by two different manufacturers. During the test, the gap in the washer was measured using a manufacturer supplied key. A load cell was used in the test setup and the load was directly measured by a digital monitor. A 600 lb-ft (813 N-m) manual torque wrench was used to apply the torque.

Preliminary tests comparing the force in the threaded bar to the gap measurement on the washer have shown that the DTI was crushing to the specified gap at a force higher than the ASTM specified minimum value [Standard 1993]. Table 4.8 shows the average crushing value of DTIs tested with the standard deviation. The force in the bar was measured using a load cell, and the load value was red when the DTI was crushed to its specified gap. The ASTM F959-93a [Standard 1993] specifies a minimum of 19 kips (84.5 kN). These tests showed that the DTI washers were very consistent in estimating the prestressing force in the bar.

4.3 Methods of Prestress Measurement

To ensure an accurate measurement of prestress, force in the bar was monitored by three means. First, three strain gages (Type CEA-06-125UW-120) were attached at the top, middle, and bottom of the bar to measure the elongation during the post-tensioning and testing stages. The strain gages were connected to a data-acquisition system to digitally record the strain. Readings were recorded until the end of each panel test. The strain readings obtained from all three gages were averaged

to determine the force in the bar for the analysis. Second, a DTI washer was employed at one end of the prestressing bar. These washers can only be used to measure the force during the post-tensioning operation. Although these washers are manufactured to crush completely at a specified minimum force, they were successfully used to apply a lesser force in the bar using the manufacturer certified relation between the force and gap in the washer. A locally purchased feeler gage was used to check the specified gap in the washer during post-tensioning. Third, a calibrated torque wrench was used for the torque application. The required torque was applied manually based on the relation developed between the force and the applied torque, prior to the post-tensioning operation. During calibration, the wrench readings were shown to be sensitive to the friction between the nut and threads of the bar, and the size of the torque increments. The wrench reading was used as an additional estimate and combined with the data obtained from the other two methods. The actual post-tensioning showed good correlation of the stress in the bar measured by the strain gages in the constructed test panels and the DTI washer gaps, but the torque wrench was found to be unreliable. The DTI washers proved to be very accurate and reliable in estimating the actual force in the bar.

4.4 Out-of-Plane Lateral Load Tests

4.4.1 Stage I Testing—Post-Tensioned Wall Panels

4.4.1.1 ***Test Description.*** The aim of the Stage I testing was to study the feasibility of post-tensioning brick masonry, its cracking strength, its flexural behavior, and the ultimate capacity of a wall to resist out-of-plane loads. In this stage, six wall specimens 3 x 6 ft (0.91 x 1.83 m) were built in the laboratory by experienced masons using standard construction methods. A typical detail of the Stage I test panel is shown in Figure 4.11. Three of the six panels were grouted to compare the results with ungrouted specimens. Ungrouted and grouted panels are designated as TPIUG and TPIG respectively. All specimens had the same level of prestress, and were tested to failure in flexure. The following sections illustrate their method of construction, testing, and the results obtained.

Panel Construction. New two-cored bricks and Type N mortar (1:1:6) were utilized to build the specimens. The wall panels were built on a wooden platform (6 in. high) to get access to the bottom of panels during the post-tensioning process. First the bottom anchorage plate was kept in position to align with the platform hole, and then the brick courses were laid. Two groups, each consisting of three panels, were built in I-shaped configuration to achieve a free support construction. The center core of each panel was kept void throughout its height in order to be able to insert the bar for post-tensioning. This was achieved by blocking the core using

a piece of wet sponge to avoid ingress of mortar during construction (see Figure 4.12). The sponge was pulled up each time a brick course was laid on top. The wall specimens were tooled on one side to accurately represent veneer construction.

Post-Tensioning Operation. One high-strength continuously threaded bar of 5/8 in. (16 mm) diameter with an ultimate strength of 120 ksi (828 MPa) was introduced into the center core of each specimen. No difficulty was experienced during this stage as the cores were clear of mortar. The prestress was applied to the specimens at the age of four days after building the wall specimens. A manual torque wrench with a capacity of 600 ft-lb (813 N-m) was used for post-tensioning. After introducing the prestressing bar through the top anchorage plate, its lower end was tightened with a nut and washer. At the top a DTI washer was placed in position between two high-strength washers, and torque was applied in steps by the turn-of-the-nut method. This task was easily performed by two persons with an extended rod attached to the torque wrench. Figure 4.13 shows a post-tensioning operation in progress on one of the specimens. The DTI washers and the torque dial were checked continuously to introduce a predetermined amount of prestress based on the previous calibration. The amount of prestress was verified by strain gages placed on the bar.

Grouting. Commercially available high-strength grout mix (Sonogrout 10 K) was used for grouting the panels TPIU1 and TPIU2. A flowable mix was prepared in the lab and poured into the core using a funnel through a hole made at the top of the specimens. Figure 4.14 shows the grouting in operation on one of the specimens. The filling of grout in the core was confirmed through another hole at the bottom of the specimen. The third panel TPIG3 was grouted using a hand-mixed grout with a proportion of 1:1/10:6 (Portland cement:lime:sand) to check its suitability as a grout. The panels TPIG1 and TPIG2 were grouted at 12 days after construction, and the third panel TPIG3 was grouted at 19 days. Panels were typically air cured for 28 days in the laboratory before testing.

Testing Procedure. The panels were tested to failure in flexure by applying loads at the middle-third points. They were seated on roller supports on either side with a span of 36 in. (0.91 m). The loads were applied with an approximate load increment of 200 lb. A manual hydraulic hand pump was used to jack the ram and the load was measured with a 50 kips load cell. Deflections at mid-span were measured on each side using potentiometers and LVDTs. During testing, strain in the steel rods was recorded from the strain gages attached to the bars. Loading, deflections, and steel strains were recorded using a data acquisition system. The compression stain of masonry at middle span was recorded using the Demec gage at the midspan. Figure 4.15 shows a test panel setup with the loading frame before

the application of the load. The load was applied incrementally until the specimens failed. The cracks that developed during loading were marked and recorded.

4.4.1.2 ***Test Results.*** The following sections outline the test results both for ungrouted and grouted panels.

Ungrouted Panels. In the case of ungrouted specimens, there was no significant increase in the load-carrying capacity beyond cracking. Table 4.8 shows the moments at cracking and ultimate strengths of individual panels. The first crack developed near the mid-span along a bed joint. One or two joint cracks developed and enlarged after further application of the load. TPIUG1 experienced a very sudden failure after cracking and the specimen broke into several pieces. TPIUG2 deflected to a maximum of approximately 2 in. (50 mm) at midspan, and residual deflection was about 1 in. (25 mm) upon removal of the load. The masonry was crushed at the compression face along the crack and some small pieces were spalling off the panel at ultimate load. The panel showed a ductile behavior by deflecting upwards upon the load removal. TPIUG3 experienced a single wide tensile crack of 3/4 in. (19 mm) nearer to the loading point in the midspan, and gave similar results as TPIUG2 panel. Figure 4.16 shows a failed ungrouted specimen after the test. The loading of TPIUG2 and TPIUG3 panels was stopped after a significant strength loss to avoid sudden failure and possible damage to the equipment.

Grouted Panels. Generally, the grouted panels had nearly twice the ultimate moment capacity of the ungrouted panels (Table 4.8). All three grouted specimens showed consistent strengths and deflections. The maximum deflection at ultimate load ranged from 2.25–2.63 in. (57–67 mm). The cracks that developed were evenly distributed in the bed joints near midspan. The panel deflections were reduced to approximately 1 in. (25 mm) after removal of the load. No difference was noticed in the results between hand-mixed grout (TPIG3) and prepackaged high-strength grout specimens (TPIG1 and TPIG2). All three specimens failed at ultimate load with a wide crack approximately 1/8 in. (3 mm) along the length of the reinforcement. The crack occurred on both sides of the panel and can be explained as a splitting crack. The panels remained intact (in one piece) even after the test, with a large amount of prestress remaining in the bar. Figure 4.17 shows a grouted test panel at ultimate load.

Figure 4.18 depicts the load-deflection curves for all six panels. Moments due to the panel's own weight, loading frame, and other additional loads placed on top of the panel during the test were considered in the analysis. It can be observed from the curves that there was very little difference between the grouted and ungrouted specimens prior to cracking. The behavior of the specimens was linear before

cracking, and the curves then diversified between grouted and ungrouted specimens. After cracking, the panels with ungrouted bars progressed rapidly to failure with very little increase in load. The panels with grouted bars showed an increased capacity up to the ultimate load of approximately two times the cracking load. No cracks were noticed in any of the panels in the anchorage zones throughout the test. Steel stresses increased only after cracking occurred and the neutral axis shifted. All the panels experienced a high post-cracking deflection at midspan. Some of the deflection was recovered when the load was removed and the cracks closed completely. Deflections at maximum capacity and failure loads for all specimens are also given in Table 4.9.

A plot of the applied load versus compression strains measured at midspan of the panels is shown in Figure 4.19. The recording of strain readings was started when the load was applied, and was stopped once the masonry started crushing during the test.

4.4.2 *Stage II Testing—Post-Tensioned Wall Panels*

4.4.2.1 *Test Description.* The Stage II testing of panels was designed to investigate the effect of different prestressing forces, the bearing conditions, and to determine how early the panels can be post-tensioned. Eight panels of the same size as Stage I (3 ft x 6 ft) were tested for out-of-plane loading. The bearing conditions included plates as used in Stage I, and shelf angles which are commonly used in the current system of veneer construction at the wall-floor connection. Two different prestressing forces were used to study their effect on the behavior, and the post-tensioning was applied at the ages of 1 day and 5 days.

Eight 3 x 6 ft (9.15 x 1.83 m) panels were built in the laboratory by experienced masons using the same bricks and mortar mix as used in Stage I. Figure 4.20 shows a constructed panel for the Stage II testing. Three of the panels were post-tensioned at the age of 1 day and the remaining panels were post-tensioned 5 days after their construction. 12 x 3 5/8 x 1 in. (305 x 92 x 25 mm) steel plates were used for three of the specimens, and the remaining panels were post-tensioned with shelf angles of 4 x 4 x 3/8 in. (102 x 102 x 16 mm). In the following sections test panels are designated as TPII-P and TPII-A for plate and angle specimens respectively. They were air-dried in the laboratory until their testing. All the panels were grouted with hand-mixed grout just prior to the application of prestress. Table 4.10 gives the details of Stage II panels along with the parameters considered.

For brevity, the procedures for panel construction and post-tensioning are not discussed here as they were similar to those used in Stage I (Section 4.2.3). In this stage, the grouting was performed in a different and simpler manner. First, the

hand-mixed grout with a proportion of 1:1:1/10 (sand:cement:lime) by weight, was poured through a funnel into the cell containing the steel bar, and then the top angle and nuts are placed in position. Then the torque was applied immediately to post-tension the panels before the grout hardened. Figure 4.21 shows the grouting operation in progress prior to post-tensioning.

The testing procedure was also very similar to the Stage I tests. The deflections were monitored at top and bottom of the panel using LVDT and potentiometers. The panels were loaded with increments of 150–200 lb (670–890 N). Figure 4.22 shows a panel being tested. The panels were loaded up to failure to get the complete load-deflection curves. Test results are plotted and shown in Figure 4.23. The applied load is corrected to get the total load by adding self weight and other superimposed loads acting during the testing. Also the theoretical dead load deflection was added to the measured values.

4.4.2.2 ***Test Results.*** From Figure 4.23 it can be observed that all the panels behaved in a similar manner, but the ultimate loads and deflections varied slightly. The 16 kips panels withstood a lesser ultimate load with the exception of plate specimen TPII-P3. The load-deflections curves are very smooth even after cracking. The ultimate load ranged from 2,635 to 3,550 lb. The deflection observed was from 1.8 in. to 2.35 in. Similar to Stage I, a longitudinal crack at the center of the panel at ultimate load was observed in all the panels. The graph between the compressive strain measured using the Demec gage and the applied load is shown in Figure 4.24.

4.5 Prestress Losses

4.5.1 Construction and Monitoring of Panels

To study the losses using the proposed system, laboratory tests were conducted over a period of 6 months. The following sections describe the construction of test specimens, post-tensioning operation, prestress loss monitoring, and the results obtained. Eight panels of 3 x 4 ft (910 x 1,220 mm), similar to the flural test specimens, were built in the laboratory by experienced masons. The new two-cored bricks were used along with Type N mortar. Figure 4.25 shows a typical test specimen.

The panels were post-tensioned between 7–9 days after construction. Grout was prepared using a proportion of 1:1/10:3 (Portland cement : Type S lime : sand) and water was added to the mixture until a flowable mix was obtained (water/cement ratio = 0.8). The hand-mixed grout was poured into the core before the top

plate/angle was placed. The panels were then post-tensioned by applying torque using a wrench. One 5/8 in. (16 mm) diameter high-strength (120 ksi) threaded rod was used as prestressing reinforcement in each panel. Table 4.11 gives the details of the test specimens.

Stresses in the steel were recorded from three strain gages attached to the bars using a data-acquisition system. Strain in the masonry was measured using a Demec gage (gage length = 8 in.). Demec locator pins were glued to the masonry surface at different locations on the panels as shown in Figure 4.26 and in Table 4.12. All panels were continuously monitored for a period of 30 days after post-tensioning inside the laboratory. Three of the test specimens were moved out of the laboratory after 30 days of post-tensioning to expose them to normal weather conditions (see Table 4.12). The readings of the strain gages and the strain in the masonry were recorded at closer intervals in the first 90 days and then the interval was increased. The maximum and minimum temperature and humidity were recorded each day.

4.5.2 Recorded Data

The following section shows the data obtained from monitoring the panels for a period of over 180 days after the post-tensioning. The temperature and humidity variation is shown in Figure 4.27. The observed masonry strain readings and steel strains are plotted with time in Figures 4.28 through 4.43. Some Demec locator pins were detached and further readings could not be taken at those locations. Some strain gages also stopped working. The graphs show all the actual readings recorded from each panel.

Dikkers and Yokel [1970] tested unreinforced brick wall panels, 4 x 8 ft, by applying uniform transverse loads, uniform axial compressive loads, or a combination of both types of loading. Test results were used to develop analytical procedures for predicting the strength of the walls subjected to axial compression and bending. The 8 ft tall brick walls behaved as slender walls with reduced moment capacity due to slenderness effects. The load capacity of the brick walls tested was closely predicted by the moment magnifier method and theoretical slenderness effects.

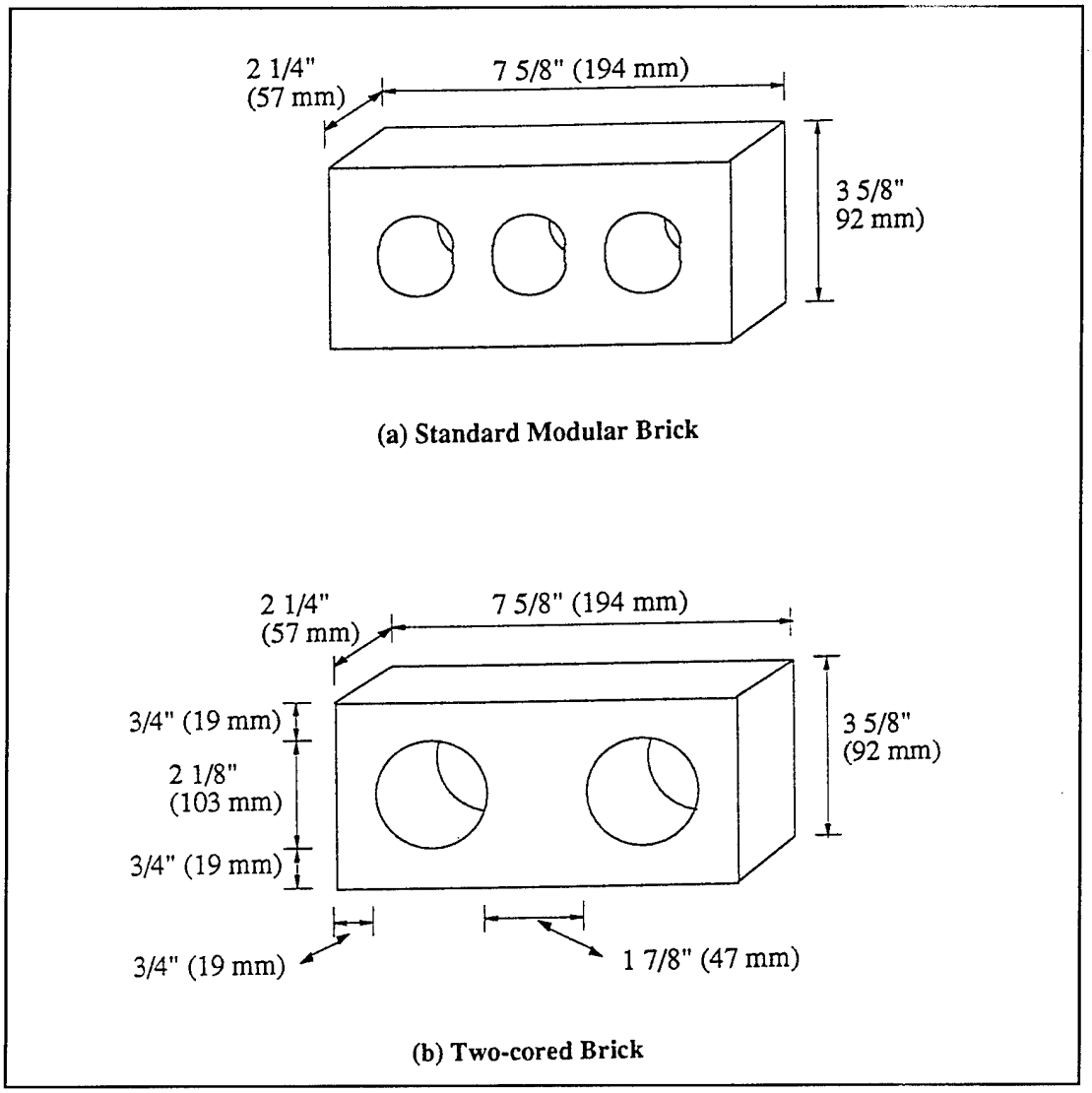

Figure 4.1. Standard and two-cored brick design diagrams.

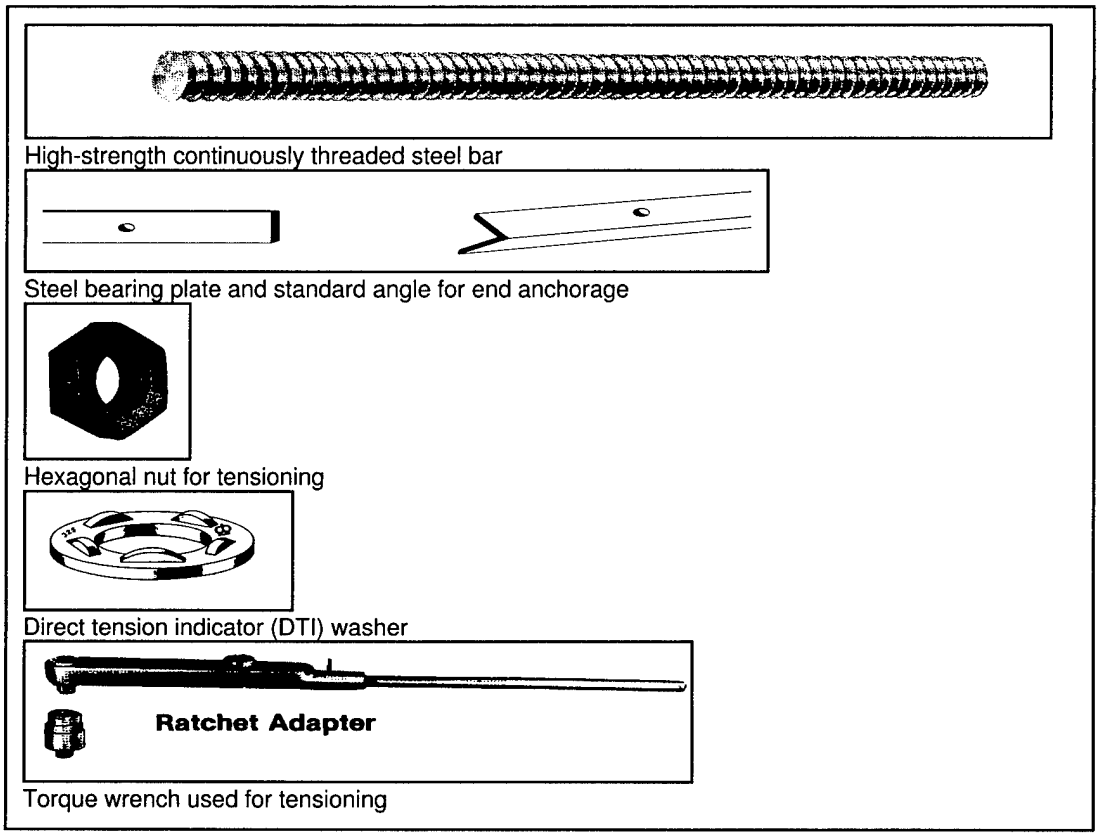

Figure 4.2. Components of post-tensioning technology for the proposed system.

Table 4.1. Laboratory test results on brick units.

Test (Five specimens used)	Experimental Value	Plant Certified Value	ASTM Requirements Average of 5 Individual	
Compressive strength, psi (MPa)	9,360 (64.5)	9,850 (67.9)	> 3,000 (20.7)	> 2,500 (17.2)
Modulus of rupture, psi (MPa)	800 (5.5)	669 (4.6)[1]	NA	NA
Absorption 24 hr. cold water (%)	5.70	5.00	< 8.00	< 10.0
Absorption 5 hr. boiling water (%)	7.93	6.30	< 17.0	< 20.0
Saturation coefficient[2]	0.72	0.79	< 0.78	< 0.80

[1] for standard modular brick
[2] waived if cold water absorption requirements are met

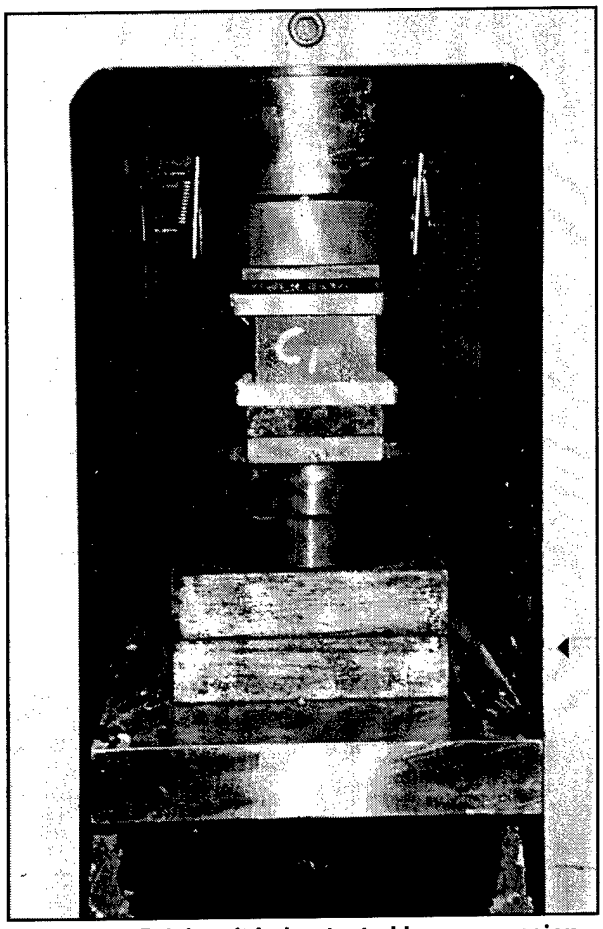

Figure 4.3. Brick unit being tested in compression.

Table 4.2. Compression tests on mortar cubes.

Testing Stage	Number of Days Cured	Number of Cubes Tested	Avg. Max. Stress psi (MPa)
Stage I panels	41	3	1,350 (9.30)
	28	3	2,190 (15.1)
	312 -383	6	2,390 (16.5)
Stage II panels	51	3	1,665 (11.5)
	302	6	2,023 (14.0)
	343	3	2,083 (14.4)
Prestress loss panels	81	3	1,495 (10.3)
	28	3	2,350 (16.2)
	60	3	2,140 (14.8)

[1] average day of post-tensioning
[2-3] begin to end of panel testing

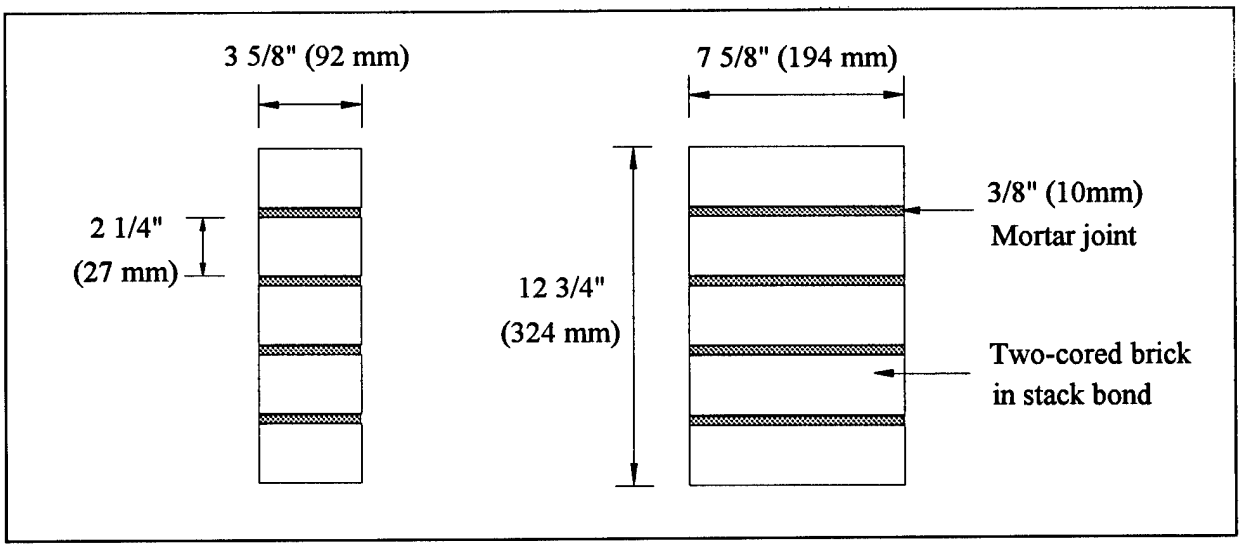

Figure 4.4. Sketch of masonry prism with dimensions.

Figure 4.5. A failed prism specimen in compression.

Table 4.3. Compression tests on masonry prisms (Stage 1)

Specimen Designation	Number of Days Cured	Stress at First Cracking psi (MPa)	Avg. Max. Stress psi (MPa)	Avg. Max. Stress psi (MPa)
SI-C04-1	4	-	2,270 (15.7)	2,225 (15.4)
SI-C04-2	4	-	2,080 (14.3)	
SI-C04-3	4	-	2,330 (16.1)	
SI-C28-2	28	1,880 (13.0)	2,290 (15.8)	2,845 (19.6)
SI-C28-3	28	2,030 (14.0)	2,580 (17.8)	
SI-CM28-1	28	3,220 (22.2)	3,480 (24.0)	
SI-CM28-2	28	2,460 (18.2)	3,340 (23.1)	
SI-C33-5	33	2,480 (17.1)	2,870 (19.8)	
SI-C33-6	33	2,710 (18.7)	2,890 (19.9)	
SI-C33-7	33	2,390 (16.5)	2,550 (17.6)	
SI-C33-9	33	2,100 (14.5)	2,740 (18.9)	
SI-C33-10	33	1,990 (13.7)	2,410 (16.6)	
SI-CM33-4	33	2,290 (15.8)	3,610 (24.9)	
SI-CM33-5	33	2,310 (15.9)	2,510 (17.3)	

Table 4.4. Compression tests on masonry prisms (Stage II).

Specimen Designation	Number of Days Cured	Stress at First Cracking psi (MPa)	Avg. Max. Stress psi (MPa)	Avg. Max. Stress psi (MPa)
SII-C01-1	1	1,955 (13.5)	2,020 (13.9)	2,145 (14.8)
SII-C01-2	1	1,880 (13.0)	2,215 (15.3)	
SII-C01-3	1	1,845 (12.7)	2,195 (15.1)	
SII-CM6-11	6	3,435 (23.7)	3,800 (26.2)	3,205 (22.1)
SII-CM6-21	6	2,930 (20.2)	3,225 (22.6)	
SII-CM6-31	6	2,370 (16.3)	2,590 (17.7)	
SII-C6-4	6	3,400 (23.5)	3,435 (23.7)	
SII-C6-5	6	2,640 (18.2)	3,010 (20.8)	
SII-C6-6	6	3,075 (21.2)	3,155 (21.8)	
SII-CM30-11	30	3,185 (22.0)	3,770 (26.0)	3,430 (23.7)
SII-CM30-21	30	2,785 (19.2)	3,395 (23.4)	
SII-CM30-31	30	3,235 (22.3)	3,235 (22.3)	
SII-CM30-41	30	3,200 (22.1)	3,400 (23.5)	
SII-CM30-51	30	2,785 (19.2)	3,345 (23.1)	
SII-CM34-11	34	3,905 (26.9)	4,160 (28.7)2	4,125 (28.5)
SII-CM34-21	34	3,230 (23.0)	4,180 (28.8)2	
SII-CM34-31	34	3,980 (27.5)	4,040 (27.9)	

[1] specimen also used for modulus of elasticity test
[2] loading stopped at the capacity of the machine

Table 4.5. Compression tests on masonry prisms (prestress loss panels).

Specimen Designation	Number of Days Cured	Stress at First Cracking psi (MPa)	Max. Stress psi (MPa)	Avg. Max. Stress psi (MPa)
PLC-1	8	-	2,925 (20.2)	2,975 (20.5)
PLC-2	8	-	3,510 (24.2)	
PLC-3	8	-	3,045 (21.0)	
PLMC-11	8	2,570 (17.7)	2,820 (19.5)	
PLMC-21	8	-	2,310 (15.9)	
PLMC-31	8	-	3,255 (22.5)	
PLC-4	28	-	3,910 (26.9)2	3,600 (24.8)
PLC-5	28	2,315 (15.7)	3,385 (23.3)	
PLC-6	28	-	3,980 (27.5)2	
PLC-7	28	-	3,430 (23.7)	
PLMC-41	28	3,040 (21.0)	3,270 (22.6)	
PLMC-51	28	-	3,655 (25.2)	
PLMC-61	28	2,570 (17.7)	3,595 (24.8)	
PLC-8	60	2,725 (18.7)	3,365 (23.2)	3,750 (25.9)
PLC-9	60	3,110 (21.5)	3,905 (27.0)	
PLP-10	60	3,690 (25.4)	3,980 (27.4)	
PLP-11	95	-	3,740 (25.8)	3,800 (26.2)
PLC-12	95	3,475 (24.0)	3,670 (25.3)	
PLC-13	95	-	3,980 (27.5)2	

[1] specimen also used for modulus of elasticity test
[2] loading stopped at the capacity of the machine not recorded or distinguished

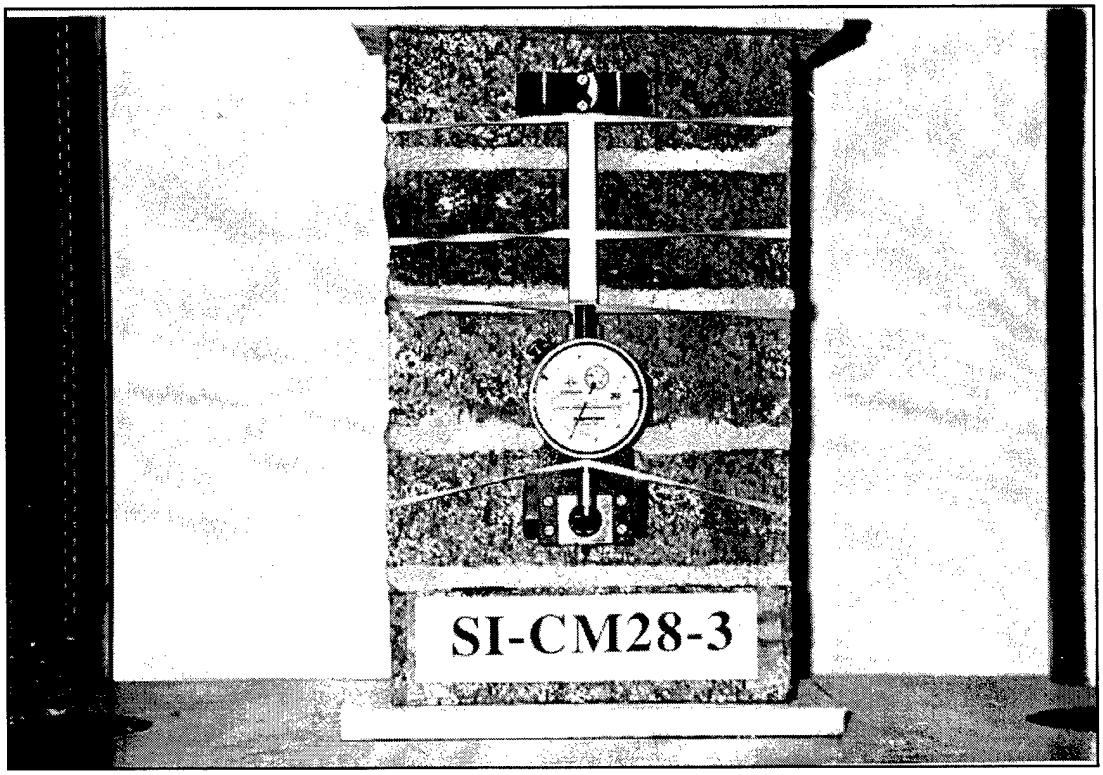

Figure 4.6. Masonry prism fitted with Demec gage for modulus of elasticity test.

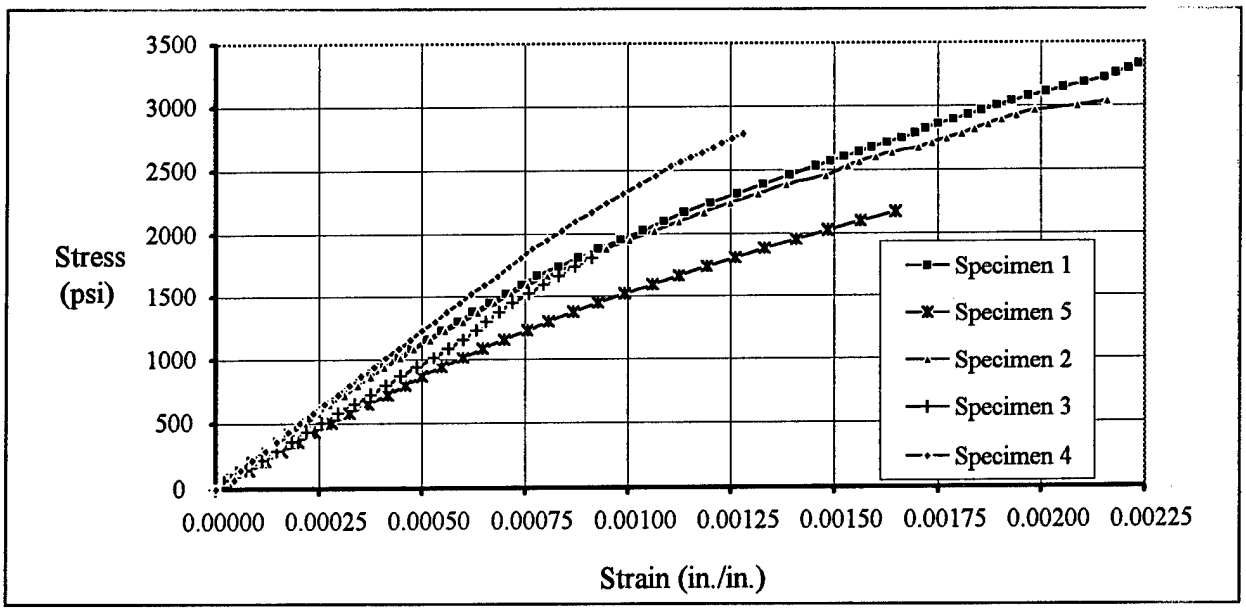

Figure 4.7. Stress-strain curves for Stage I masonry specimens.

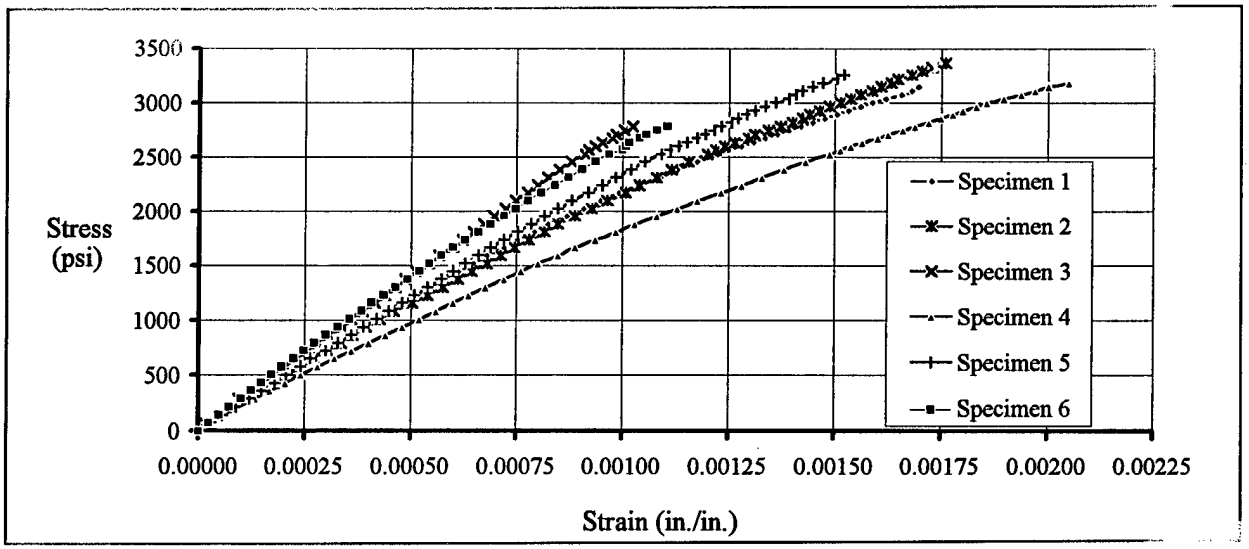

Figure 4.8. Stress-strain curves for Stage II masonry specimens.

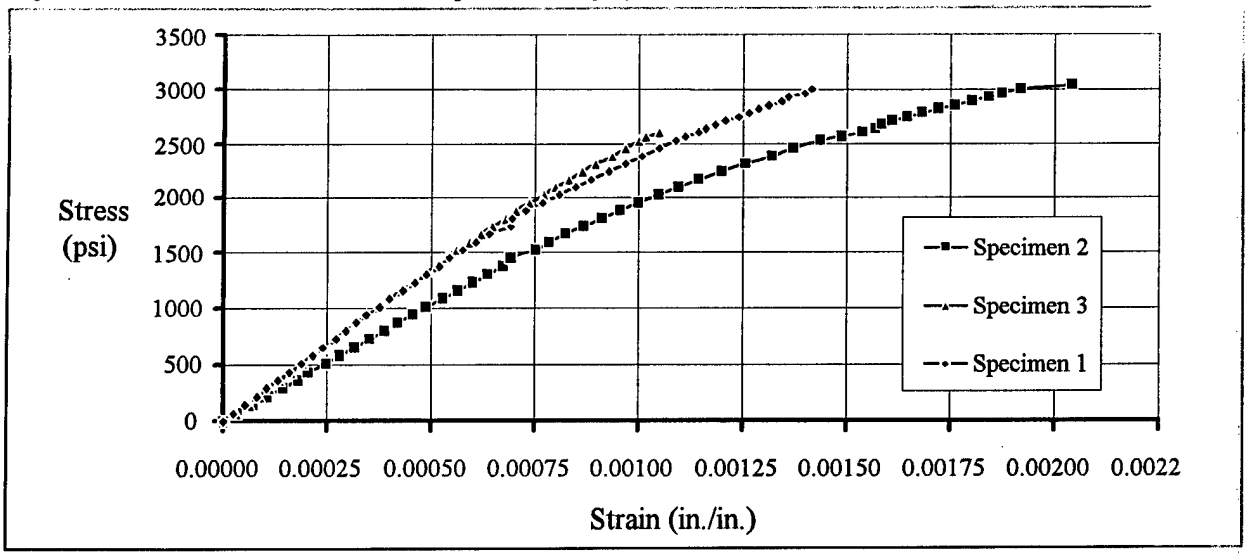

Figure 4.9. Stress-strain curves for prestress loss study specimens.

Table 4.6. Modulus of elasticity tests on masonry prisms.

Stage	Number of specimens	Average Compressive Strength, psi (MPa)	Modulus of Elasticity, psi (MPa)	Equivalent Compressive Strength
Stage I	5	2,845 (19.6)	2.162 × 106 (14,900)	760 f'_m
Stage II	6	3,430 (23.7)	2.401 × 106 (16,560)	700 f'_m
Prestress Loss	3	3,600 (24.8)	2.486 × 106 (17,145)	690 f'_m

Table 4.7. Prestressing steel test results.

Specimen Number	Gage Length (in.)	Yield Strength[1] psi (MPa)	Ultimate Tensile Strength psi (MPa)
G1-1	2 3/8		132,080 (910.9)
G1-2	2 3/16		132,080 (910.9)
G1-3	2 7/16		131,860 (909.4)
G1-4	2 9/16		131,195 (904.8)
G2-1	14 11/16	105,000 (724.0)	129,690 (894.4)
G2-2	14 11/16	102,000 (703.5)	125,485 (865.4)
G2-3	15 1/16	110,000 (758.6)	128,550 (886.6)
G2-4	15 3/16	110,000 (758.6)	125,240 (7)

[1] 0.2 percent offset method

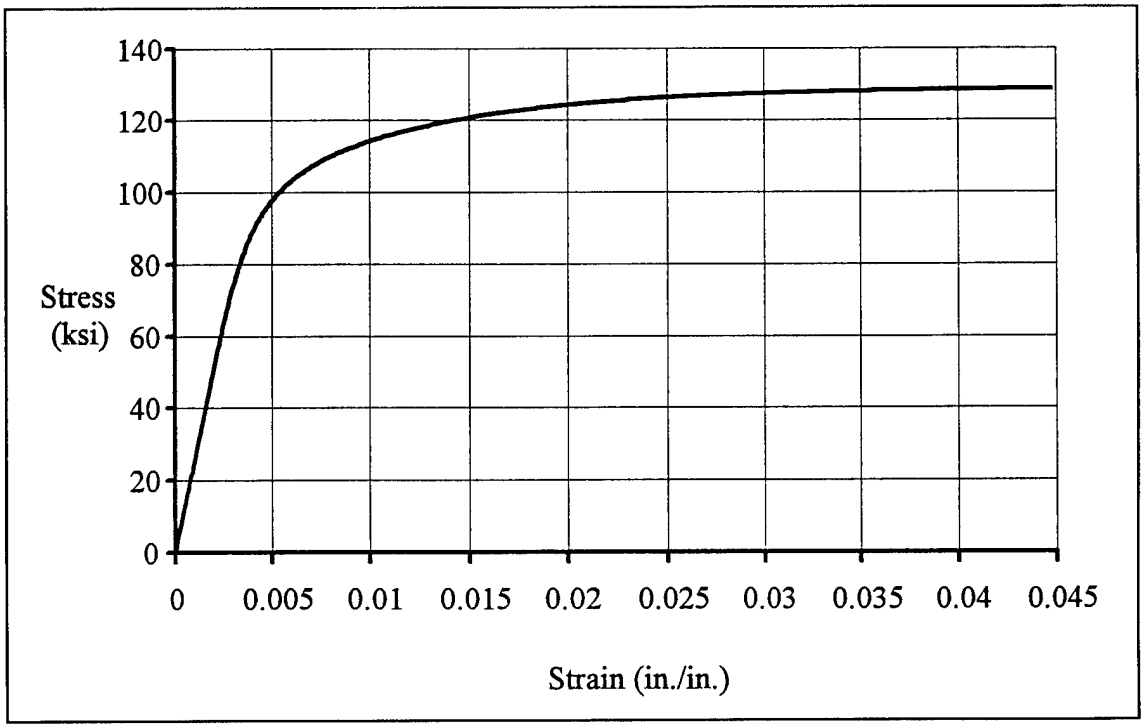

Figure 4.10. Stress-strain relation for post-tensioning steel.

Table 4.8. Direct tension indicator washer test results.

Number of Samples Tested	Average Crushing Load [lb (kN)]	Standard Deviation lb (kN)
48	19,043 (84.7)	591.8 (2.63)

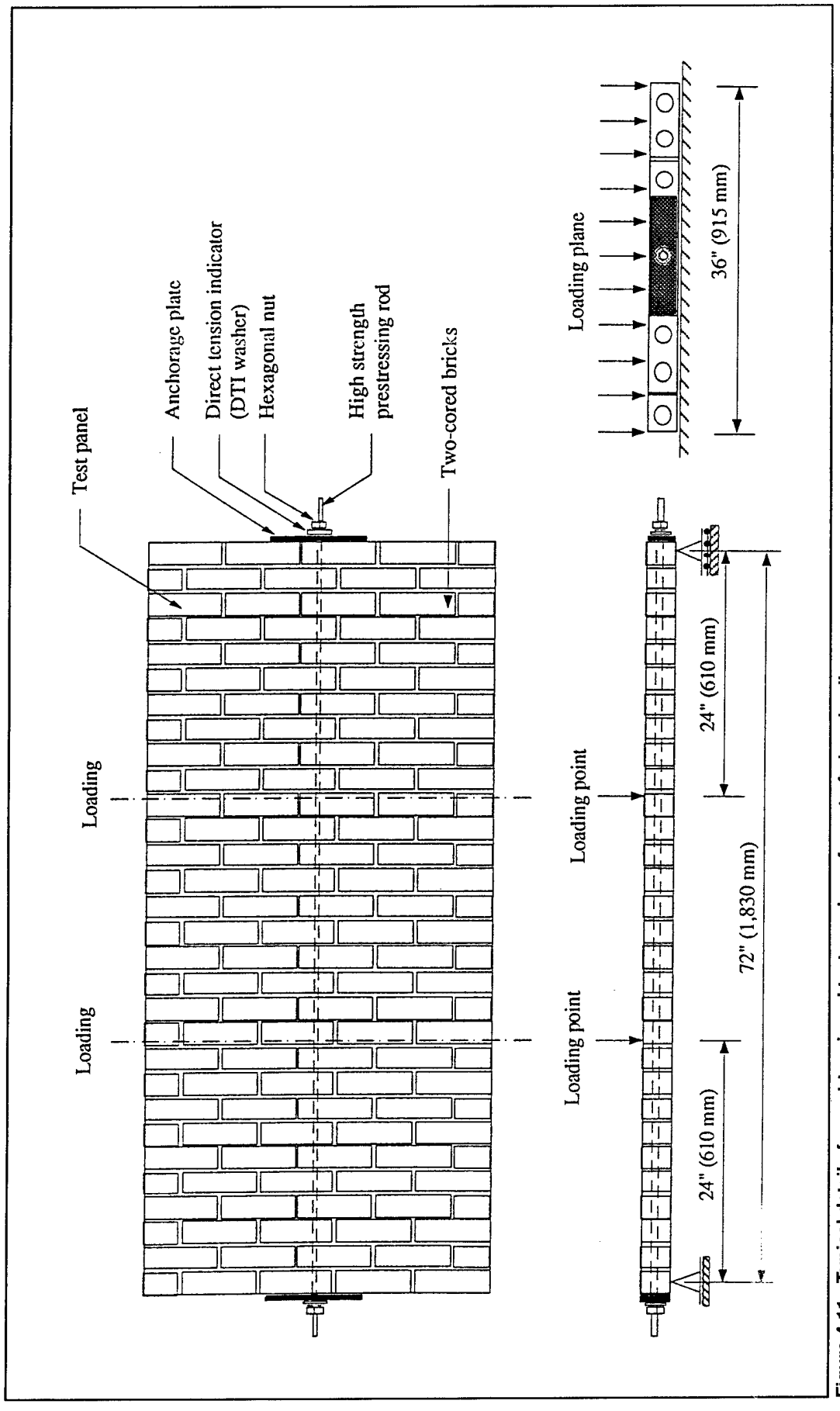

Figure 4.11. Typical detail of a post-tensioned test specimen for out-of-plane loading.

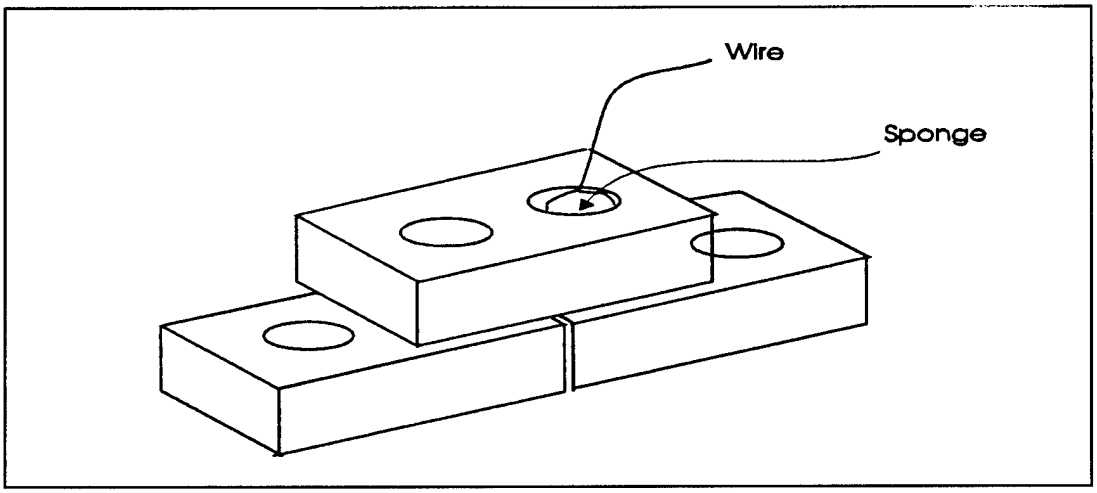

Figure 4.12. Blocking the core using a wet sponge.

Figure 4.13. Post-tensioning operation in progress.

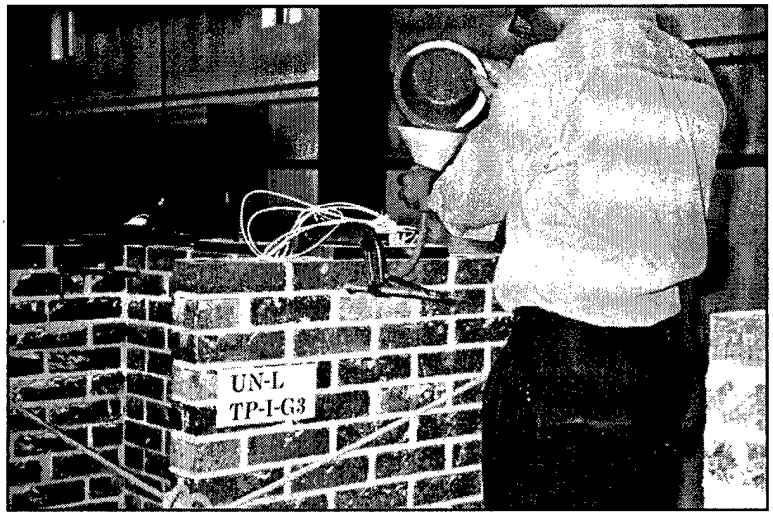

Figure 4.14. Grouting the panel after post-tensioning.

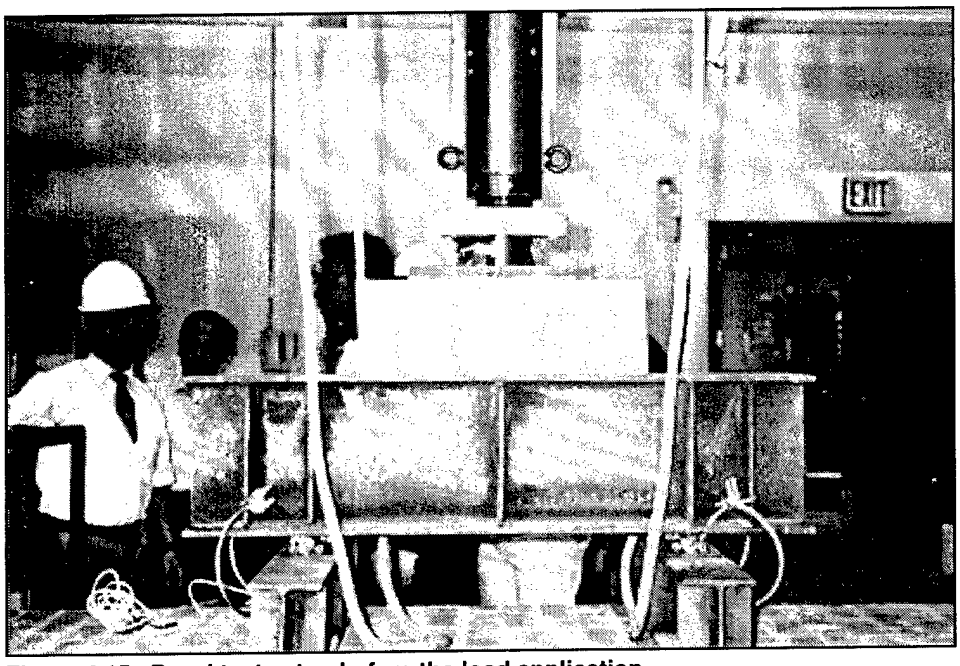

Figure 4.15. Panel test setup before the load application.

Table 4.9. Moments and midspan deflections of test specimens.

Specimen Designation	Load at Cracking Moment lb (kN)	Load at Ultimate Moment Capacity lb (kN)	Deflection at Maximum Capacity in. (mm)	Deflection at Failure Load in. (mm)
TPIUG1	1,230	2,050 (9.1)	0.26 (6.6)	2.50 (63.5)
TPIUG2	1,145	2,220 (9.9)	0.70 (17.8)	2.10 (53.3)
TPIUG3	1,000	1,940 (8.6)	0.70 (17.8)	3.00 (76.2)
TPIG1	1,050	3,770 (16.8)	1.10 (27.9)	2.25 (57.2)
TPIG2	1,200	3,690 (16.4)	1.55 (39.4)	2.60 (66.0)
TPIG3	1,200	3,720 (16.5)	1.22 (3.1)	2.25 (57.2)

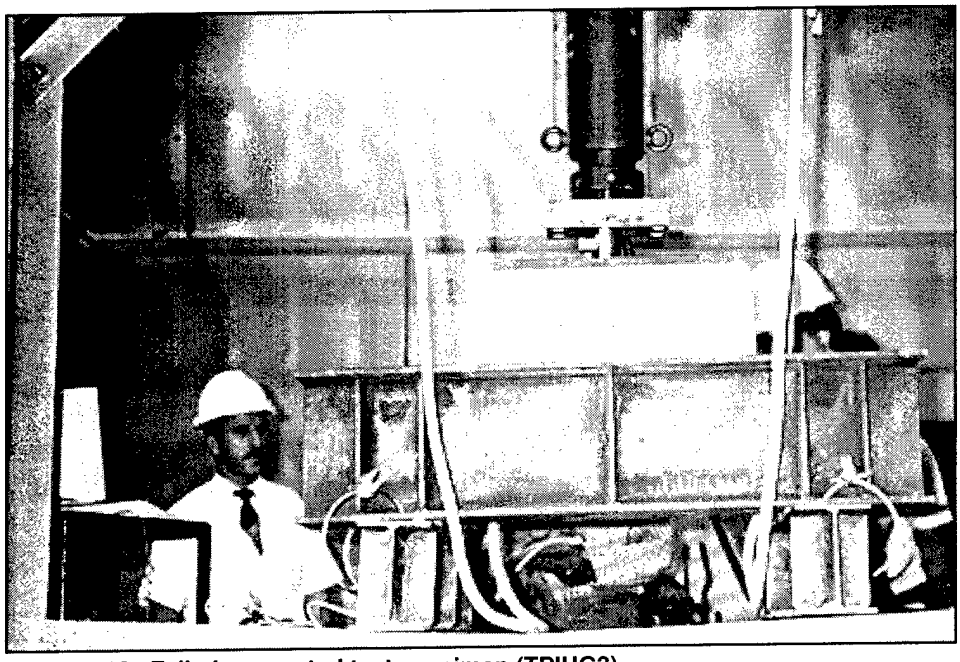

Figure 4.16. Failed ungrouted test specimen (TPIUG3).

Figure 4.17. Failed grouted test specimen (TPIG1).

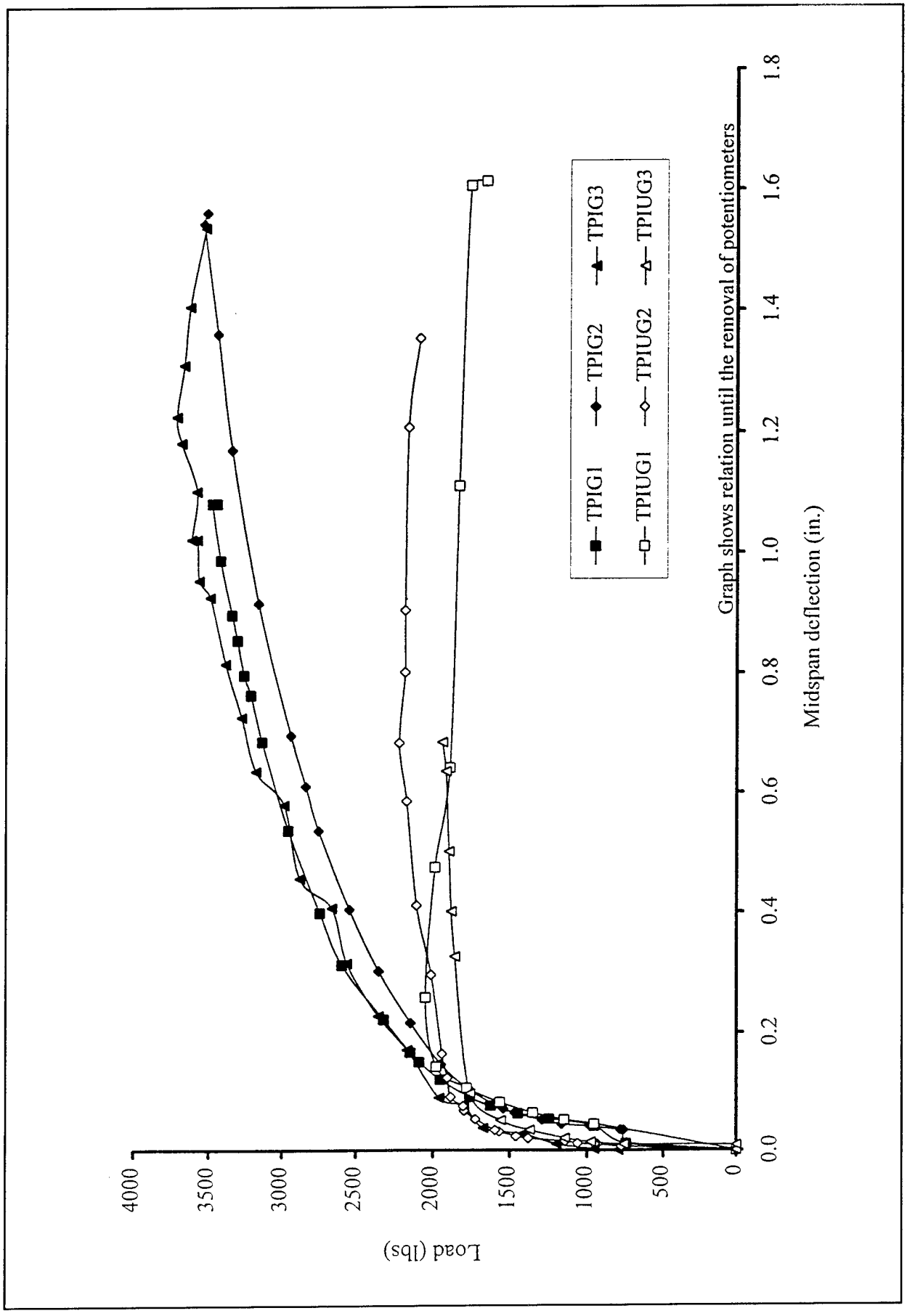

Figure 4.18. Load-deflection curves for Stage I test specimens.

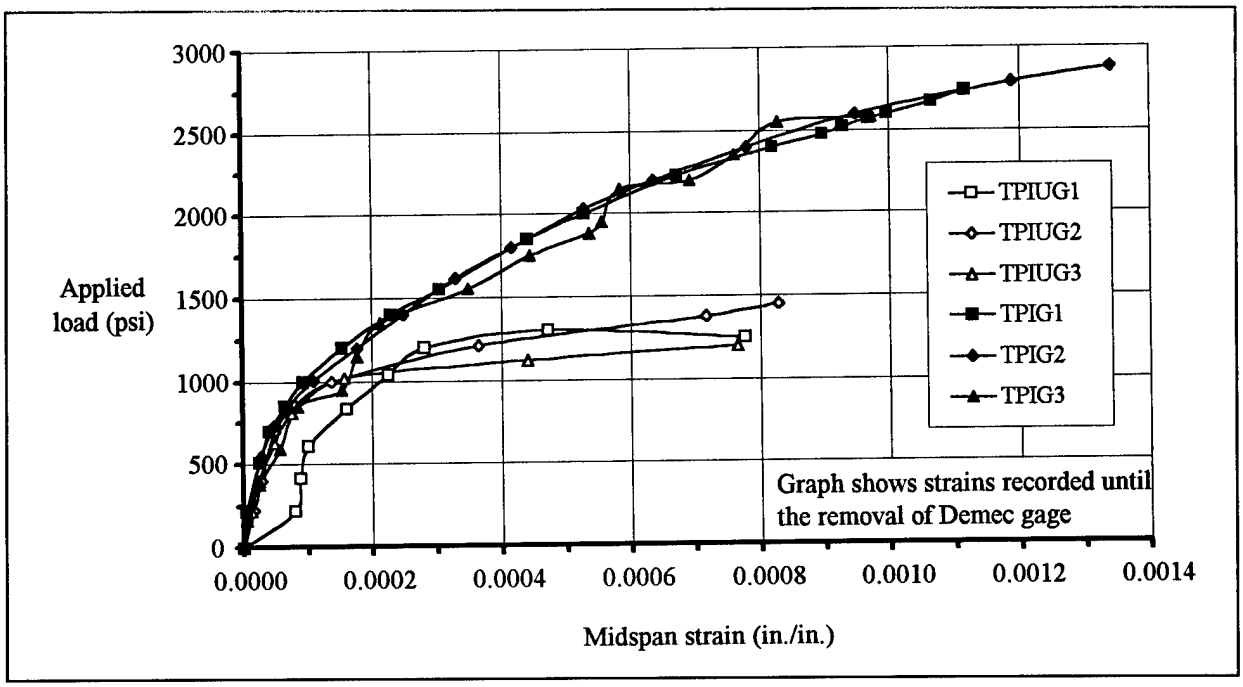

Figure 4.19. Applied load versus compressive strain of Stage I test specimens.

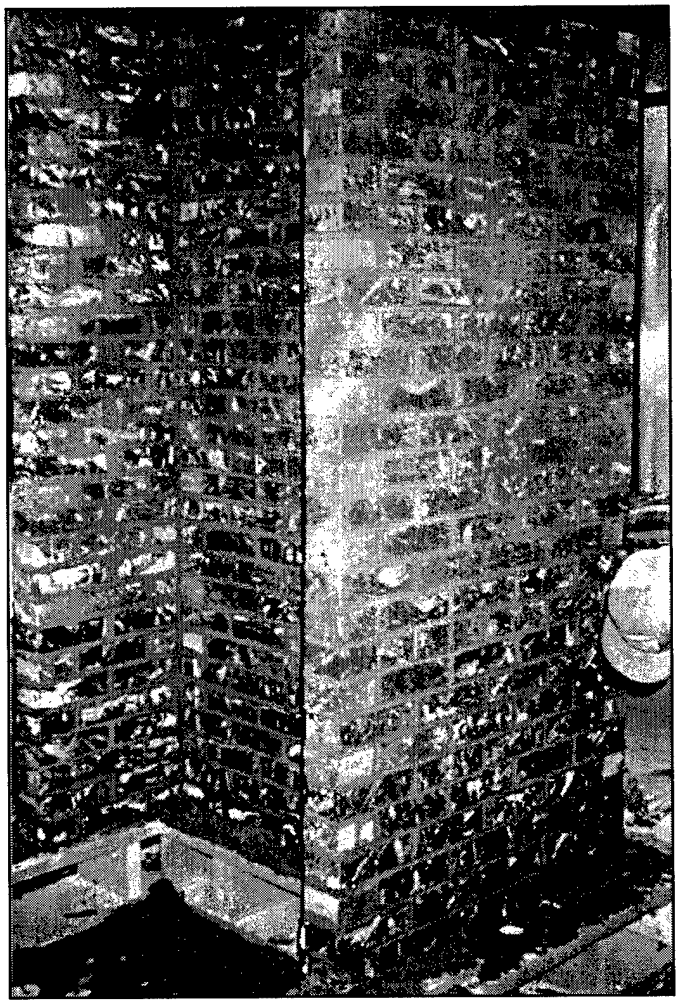

Figure 4.20. A constructed panel for Stage II testing.

Table 4.10. Details of Stage II panels.

Panel Designation	Age at Post-tensioning	End Bearing Condition	Prestressing Force kips (kN)
TPII-A1	1	Angle	19 (84.5)
TPII-A2	1	Angle	19 (84.5)
TPII-P1	1	Plate	19 (84.5)
TPII-A3	5	Angle	16 (71.2)
TPII-A4	5	Angle	16 (71.2)
TPII-P2	5	Plate	16 (71.2)
TPII-P3	5	Plate	16 (71.2)
TPII-A5	5	Angle	19 (84.5)

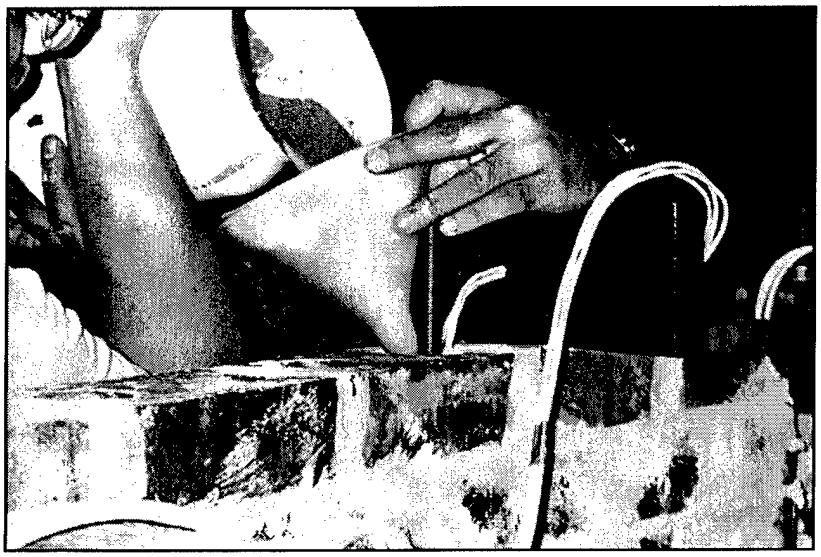

Figure 4.21. Grouting of a Stage II panel in operation.

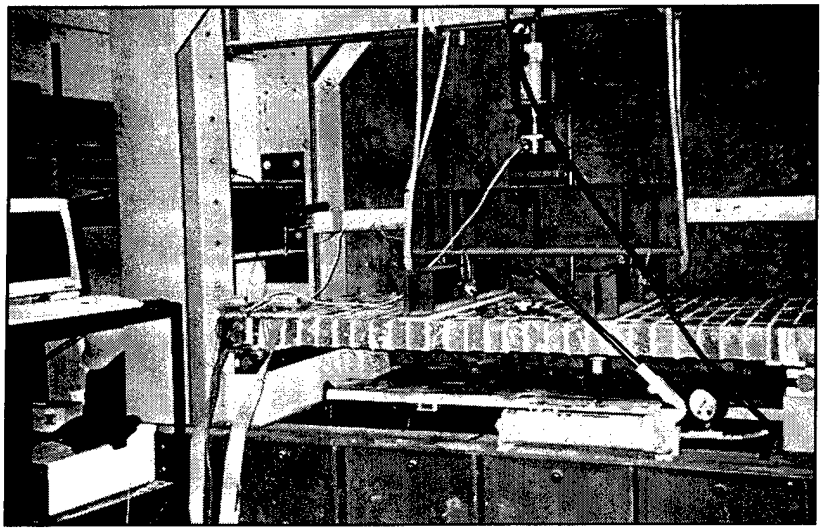

Figure 4.22. Test setup for Stage II testing.

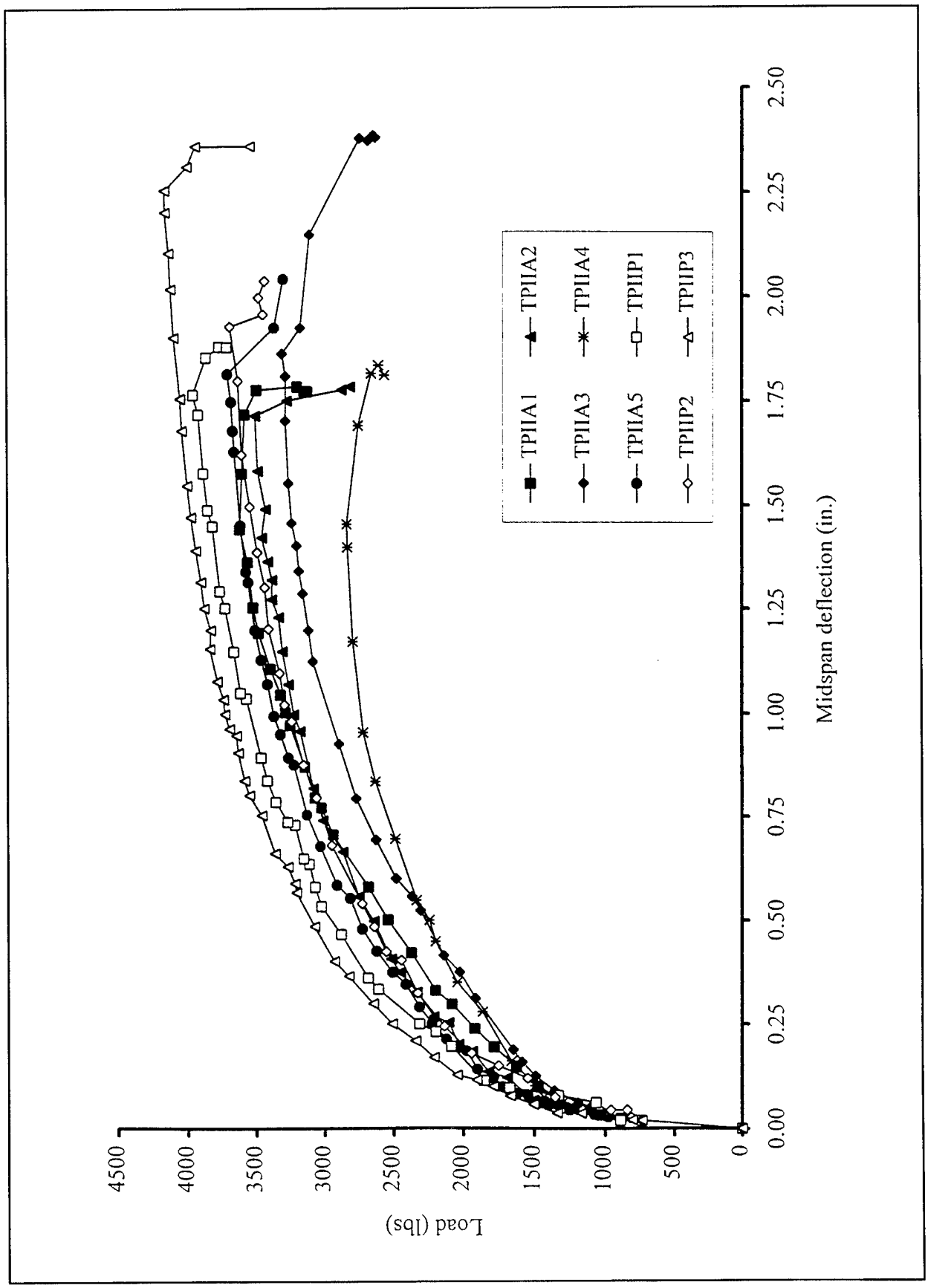

Figure 4.23. Load-deflection curves for Stage II test specimens.

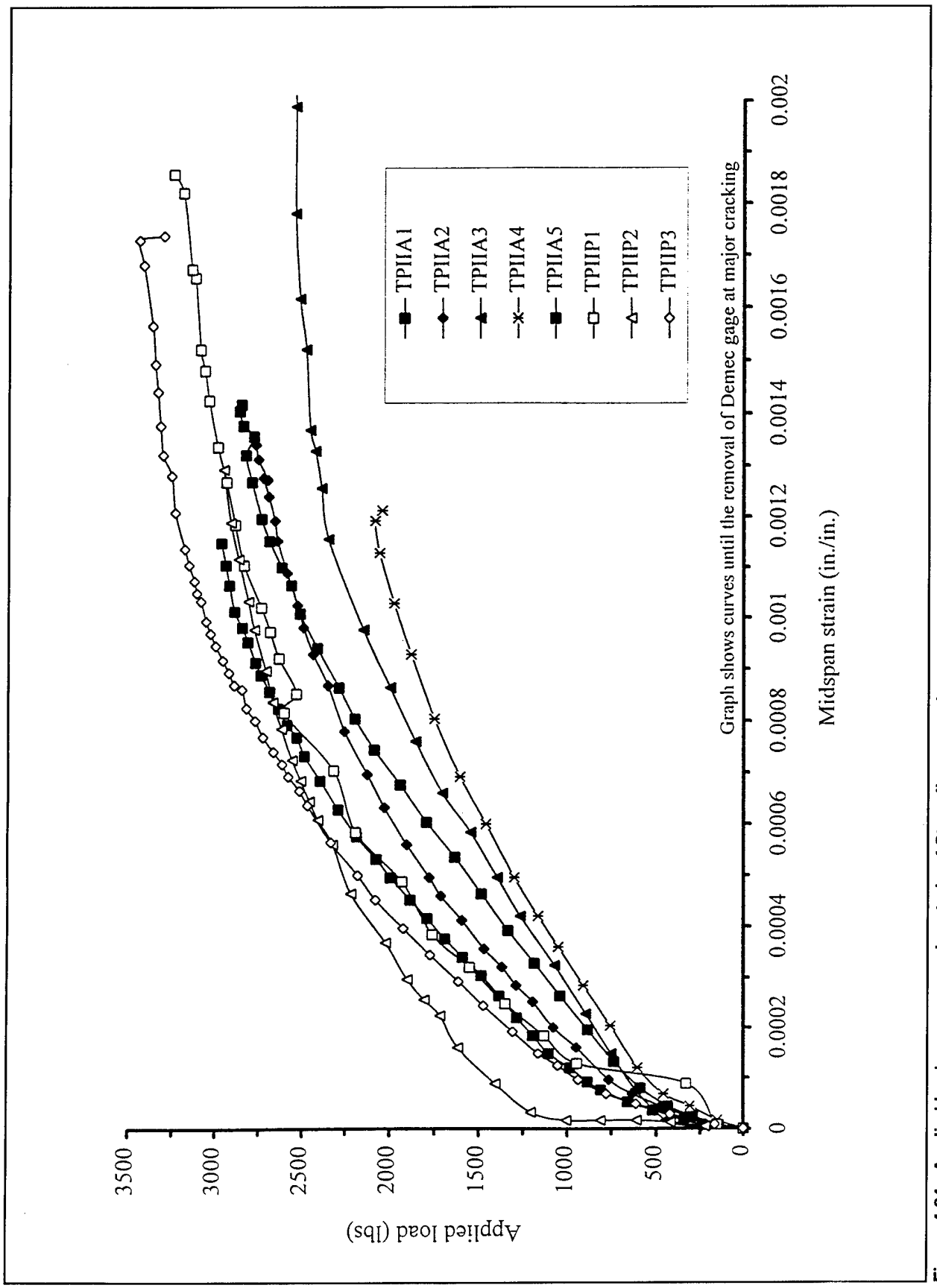

Figure 4.24. Applied load vs. compressive strain of Stage II test specimens.

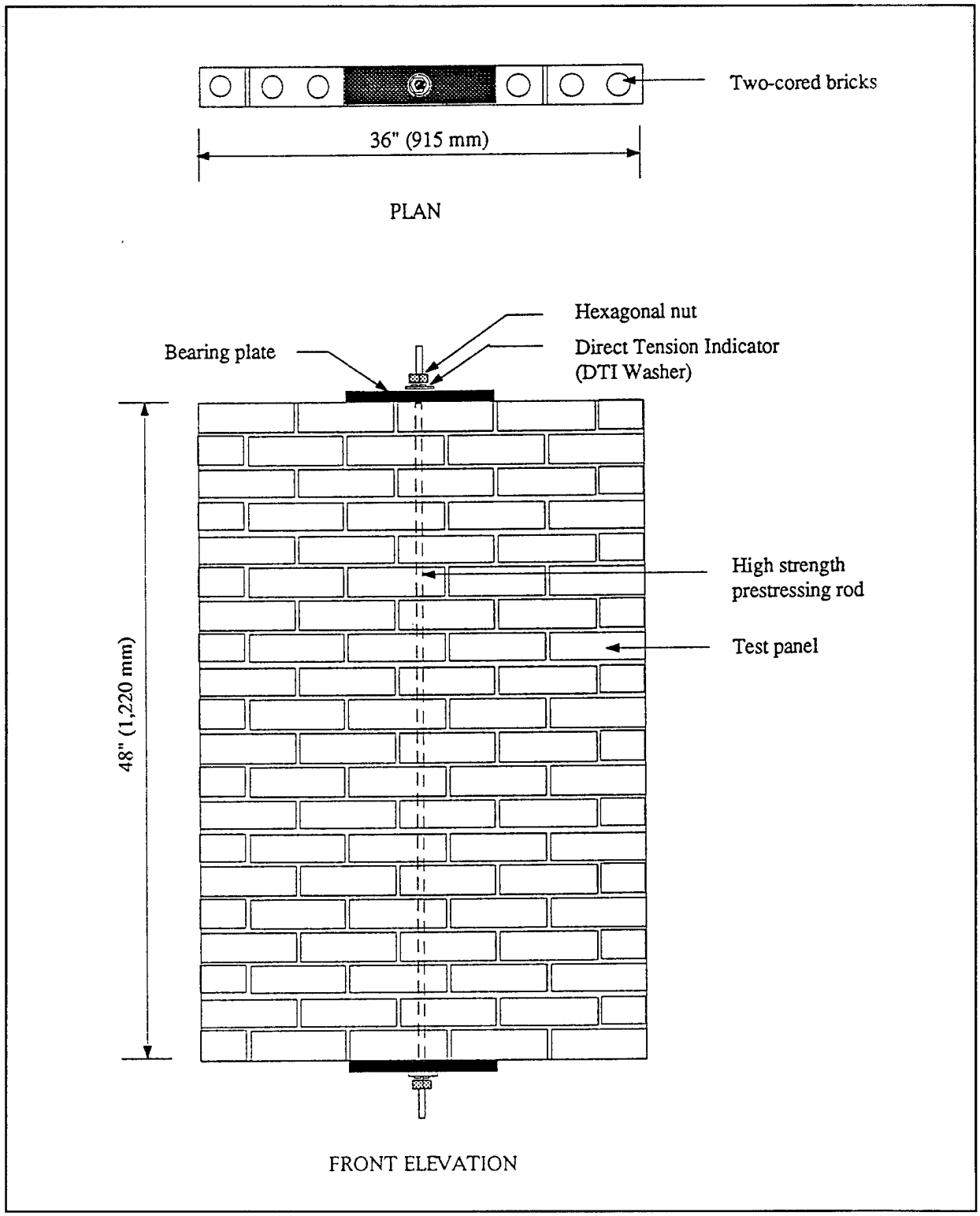

Figure 4.25. Typical details of test panel for prestress loss study.

Table 4.11. Description of test specimens.

Panel Designation	Dimension (in.)	Prestressing Force (lb)	End Bearing Condition
PLP-1	36 x 48	19,000	12 x 3 5/8 x 1 in. Plate
PLP-2	36 x 48	19,000	12 x 3 5/8 x 1 in. Plate
PLA-1	36 x 48	19,000	4 x 4 x 3/8 in. - 36 in. long Angle
PLA-2	36 x 48	19,000	4 x 4 x 3/8 in. - 36 in. long Angle
PLA-3	36 x 48	19,000	4 x 4 x 3/8 in. - 36 in. long Angle
PLA-4	36 x 48	16,000	4 x 4 x 3/8 in. - 36 in. long Angle
PLA-5	36 x 48	16,000	4 x 4 x 3/8 in. - 36 in. long Angle
PLA-6	36 x 48	16,000	4 x 4 x 3/8 in. - 36 in. long Angle

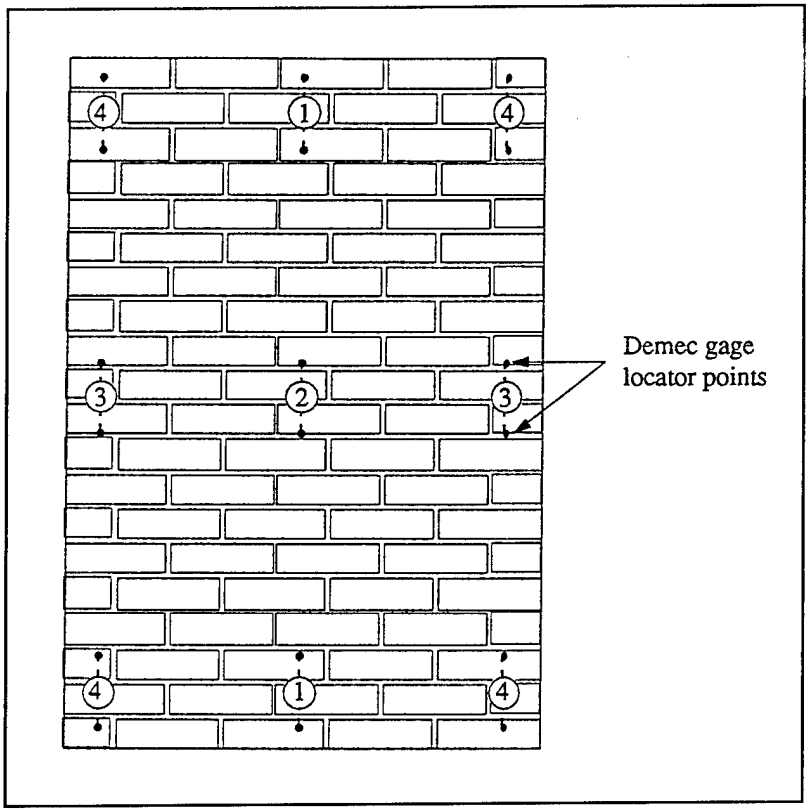

Figure 4.26. Locations of masonry strain measurement.

Table 4.12. Parameters of test specimens.

Panel Designation	Number of Strain Gages	Positions of Strain Measurement[1]	Exposure Condition (Days After Post-Tensioning)
PLP-1	3	1, 3, 5, & 7	laboratory environment
PLP-2	3	2, 4, 5, & 7	0 - 33 inside the laboratory 33 - 180 outside weather
PLA-1	3	3, 4, 5, & 7	laboratory environment
PLA-2	3	1, 3, 6, & 8	0 - 33 inside the laboratory 33 - 180 outside weather
PLA-3	3	5, 7, 10, & 12	laboratory environment
PLA-4	3	6, 8, 9, & 11	0 - 31 inside the laboratory 31 - 180 outside weather
PLA-5	3	1, 5, 7, & 12	laboratory environment
PLA-6	3	4, 6, 7, & 9	laboratory environment

[1] see Fig. 4.21 for Demec point locations

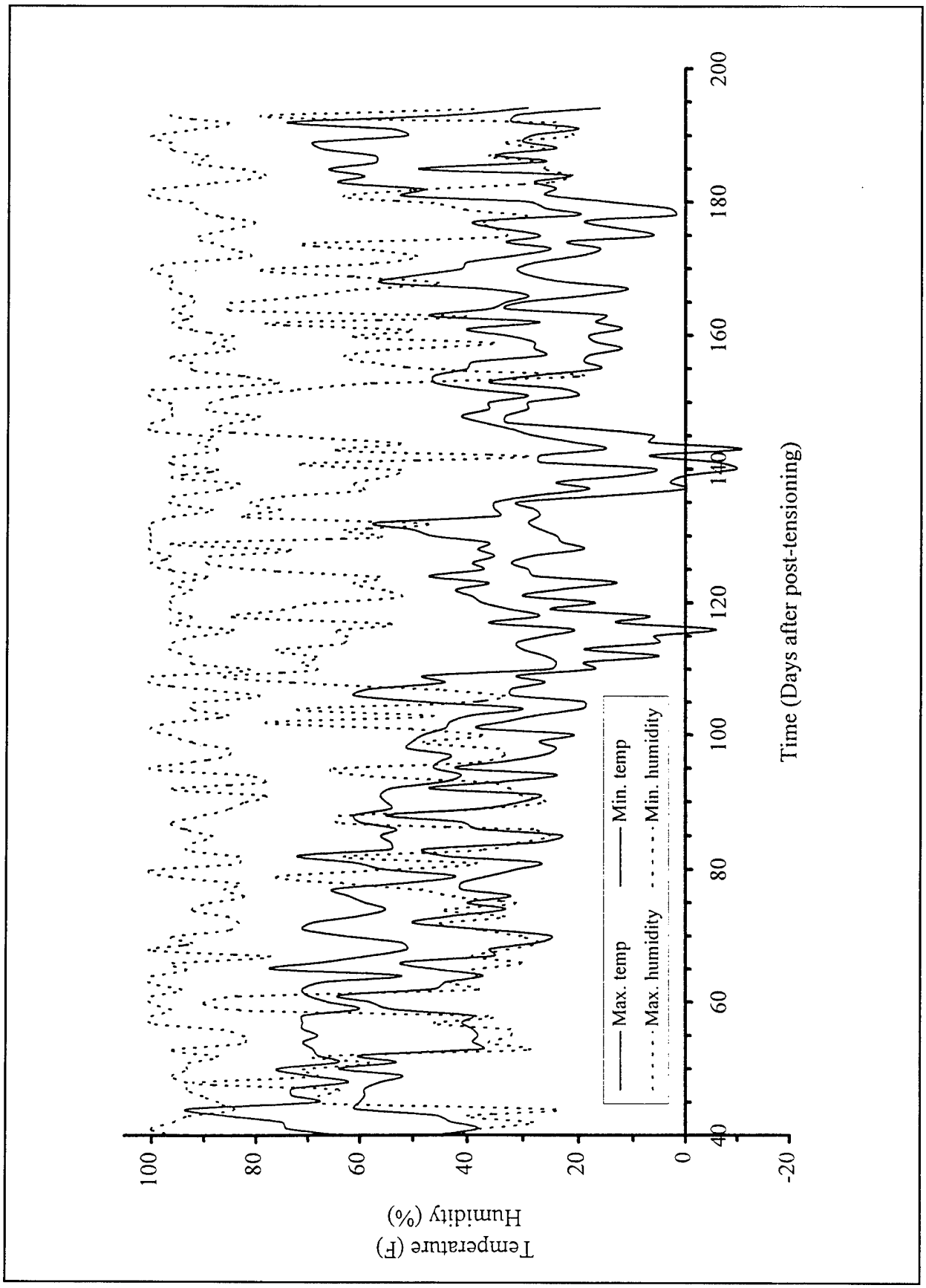

Figure 4.27. Variation of temperature and humidity with time.

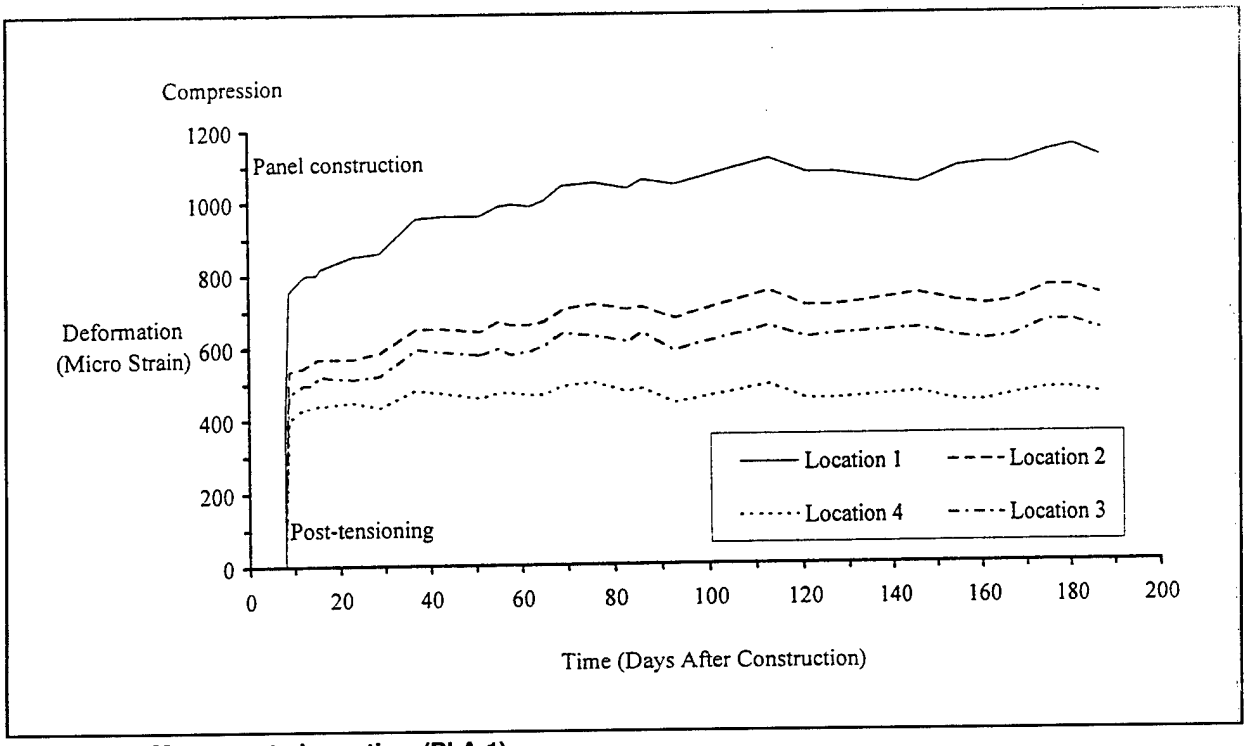

Figure 4.28. Masonry strain vs. time (PLA-1).

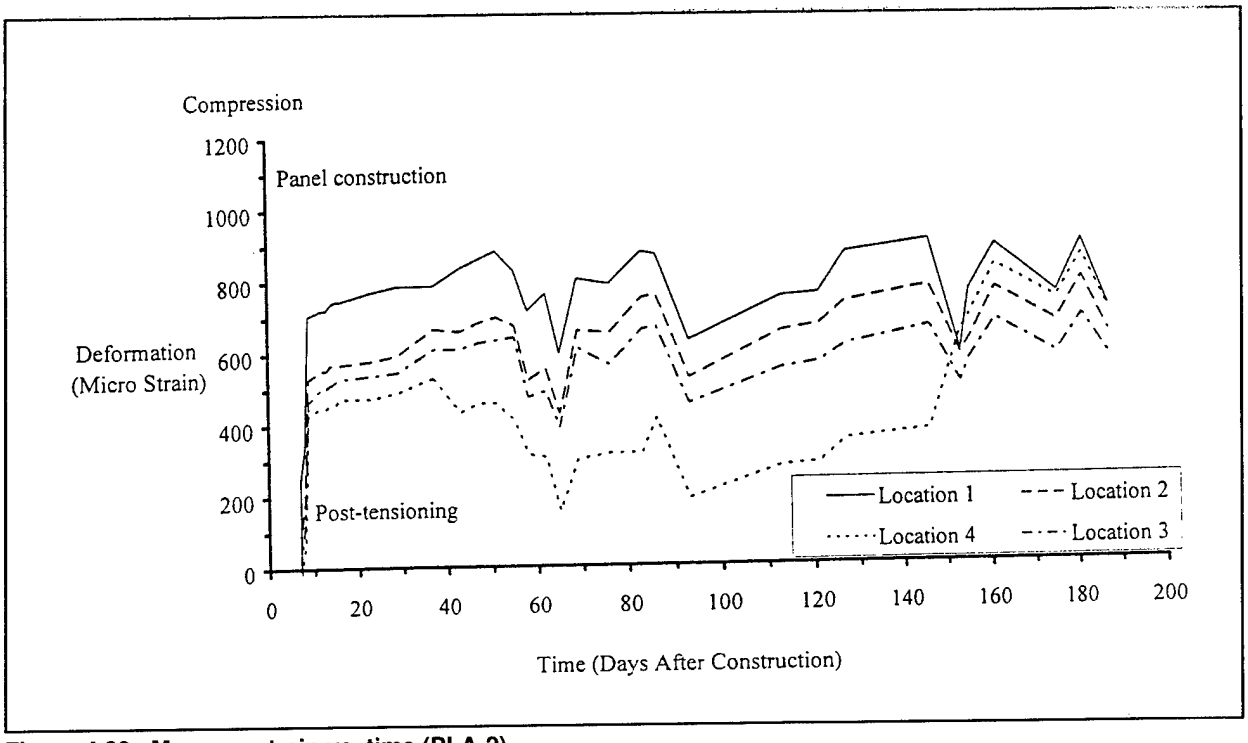

Figure 4.29. Masonry strain vs. time (PLA-2).

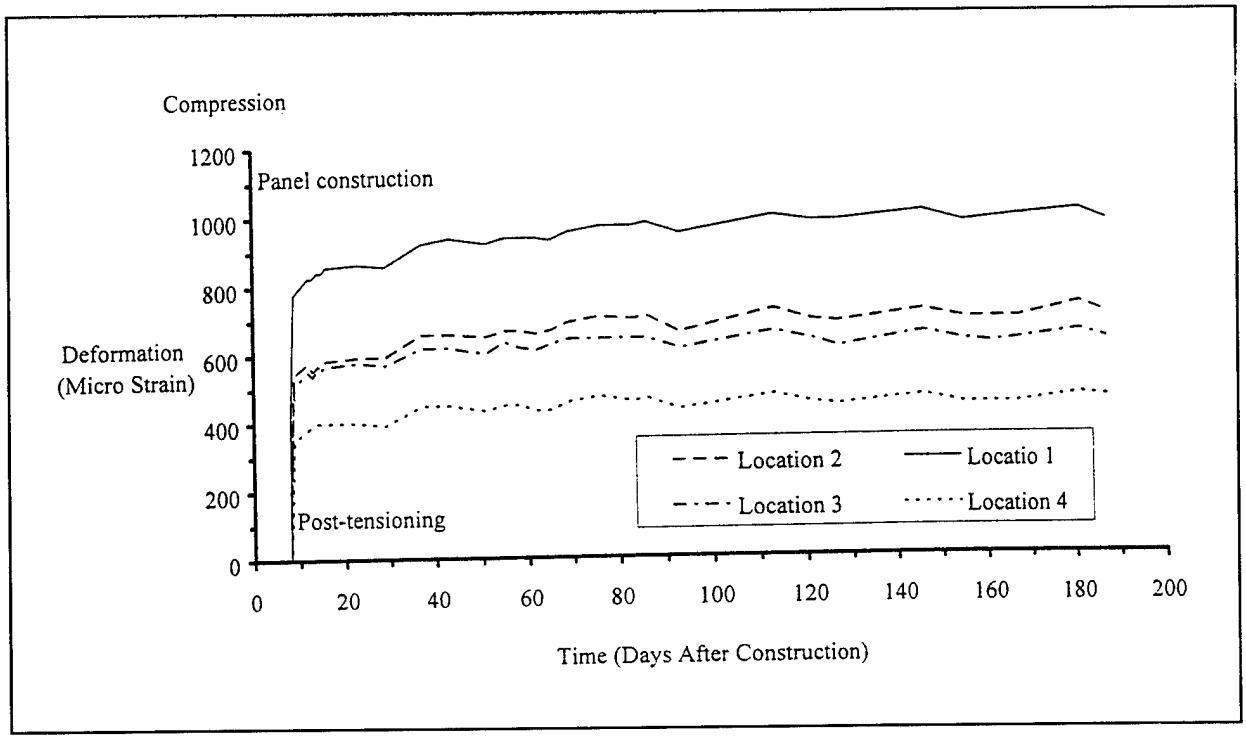

Figure 4.30. Masonry strain vs. time (PLA-3).

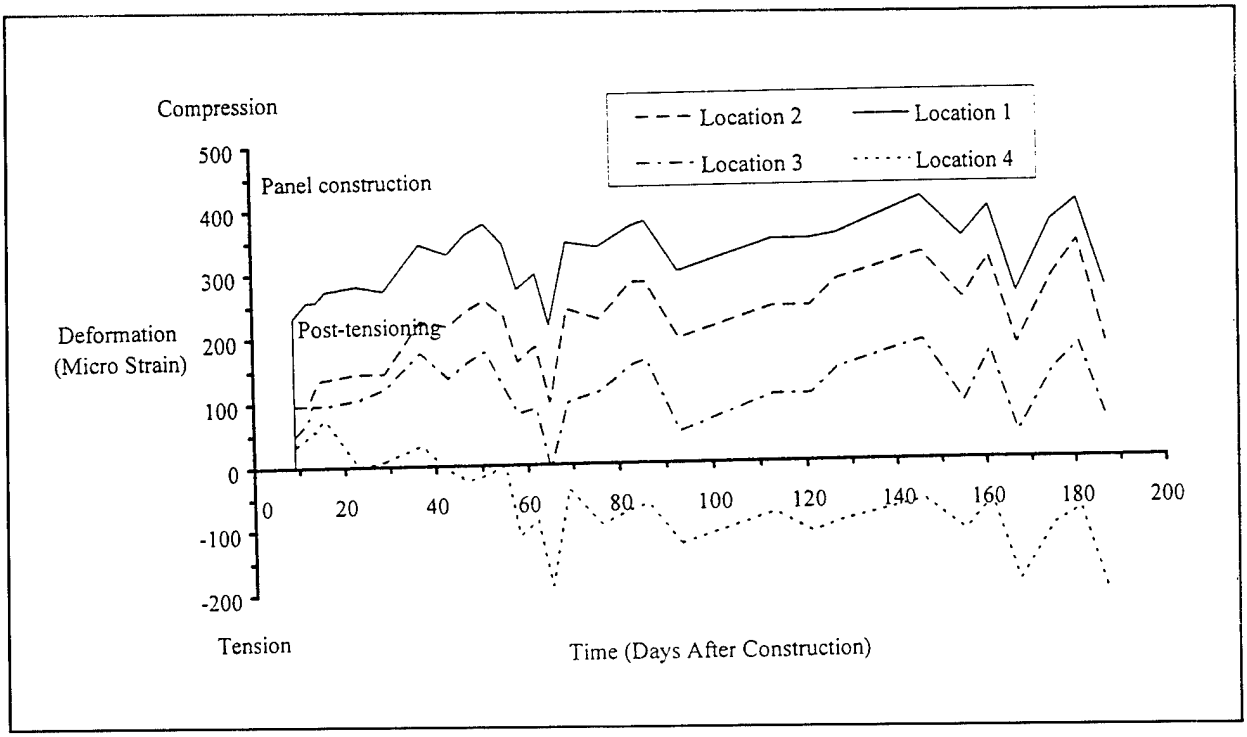

Figure 4.31. Masonry strain vs. time (PLA-4).

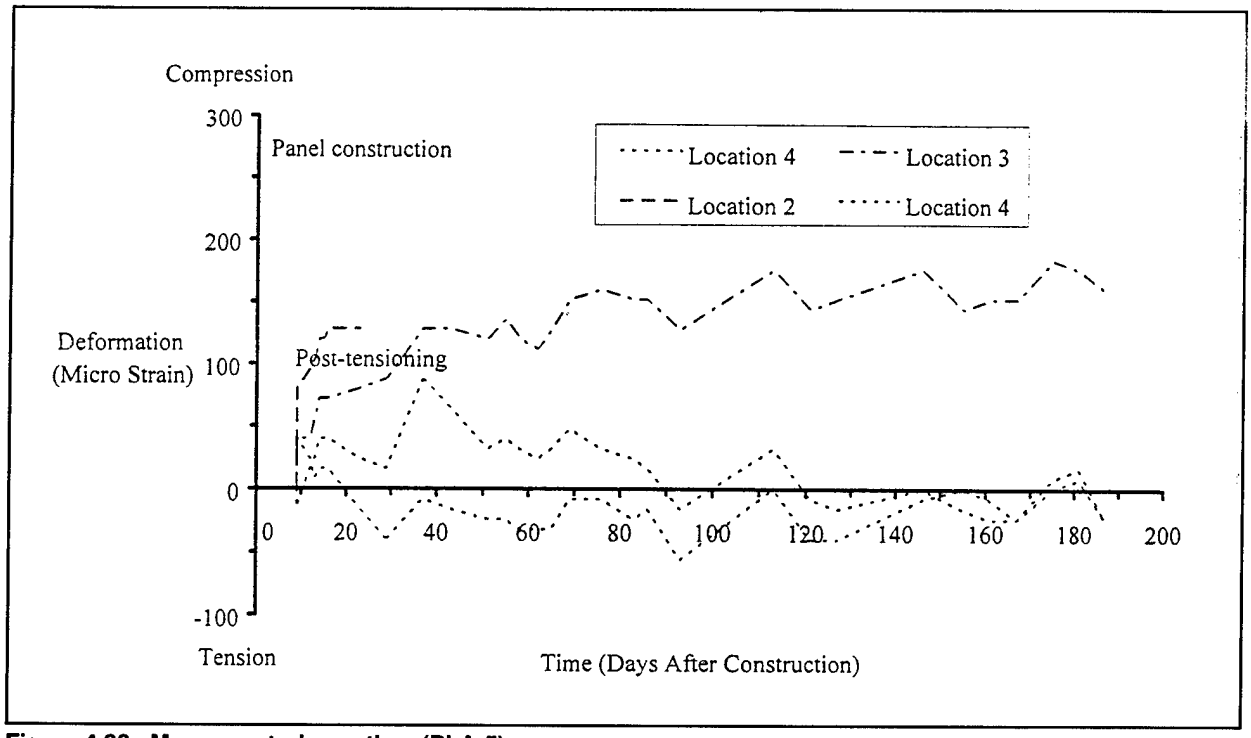

Figure 4.32. Masonry strain vs. time (PLA-5).

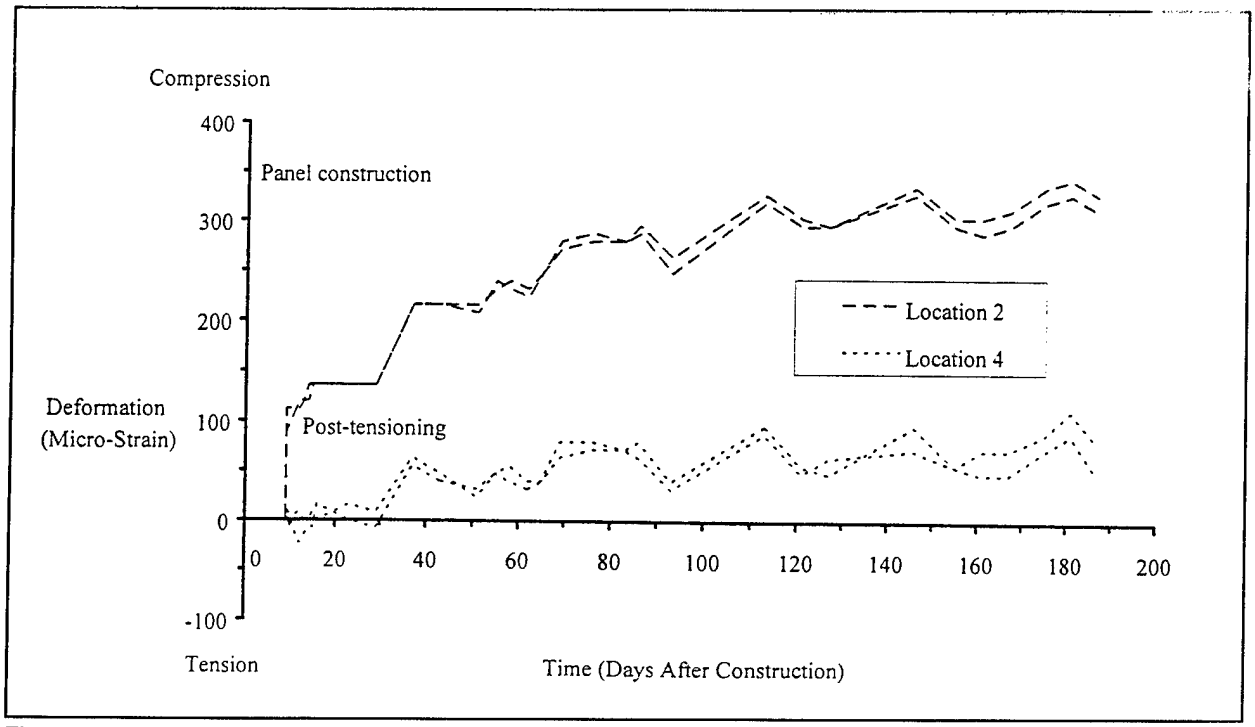

Figure 4.33. Masonry strain vs. time (PLA-6).

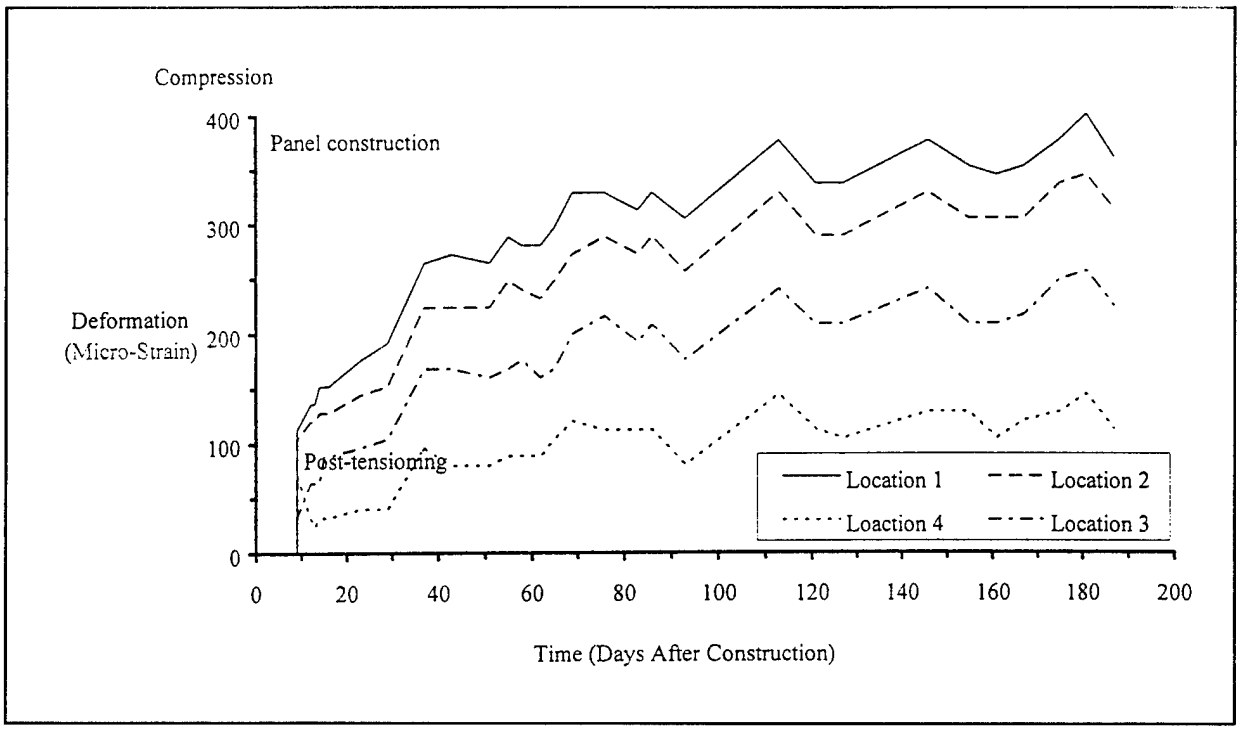

Figure 4.34. Masonry strain vs. time (PLP-1).

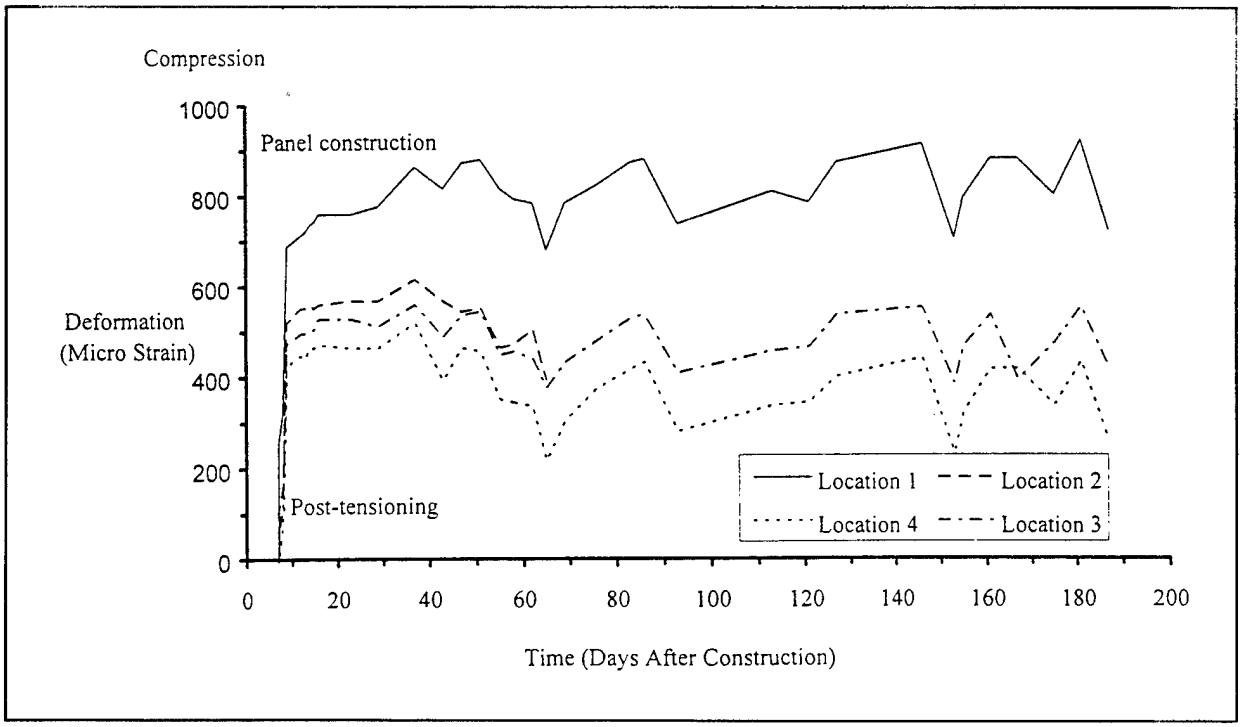

Figure 4.35. Masonry strain vs. time (PLP-2).

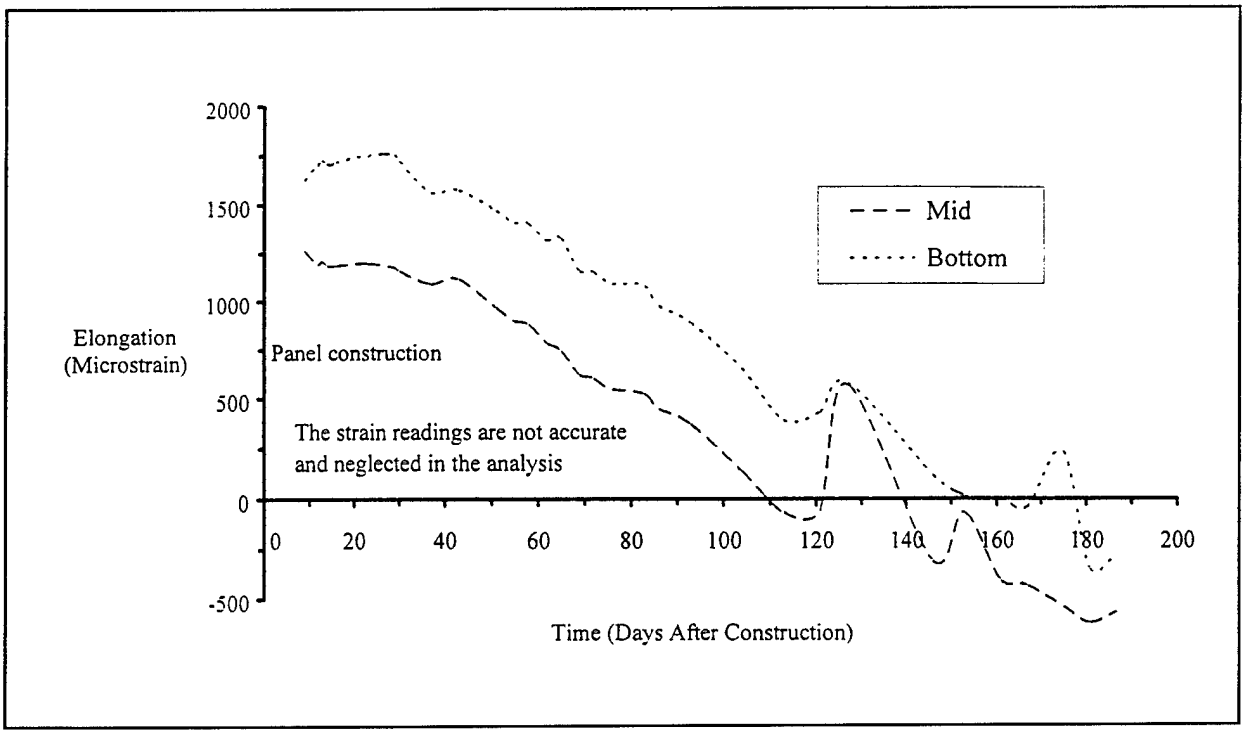

Figure 4.36. Steel strain gage readings vs. time (PLA-1).

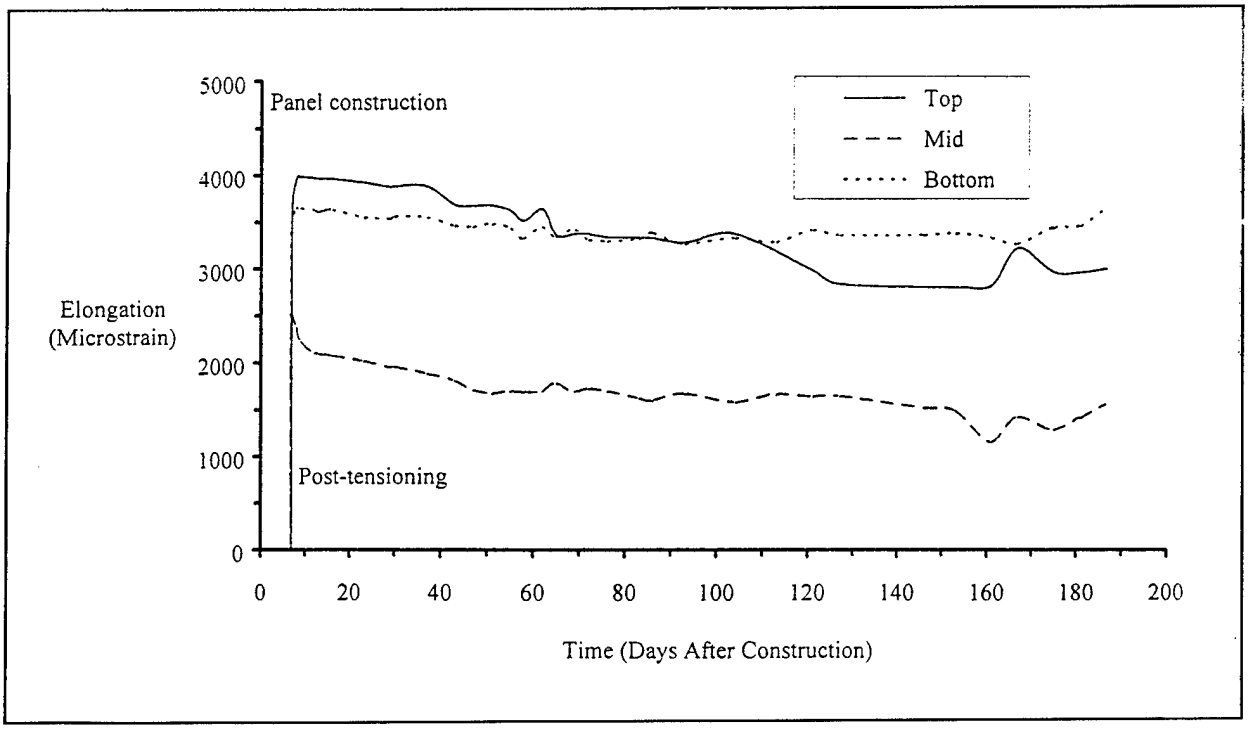

Figure 4.37. Steel strain gage readings vs. time (PLA-2).

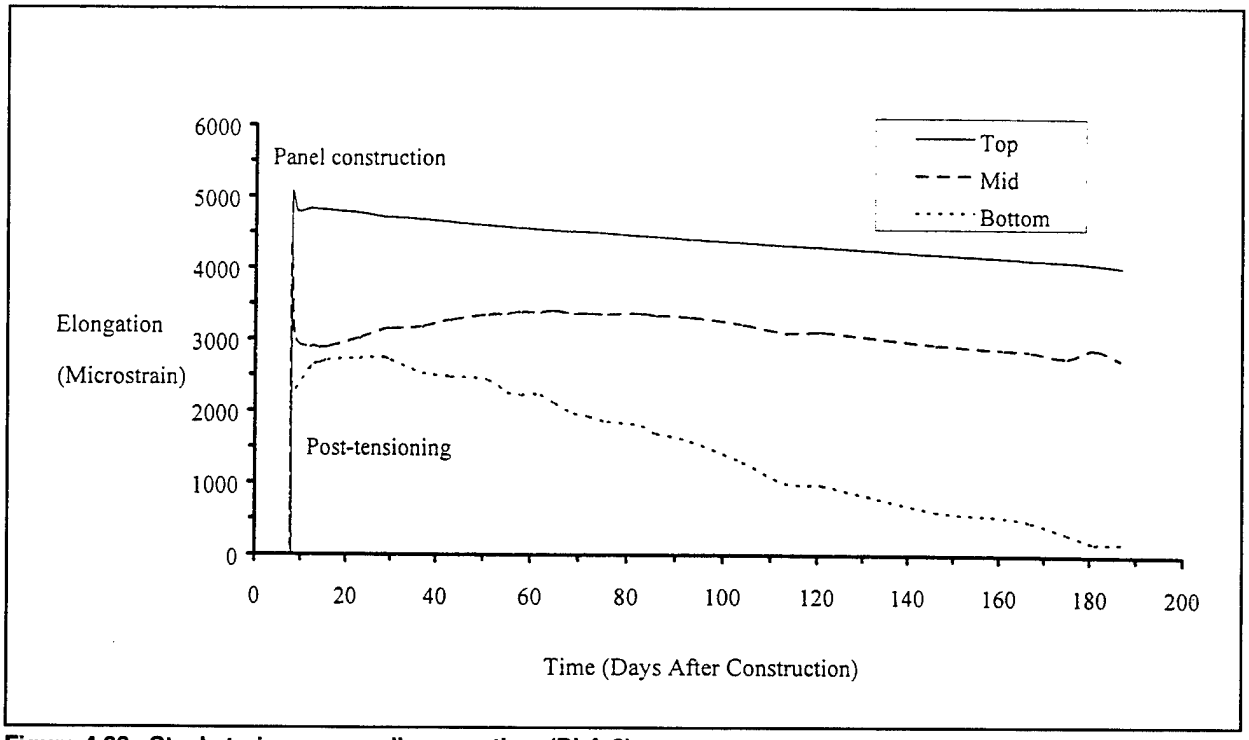

Figure 4.38. Steel strain gage readings vs. time (PLA-3).

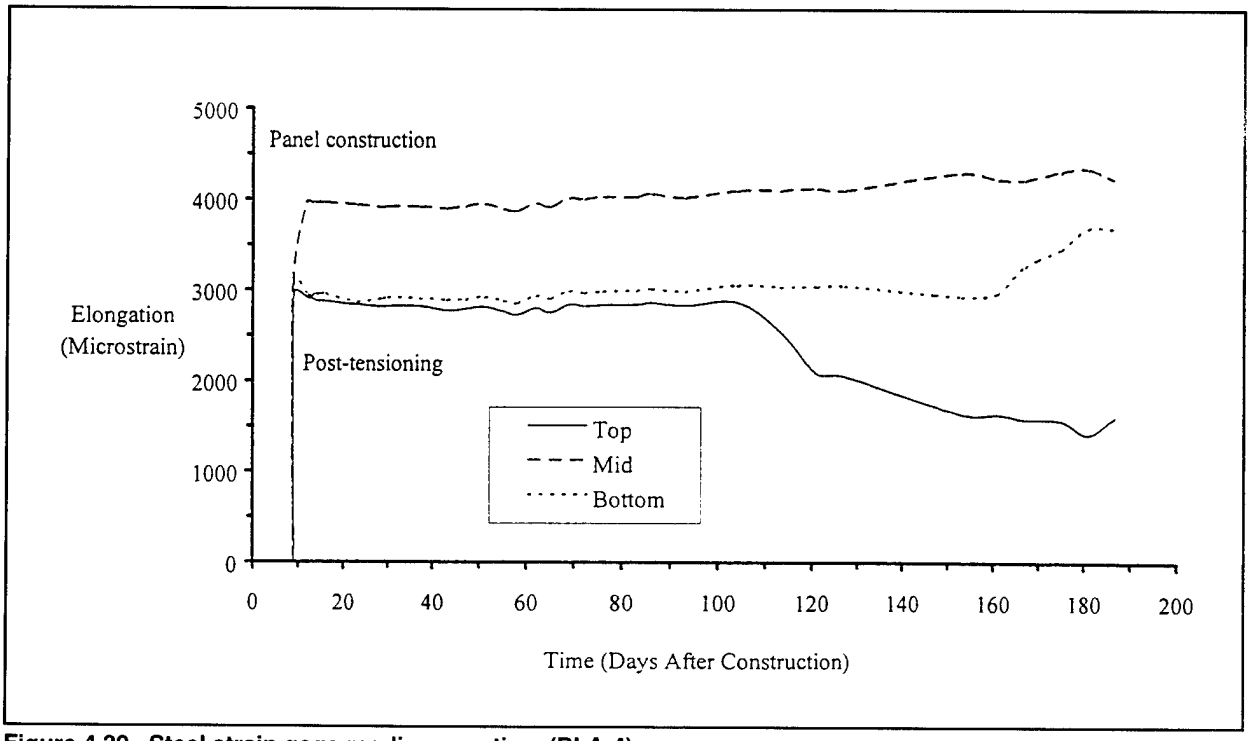

Figure 4.39. Steel strain gage readings vs. time (PLA-4).

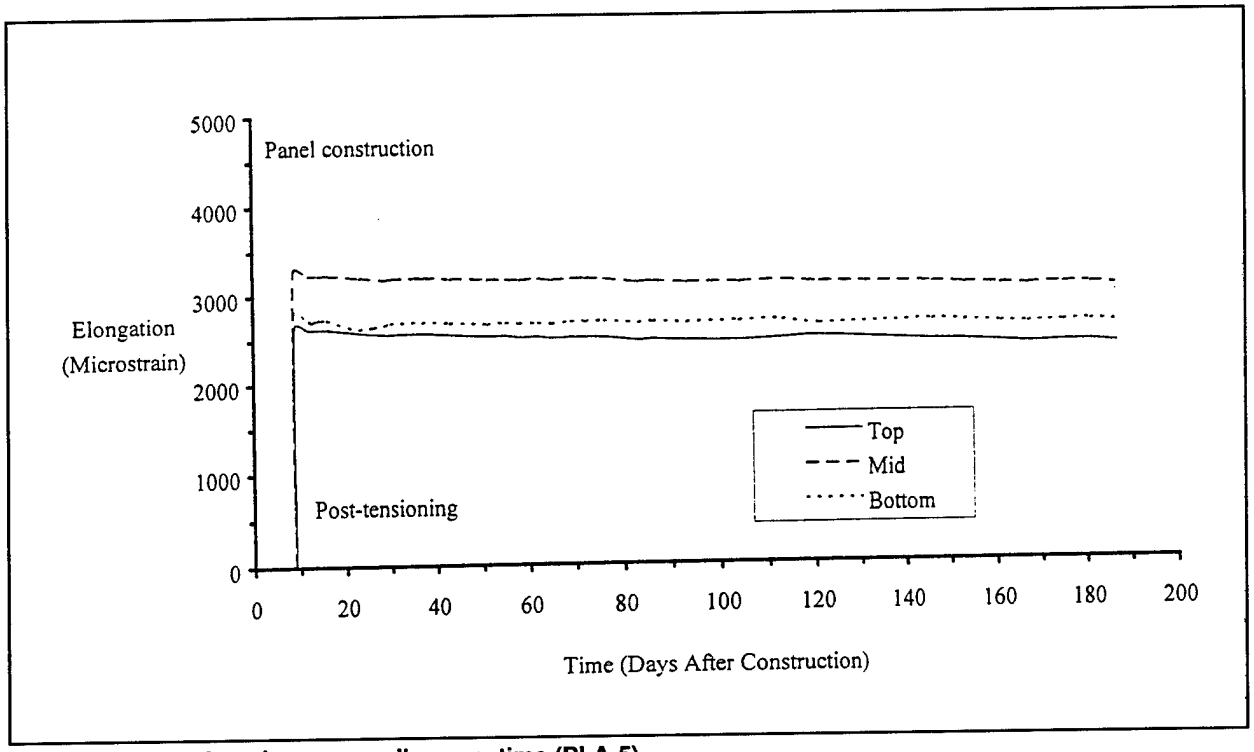

Figure 4.40. Steel strain gage readings vs. time (PLA-5).

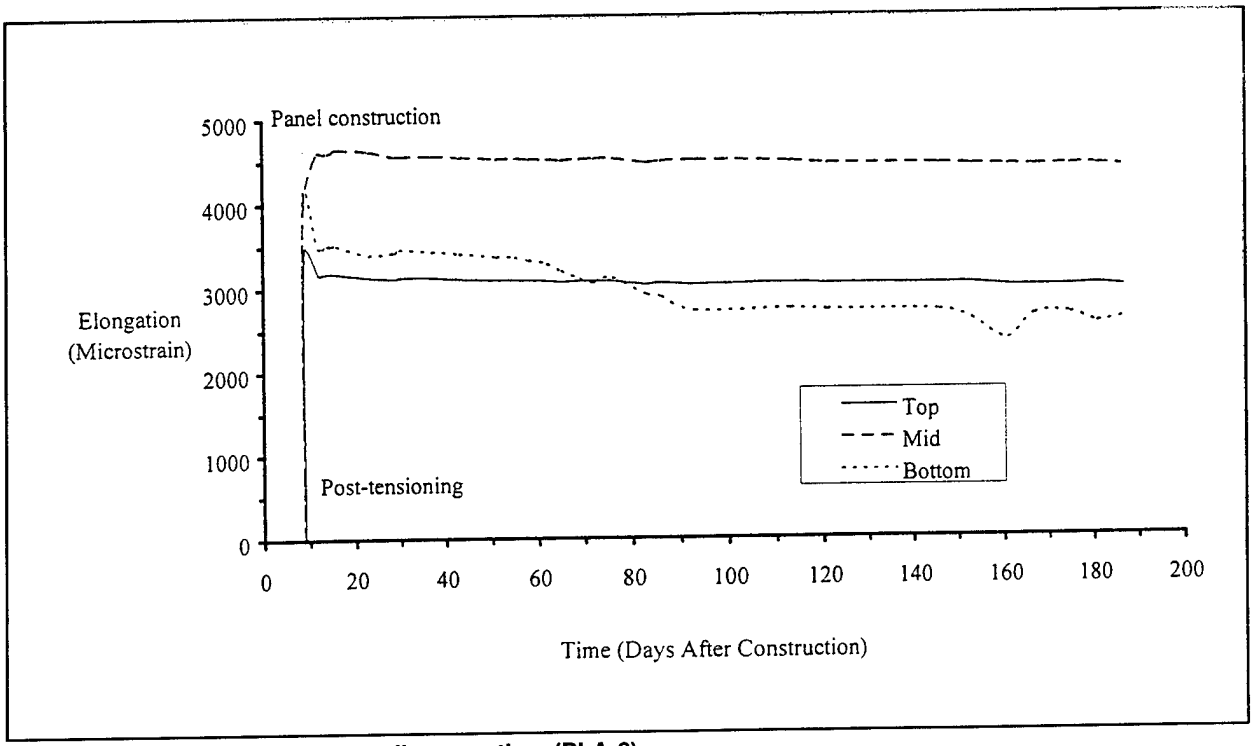

Figure 4.41. Steel strain gage readings vs. time (PLA-6).

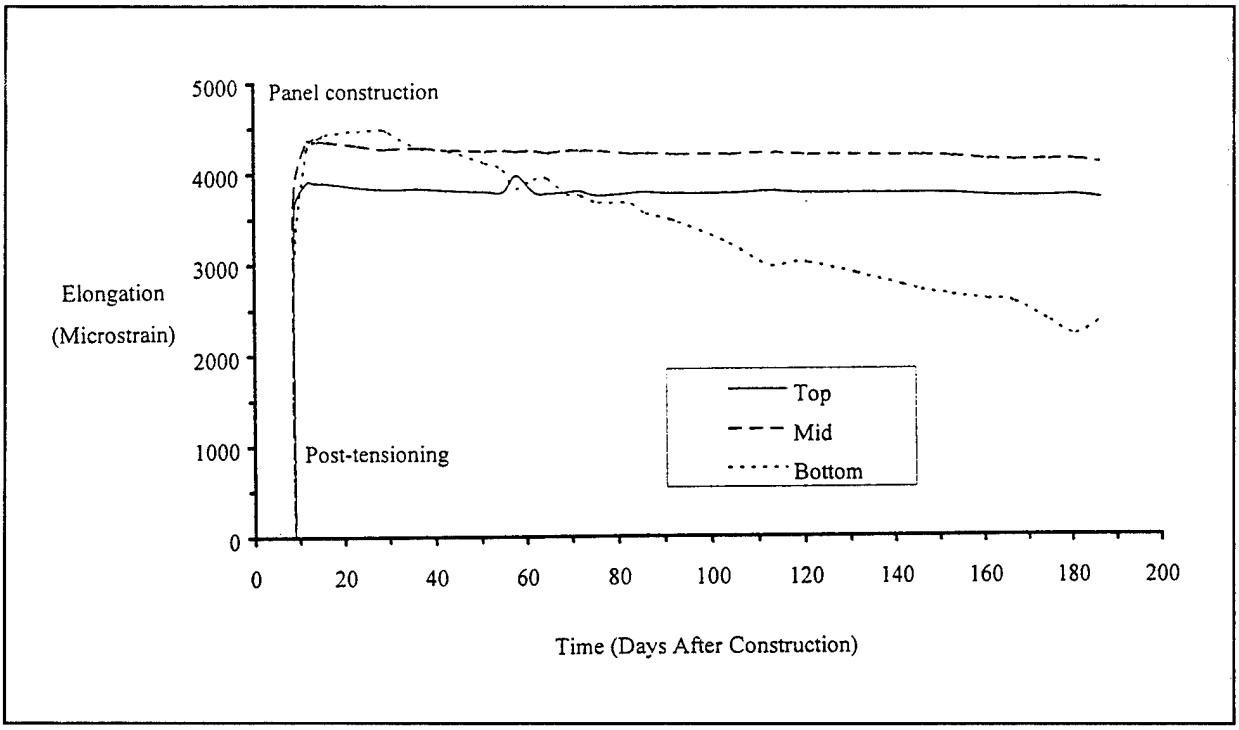

Figure 4.42. Steel strain gage readings vs. time (PLP-1).

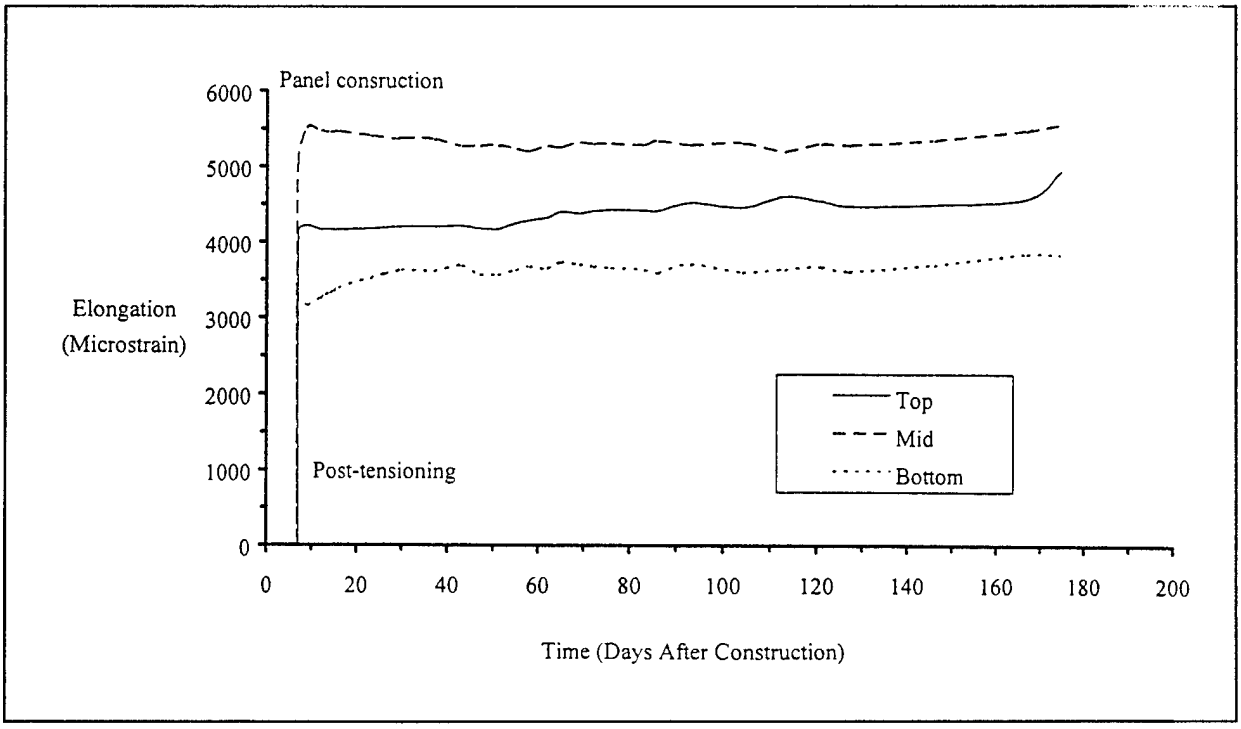

Figure 4.43. Steel strain gage readings vs. time (PLP-2).

5 Comparison and Discussion of Results

The results of the experimental work described in Chapter 4 are discussed here. Wall strength comparisons are made between the grouted and ungrouted panels. The wall capacities required by the UBC for wind loading are discussed. Some typical design charts showing the capacity of wall panels versus steel spacing and wall height are plotted. The prestress losses were evaluated over a period of 180 days and are discussed in Section 5.4.

5.1 Compressive Strain Comparison

Applied load versus compression strains measured at midspan of both Stage I and Stage II panels using a Demec gage are plotted in Figures 5.1 and 5.2 along with the theoretical curve. The recording of strain readings was started when the load was applied to the panel and was stopped once the masonry started crushing during the test. The theoretical curve was calculated based on the moment-curvature method given in Chapter 3 (Section 3.1) using the actual material properties. A good correlation can be seen between the two sets of curves, indicating that the moment curvature method can closely predict the behavior of the prestressed clay brick panels even in the post-cracking range.

5.2 Comparison of Wall Strength

The capacities of the wall panels tested in Stages I and II along with the parameters considered in each stage are compared in this section. The parameters included the presence of grout, different end bearing conditions, and the magnitude of initial prestressing force. Comparisons are made at both cracking and ultimate stages. The theoretical analysis at ultimate load of both grouted and ungrouted panels is also included in this section.

5.2.1 Cracking Moment

The load-deflection behavior of both the grouted and ungrouted panels of Stage I is shown in Chapter 4, Figure 4.19. The cracking moment capacity of all six panels was averaged to 1,840 lb-ft (2,495 N-m). The theoretical cracking moment

calculated based on the UBC [1994] specified modulus of rupture value of $2.5\sqrt{f'_m}$ was equal to 1,780 lb-ft (2,415 N-m), which is lower by only 3.3 percent (see Figure 5.3). Based on the experimental cracking moment of Stage I panels, the modulus of rupture of the specimens was found to be equal to $2.66\sqrt{f'_m}$.

The cracking moment in the case of Stage II could not be clearly distinguished since the curves were smoother (see Figure 4.24). The average experimental cracking moment of stage II panels (four panels) with initial prestressing force of 19 kips (84.5 kN) was approximated to be 2,012 ft-lb (2,728 N-m) from the load-deflection curves. The theoretical value according to UBC [1994] is equal to 1,870 ft-lb (2,532 N-m) which is 7.1 percent lower than the test results (see Figure 5.4). The panels with an initial prestressing force of 16 kips (71.2 kN), experienced an average cracking moment of 1,868 ft-lb (2,533 N-m), similarly approximated from the load-deflection curves. These experimental values obtained correspond to a modulus of rupture of approximately $2.87\sqrt{f'_m}$.

5.2.2 *Ultimate Moment Capacity*

The theoretical nominal moment capacities were calculated for both grouted and ungrouted panels. Appendix B illustrates the detailed procedure for calculating the ultimate capacity of each panel. The experimental average ultimate capacity of grouted and ungrouted panels of Stage I was 3,620 lb-ft (4,908 N-m) and 2,070 ft-lb (2,806 k-N) respectively. Figure 5.5 shows a comparison between the experimental and analytical results.

As can be seen from Figure 5.5, the theoretical analysis of ungrouted panels using the MSJC Code [Prestressed 1995] provisions yielded a significantly lower value (see Appendix B). The equation given in the code was used to calculate the stress in the steel at ultimate flexure. The theoretical moment capacity was equal to 1,450 lb-ft (1,966 N-m). This large disparity in the results could be attributed to the accuracy of the equation for unbonded tendons.

The grouted panels had nearly double the ultimate capacity of ungrouted specimens. The major contribution to this strength is the constant effective depth of steel along the entire span. The strain compatibility analysis predicted the ultimate moment very closely with test results. The actual material properties were used in the analysis. The steel stress was determined from the steel stress-strain diagram, and the compressive strength of masonry from prism tests. Prestress loss was assumed to be 5 percent at the time of testing the specimens.

The average ultimate capacity of Stage II specimens (eight panels) was equal to 3,606 lb-ft (4,888 N-m). The load-deflection curves (Figure 4.24) show a wide range

of ultimate strength values varying from 2,837 lb-ft (3,846 N-m) to 4,180 lb-ft (5,667 N-m). The theoretical value calculated based on strain compatibility for these panels was 3,805 lb-ft (5,159 N-m) which is 5.5 percent higher than the average experimental value. This lower experimental average value can be attributed to the lesser strengths of TPIIA3 and TPIIA4 panels, and it is an average of all eight panels. The presence of grout in the core helped to restrain the steel at a constant effective depth throughout the member.

The behavior between the panels fitted with plates and shelf angles did not show any noticeable difference either in their strength or deflections (see Figure 4.24). Also from Figure 4.24 it can be seen that the panels post-tensioned at the age of 1 day and 5 days did not any have significant difference in their behavior.

5.3 Comparison With Wind Loads

5.3.1 UBC Design Wind Pressure

The capacity of the panels tested from both Stage I and Stage II are compared with the UBC [1994] design wind loads. The design wind pressures are calculated based on the following example and the data assumed. The wind pressures obtained are plotted along the wall height, as shown in Figure 5.6. Table 5.1 gives the values of wind pressures at different heights with different exposure conditions and wind speeds.

Example Calculation	UBC Section
Height of the wall = 60 ft	NA
Exposure = B, Gust factor coefficient C_e (based on height)	1614, Table 16-G
Wind speed = 80 mph, Stagnation pressure, q_s = 16.4	1614, Table 16-F
Pressure coefficient (method 1), C_q = 0.8 (inward)	Table 16-H
Importance factor, I_w = 1.00 (standard)	Table 16-K

The design wind pressure is given by the formula:

$$P = C_e C_q q_s I_w \qquad \text{[Eq 5.1]}$$

5.3.2 Wall Capacities for Out-of-Plane Loading

Based on the experimental test results of grouted post-tensioned wall panels, the following wall designs were made. The allowable deflection from UBC [1994] was limited to $0.007h$, where h is the height of the wall. This UBC allowable deflection

for walls with a height of 10 ft and 12 ft corresponds to 0.84 in. and 1.01 in. respectively. Calculations based on the assumptions of the example below show midheight deflections of walls with a height of 10 ft and 12 ft to be equal to 0.101 in. and 0.145 in. respectively at the cracking moment stage. These calculations showed that the cracking moment will be reached before the deflection limit is exceeded for these prestressed masonry walls. Hence the satisfactory allowable service loading was assumed to be that which causes the cracking of wall panels. A sample calculation is shown below.

Data for the Example:

Height of the Wall, h = 10 ft
Wall thickness, t = 3 5/8 in. (4 in. nominal)
Section modulus, S = 78.84 in.^{3}
Compressive strength of masonry, f'_m= 3,000 psi
Effective prestressing force, P_e = 18,000 lbs
Diameter of prestressing steel bar = 5/8 in.
Spacing of the bars, s = 36 in.
Modulus of rupture, f_r = 137 psi
Design

$$\text{Precompression stress} = \frac{P}{A} = \frac{18{,}000}{36(3.625)} = 138\text{psi}$$

Stress in the tension fiber at cracking, f_b = 137 + 138 = 275 psi
Moment required to crack = f_b S = 275 (78.84) = 21,675 lb-in.

$$\text{Moment due to uniformly distributed load, } M = \frac{wl^2}{8}$$

$$\text{Therefore, distributed load, } w = \frac{8(M)}{l^2} = \frac{8(21{,}675)}{(12 \times 10)^2} = 12.04\ lb\text{-}in. = 48.2\ psf$$

Design charts were created for different parameters involved in the design of panels at service loading and are shown in Figures 5.7 to 5.12. From the above calculation it can be seen that the wall capacity has a factor of safety of 3.9 compared with the UBC design wind pressure for a 60 ft tall wall with exposure B and a wind speed of 80 mph (see Figure 5.6).

Figure 5.13 compares the cracking capacity of walls with the UBC wind loads. A 60 ft tall building wall was assumed with a first floor height of 12 ft, and additional floor heights of 10 ft each. The chart is based on the following assumptions: (1) effective prestress = 18,000 lbs, (2) spacing of 5/8 diameter bars = 36 in., and (3) modulus of rupture of masonry = $2.5\sqrt{f'_m}$. For the cases considered above, the

walls have a factor of safety of 3.9 to 4.3 against cracking throughout the height of the wall. Even considering the worst wind load combinations from Table 5.1 (exposure = C and wind speed = 90 mph), the walls still have a factor of safety against cracking of 1.8 to 1.9. It should be noted that using cracking as the serviceability limit state is conservative. The UBC allows service load deflection well beyond cracking.

Similarly, the wall capacities were compared with the wind loads from UBC at ultimate stage. UBC [1994] specifies a maximum load factor of 1.3 for wind load. This value has been used to check the factor of safety with nominal strengths of the panels. For comparison at ultimate strengths, Stage II panels were used since they had slightly lower strength compared to Stage I test specimens. The average ultimate capacity of the panels was 3,605 lb-ft (4,888 N-m), which is converted to distributed load capacity of the panels. The UBC wind loads for service loading (Table 5.1) were multiplied with the load factor to obtain the ultimate values. Figure 5.14 shows the wall capacities and UBC loads at ultimate for Stage II test panels. The data used in deriving the panel strengths was the same as for the service loads. The minimum factor of safety is approximately equal to 6.5. Hence the design limitations will be besed on service loads.

5.4 Prestress Loss Analysis

The analysis of the prestress losses occurring in the panels up to 187 days after construction are discussed in this section. The changes in the masonry strain due to creep, shrinkage, and moisture expansion recorded using a Demec gage were shown in Chapter 4. The strains occurring in the prestressing bars recorded continuously from the strain gages were also shown in Chapter 4.

5.4.1 Analysis of Masonry Stresses

The masonry strains from each panel recorded at different stages are given in Table 5.2. The locations of strain measurements were shown in Figure 4.29. It should be noted that there was no loss of prestress due to elastic deformation of masonry, as it occurred during the prestress application (torquing).

The distribution of strains shows that the prestressing force was not uniformly distributed in the cross section (see Table 5.2). Some variation can be noticed at the middle span where the stresses are expected (assumed for strength calculations) to be uniformly distributed in the cross section. The theoretical initial elastic deformations in the masonry panels during the post-tensioning stage, calculated from the modulus of elasticity, were 0.0000601 and 0.0000506, with an initial prestressing

force of 19 kips (84.5 kN) and 16 kips (71.2 kN) respectively. These theoretical values are based on the assumption that the initial prestress is uniformly distributed in the cross section of the panels. A large stress variation can be seen even within each panel itself.

Panels PLP-2 and PLA-2 developed a small tensile stress at location 4 during the post-tensioning. Prestress was concentrated along the steel bar (location path 1-2-1) at the center of the panel. Immediately below the anchorage (Location 1), the stress values were high. This is due to the anchorage zone effect, where high compressive stresses result from the transfer of prestress to the masonry panel over a small area. The stresses were better distributed at Locations 2 and 3 at the midspan. The high anchorage stresses can also be attributed to the uneven contact surface of the masonry at the bearing location. The average stresses of all panels immediately after prestress application are shown in Table 5.3. No distinction was made between the panels fitted with plate and angles, as they experienced similar distribution of stresses.

Table 5.3 shows that Location 1 was the place of maximum stress in all the panels. This indicates that the applied prestress was transferred over a small area below the anchorage. For example, assuming the average value of 674.2 psi (4.65 MPa), and that the prestress distribution was uniform, the force would be distributed over a length of only 7.75 in. (197 mm). At middle span of the panel (Location 2), the stress was higher than the theoretical value, and at location 3, the stress was close to the theoretical value. The corners (Location 4) experienced only a maximum of one-third of the theoretical stress value. Again no significant difference was noticed in the stress distribution between the panels fitted with plates and angles.

The masonry strains kept increasing at a higher rate immediately after post-tensioning. Panels PLP-2, PlA-2, and PLA-4 were exposed to exterior weather conditions starting from the age of 40 days after construction. From Table 5.2, it can be noticed that the compressive strains started decreasing in the outside panels as opposed to panels stored inside the laboratory. Between 40 and 187 days, the strain in all outside panels decreased. This was most likely due to the moisture expansion of masonry. During this period, the inside panels experienced further creep/ shrinkage. The masonry deformation coefficients at each location are shown below in Table 5.4. These coefficients were calculated by assuming a value of unity (1.0) for the strains at post-tensioning, and dividing the strain values at other locations by the strain at post-tensioning. Figures 5.15 and 5.16 show the average deformation coefficients between the inside and outside panels, respectively.

5.4.2 Steel Stresses

It can be noticed from Figures 4.37 to 4.44 (Chapter 4) that the steel strain gage readings showed a large variation at the post-tensioning stage. The values changed significantly even during the course of the study. Though the strain gages were attached to the bars following the manufacturer's recommendations, some of the readings were found to be inaccurate. Some of the unsatisfactory readings can be attributed to ingress of water (poor water sealant) from the grout preceding the post-tensioning operation. Another possibility was that the strain gages may have debonded from the steel bars during post-tensioning. The steel strains corresponding to an initial prestressing forces of 16,000 lb (71.2 kN) and 19,000 lb (84.5 kN) should be 0.002910 and 0.003540 respectively (from stress-strain relationship of steel). Hence, by judging the steel strain corresponding to the initial prestressing force applied, some of the recorded data were neglected in the prestress loss analysis. The steel strain gage readings ranged from a value of 1,250 x 10^{-6} to 5,500 x 10^{-6} at post-tensioning.

In panel PLA-1, only two strain gages (middle and bottom) were functioning, and they were neglected in the analysis due to inaccuracy in the readings. Panel PLA-2 had all three strain gages functioning, but the middle gage showed an extremely low value at post-tensioning, and thus was ignored. The top strain gage readings were also neglected due to large fluctuations in the readings. In panel PLA-3, only the middle strain gage showed a reasonable strain value (0.003003) at post-tensioning. This is the only gage reading used in the loss calculation for this panel.

In panel PLA-4, the bottom gage readings were found to be satisfactory up to 160 days. The readings from the top and middle gages were too erratic to be considered in the analysis. All three strain gages in PLA-5 showed a good record of strain readings until the end of the study. Hence all gage readings were considered for the analysis. The panel PLA-6 had only one gage (top) which showed accurate readings. The other two strain readings (middle and bottom) were dropped from the analysis.

The panels PLP-1 and PLP-2 fitted with plates had an initial prestress of 19,000 lb (84.5 kN) which corresponds to a strain of 0.003540. The bottom gage in panel PLP-1 and middle gage in PLP-2 were neglected due to their high strain values at post-tensioning.

The changes in the strain values of prestressing steel plotted against time are shown in Figure 5.17. The strain gage readings in each bar were averaged in panels where two or more gage readings were considered. The corresponding stress losses were determined using the stress-strain relation developed earlier (Figure 4.11). The recorded loss of prestress for each panel is given in Table 5.5.

In Table 5.5, positive values indicate an increase in stress (gain), while negative value indicates a decrease in stress (loss). The change in the prestress reflects collective long-term effects such as the steel relaxation, creep, and shrinkage/expansion of masonry. The steel relaxation could not be differentiated from the net effect, as the specimes were grouted. The results showed that the change in prestress in the bars range from a 15.01 percent gain to a 8.76 percent loss. These values are comparable to loss/gain values reported by other investigators.

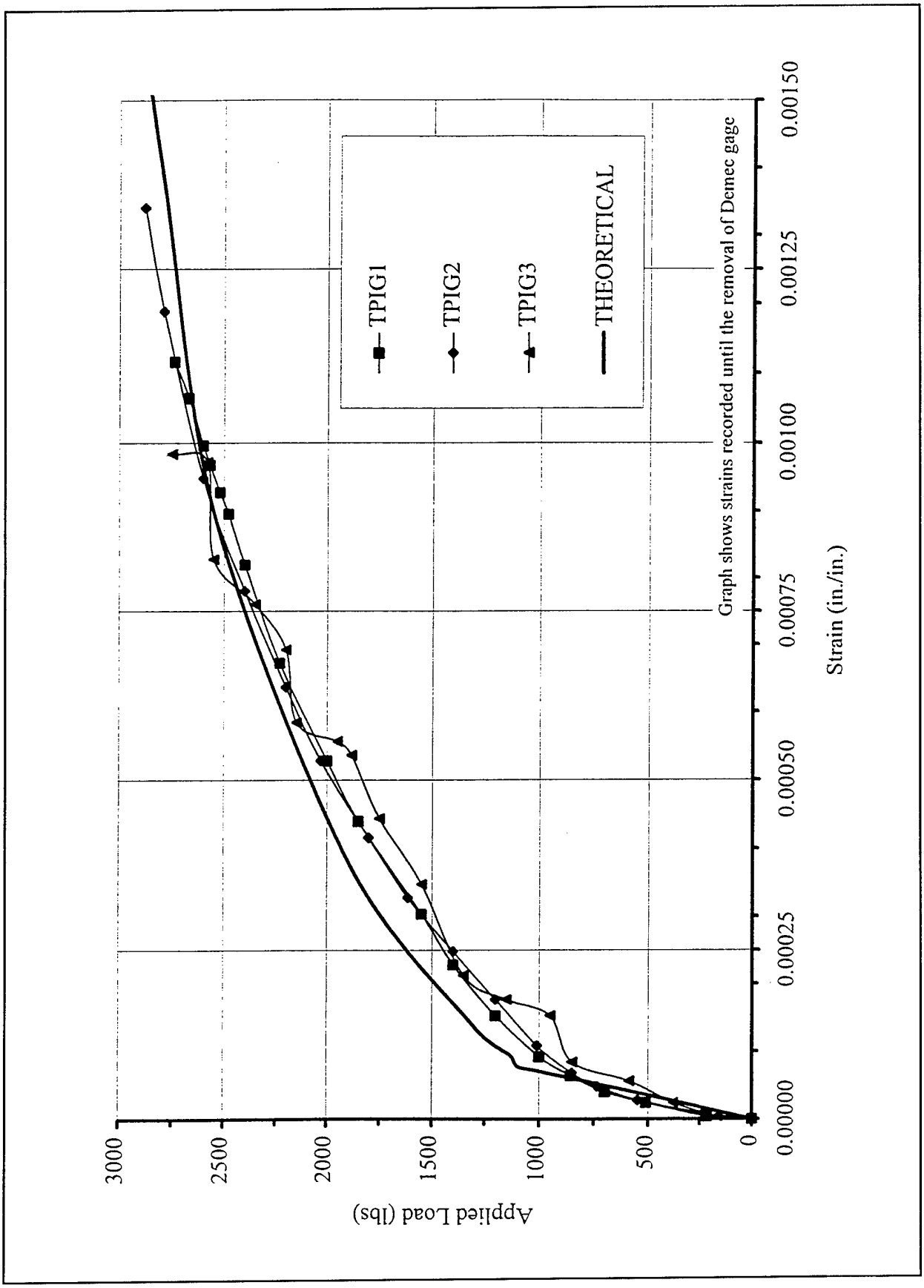

Figure 5.1. Load vs. compressive strain of Stage I test specimens.

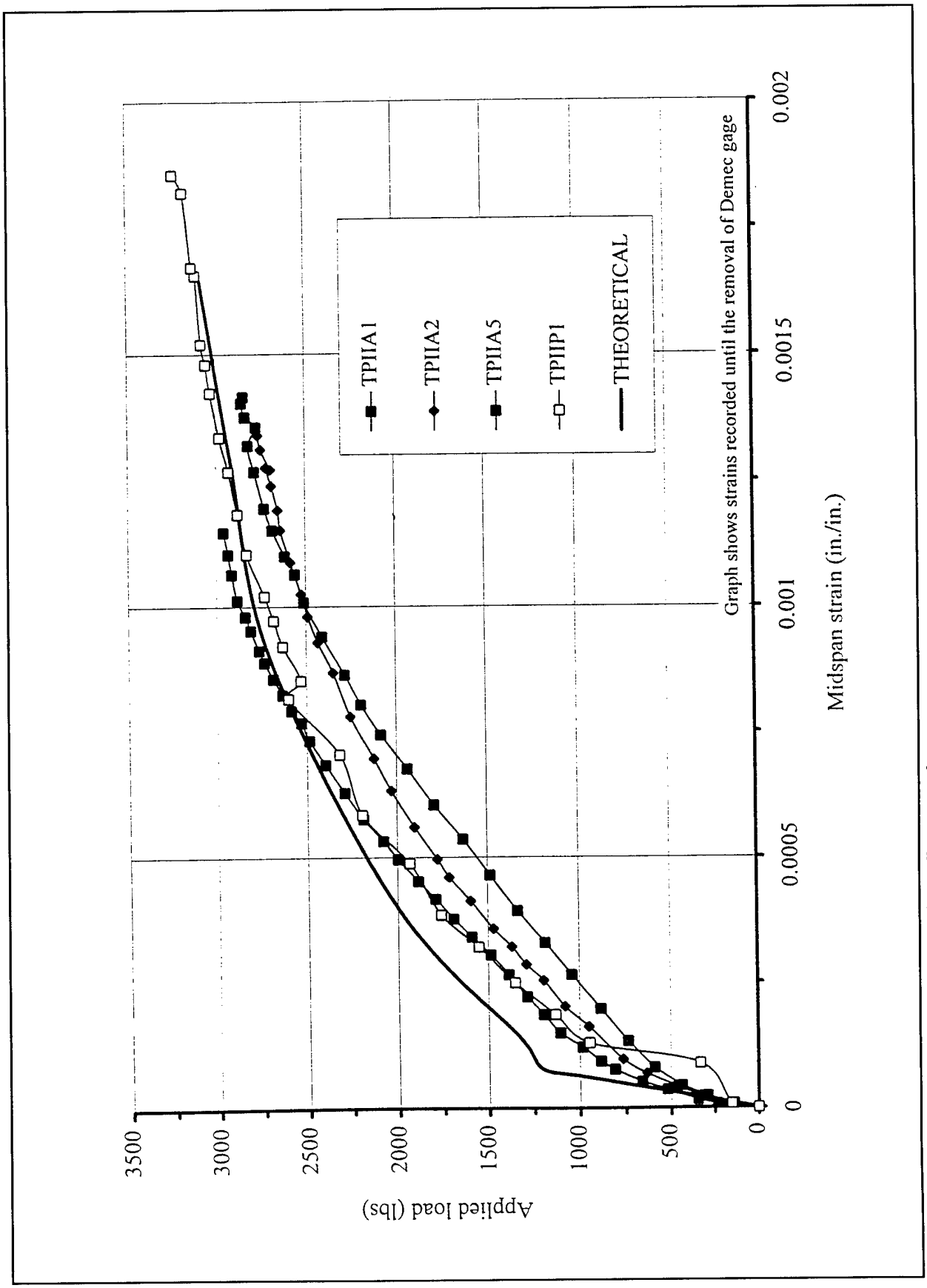

Figure 5.2. Load vs. compressive strain of Stage II test specimens.

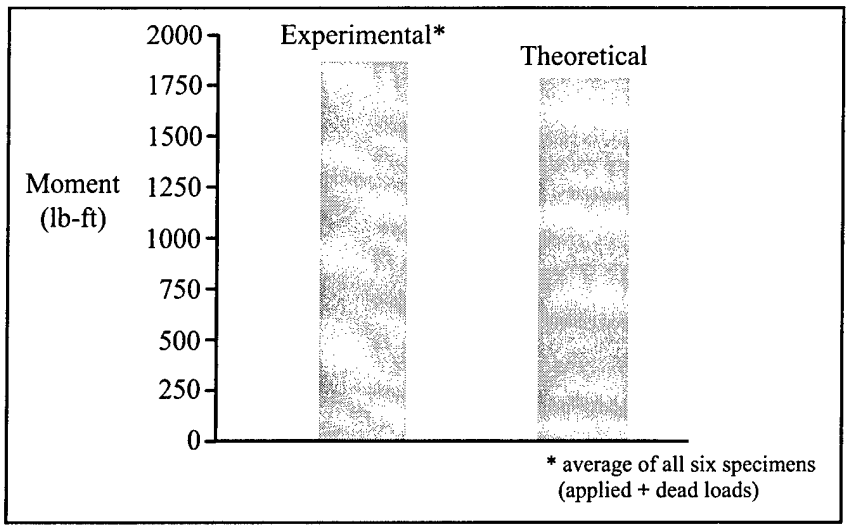

Figure 5.3. Comparison of cracking moments (Stage I).

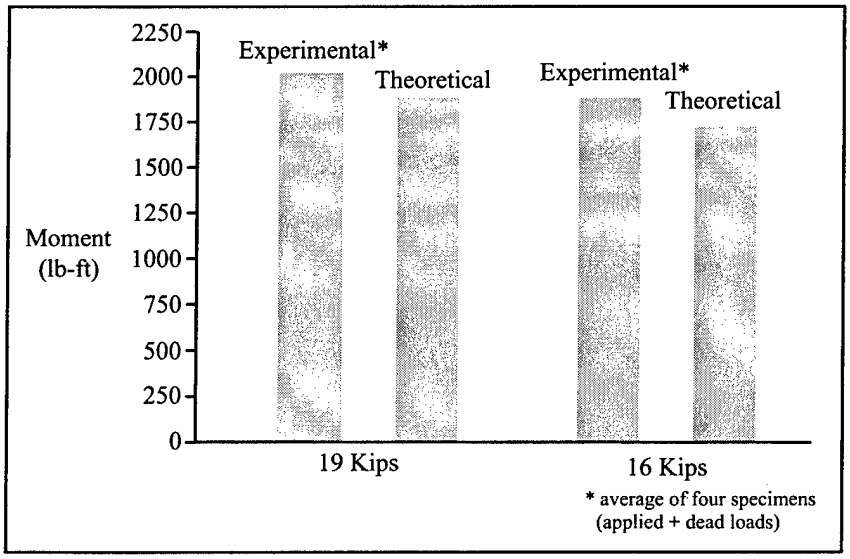

Figure 5.4. Comparison of cracking moments (Stage II).

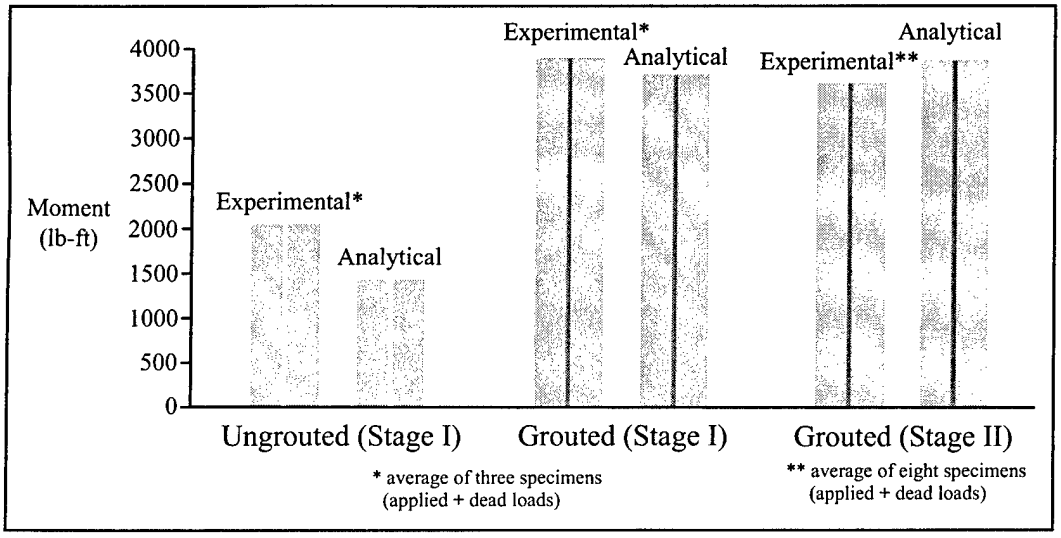

Figure 5.5. Comparison of ultimate strengths (Stages I and II).

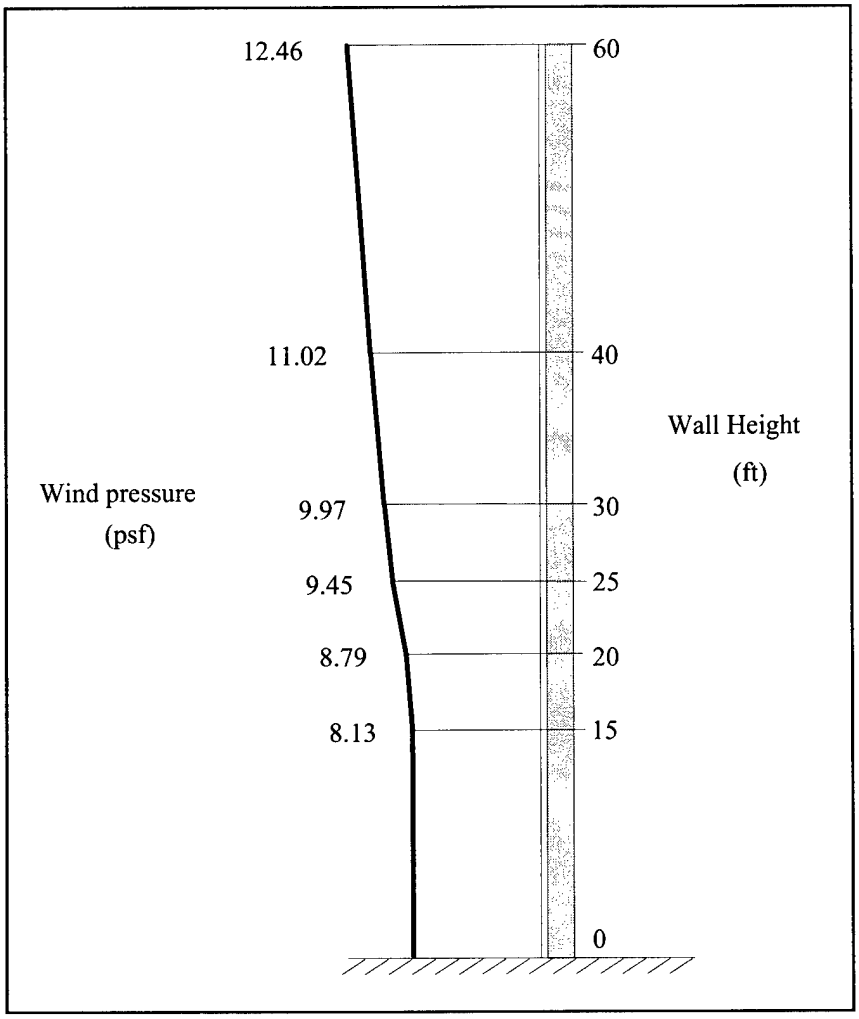

Figure 5.6. UBC design wind pressure.

Table 5.1. Design wind pressures from UBC.

Wall Height (ft)	Exposure B Wind Speed = 90 mph	Exposure C Wind Speed = 80 mph	90 mph
0-15	10.32	13.91	17.64
20	11.15	14.83	18.80
25	11.98	15.61	19.80
30	12.65	16.14	20.47
40	13.98	17.19	21.80
60	15.81	18.76	23.80

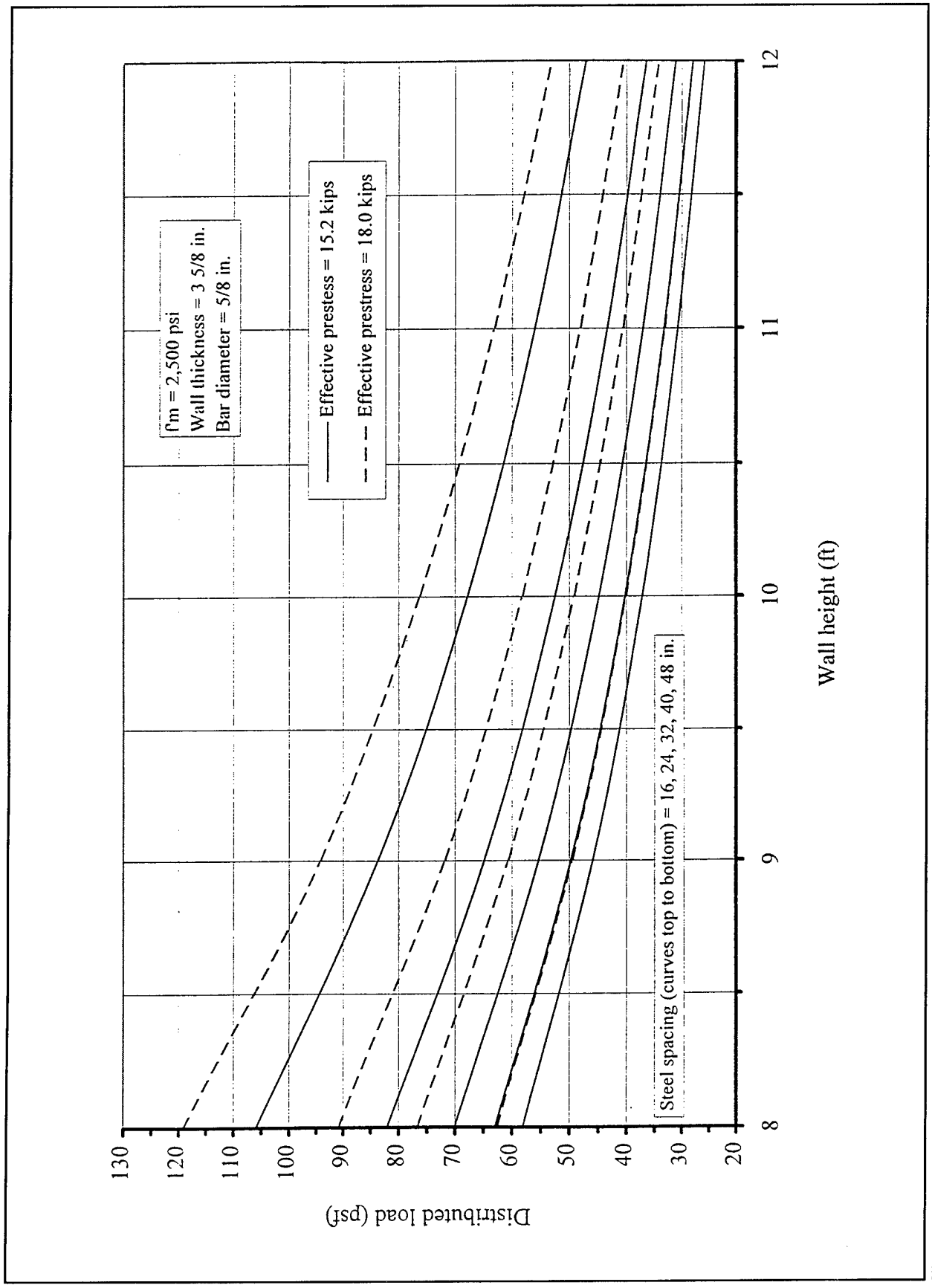

Figure 5.7. Wall capacity at cracking vs. height of wall.

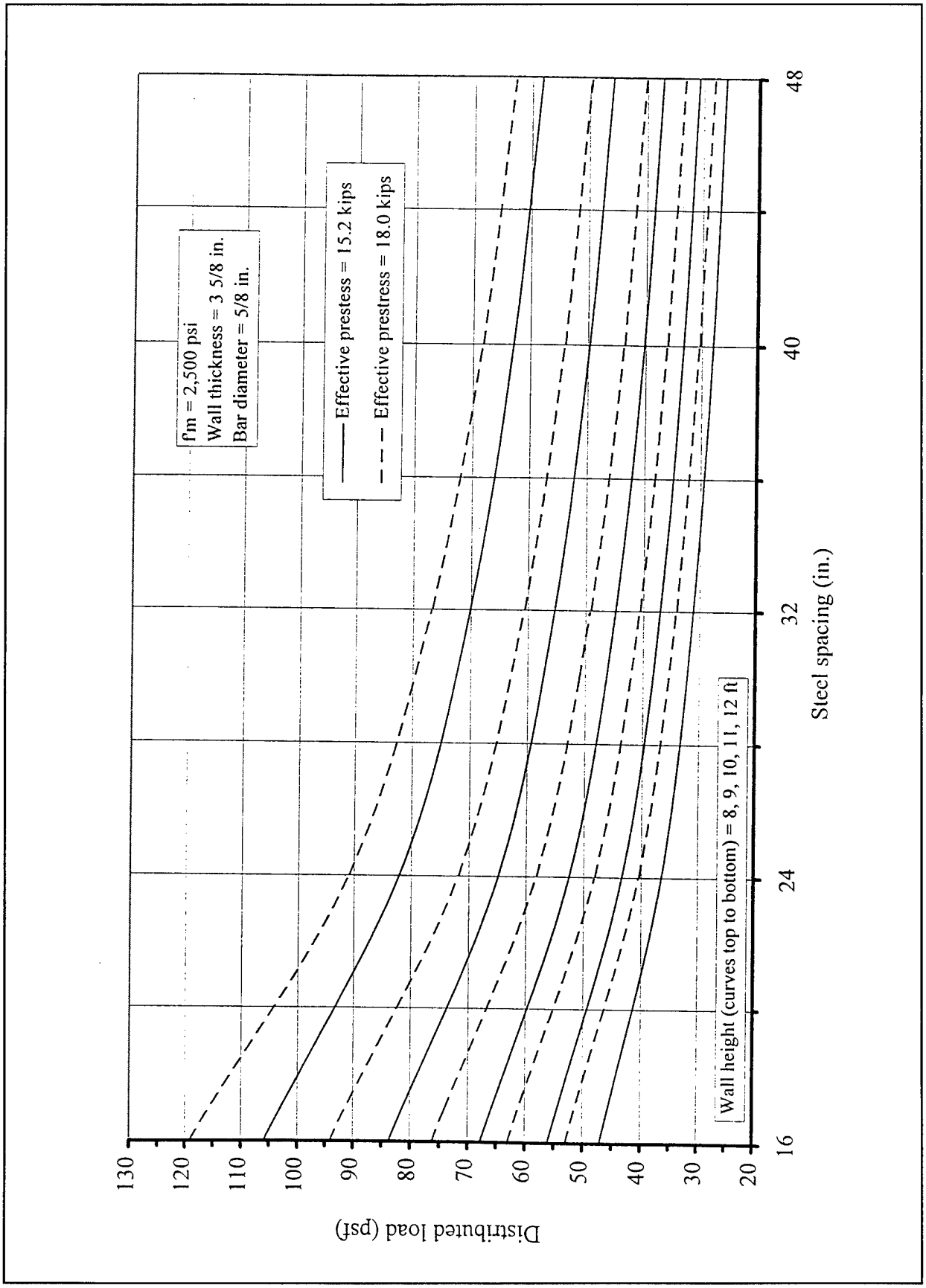

Figure 5.8. Wall capacity at cracking vs. steel spacing.

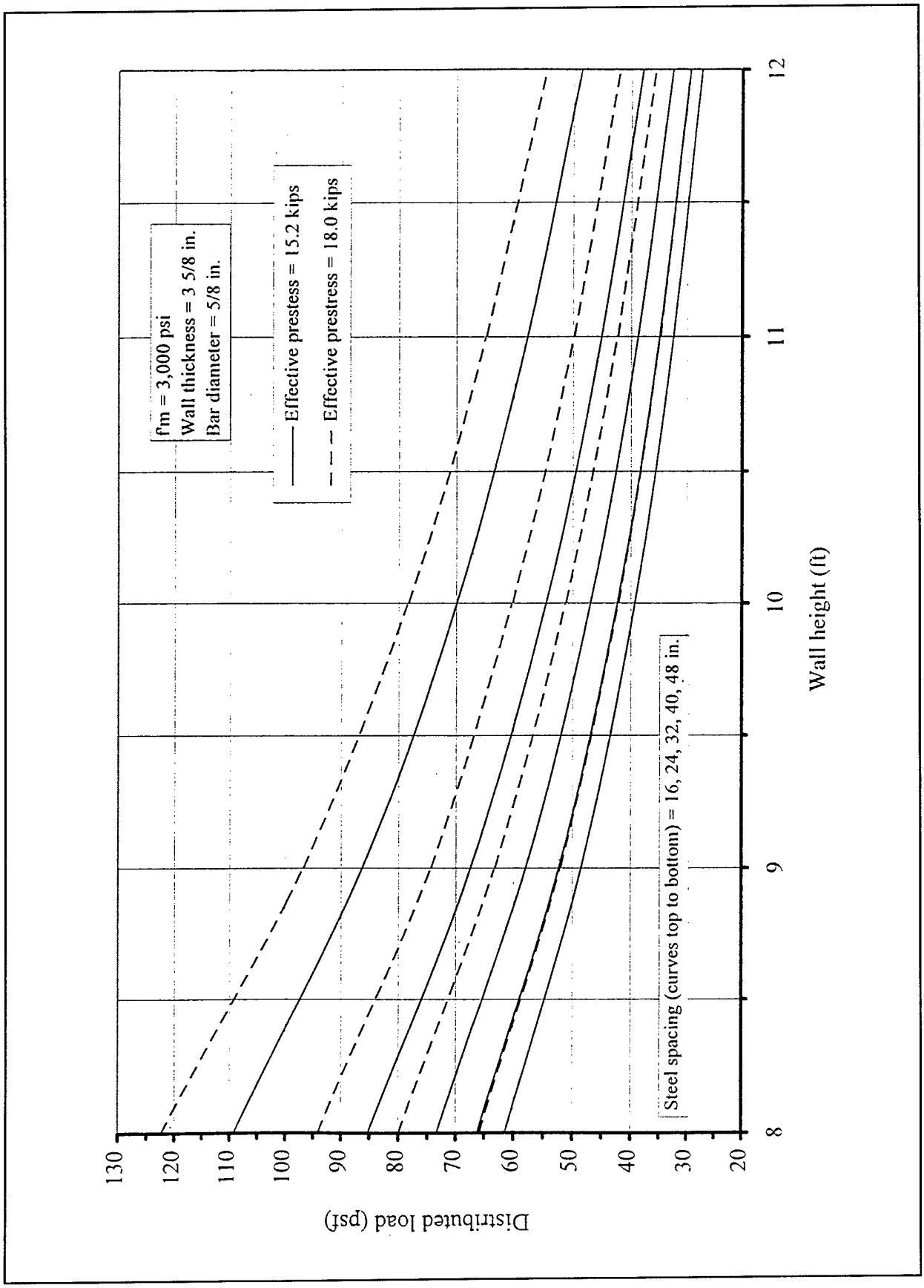

Figure 5.9. Wall capacity at cracking vs. height of wall.

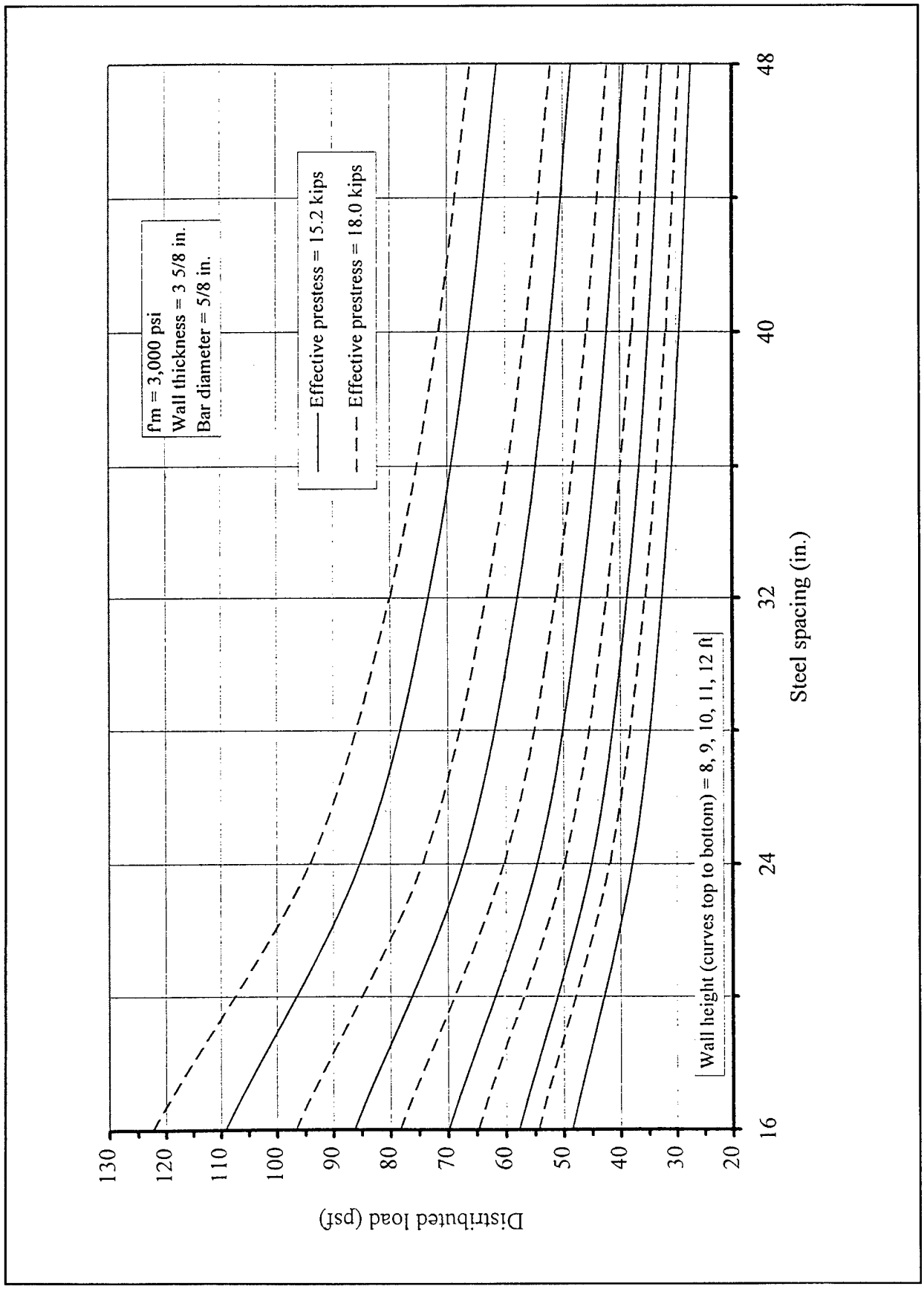

Figure 5.10. Wall capacity at cracking vs. steel spacing.

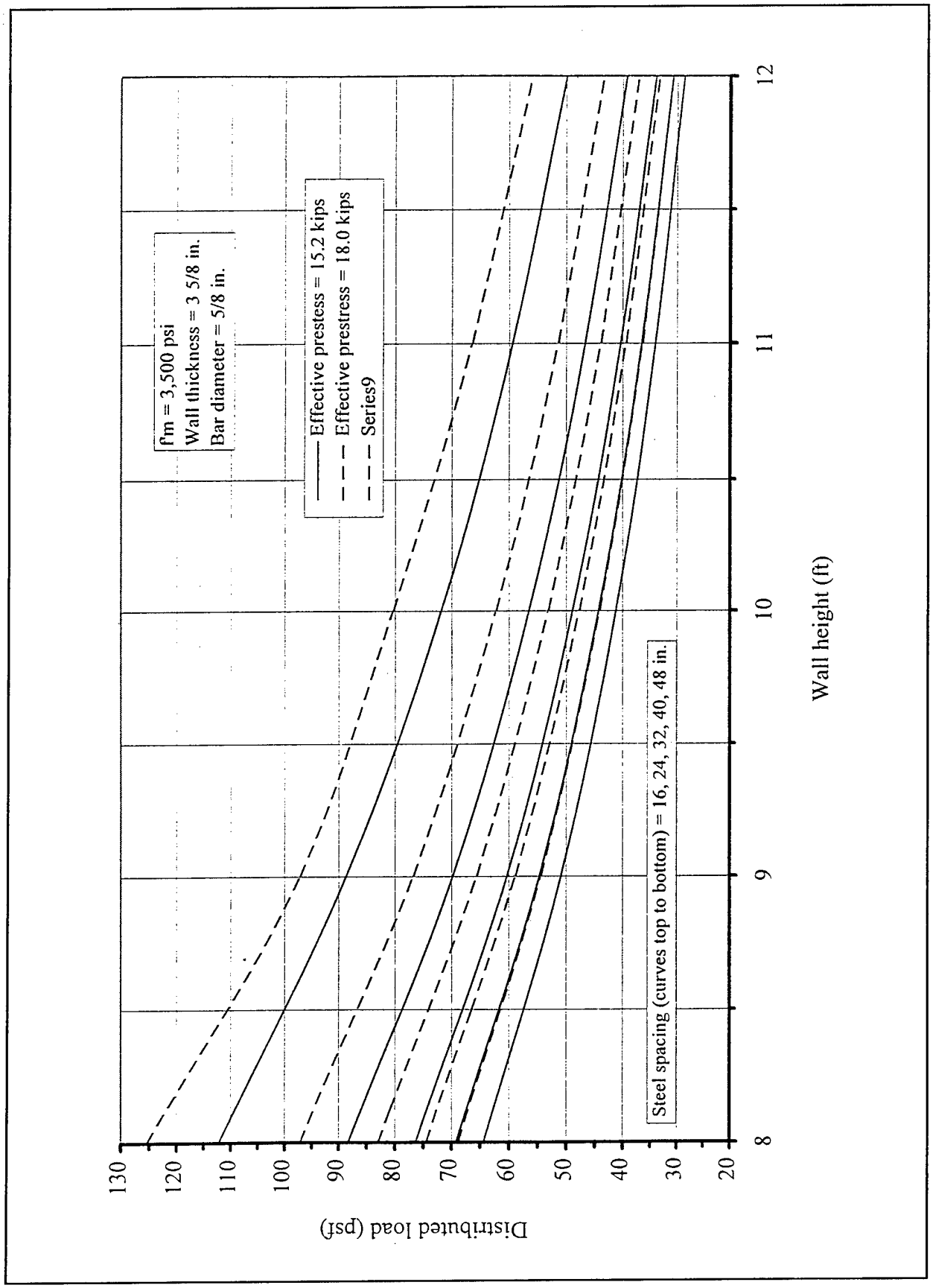

Figure 5.11. Wall capacity at cracking vs. height of wall.

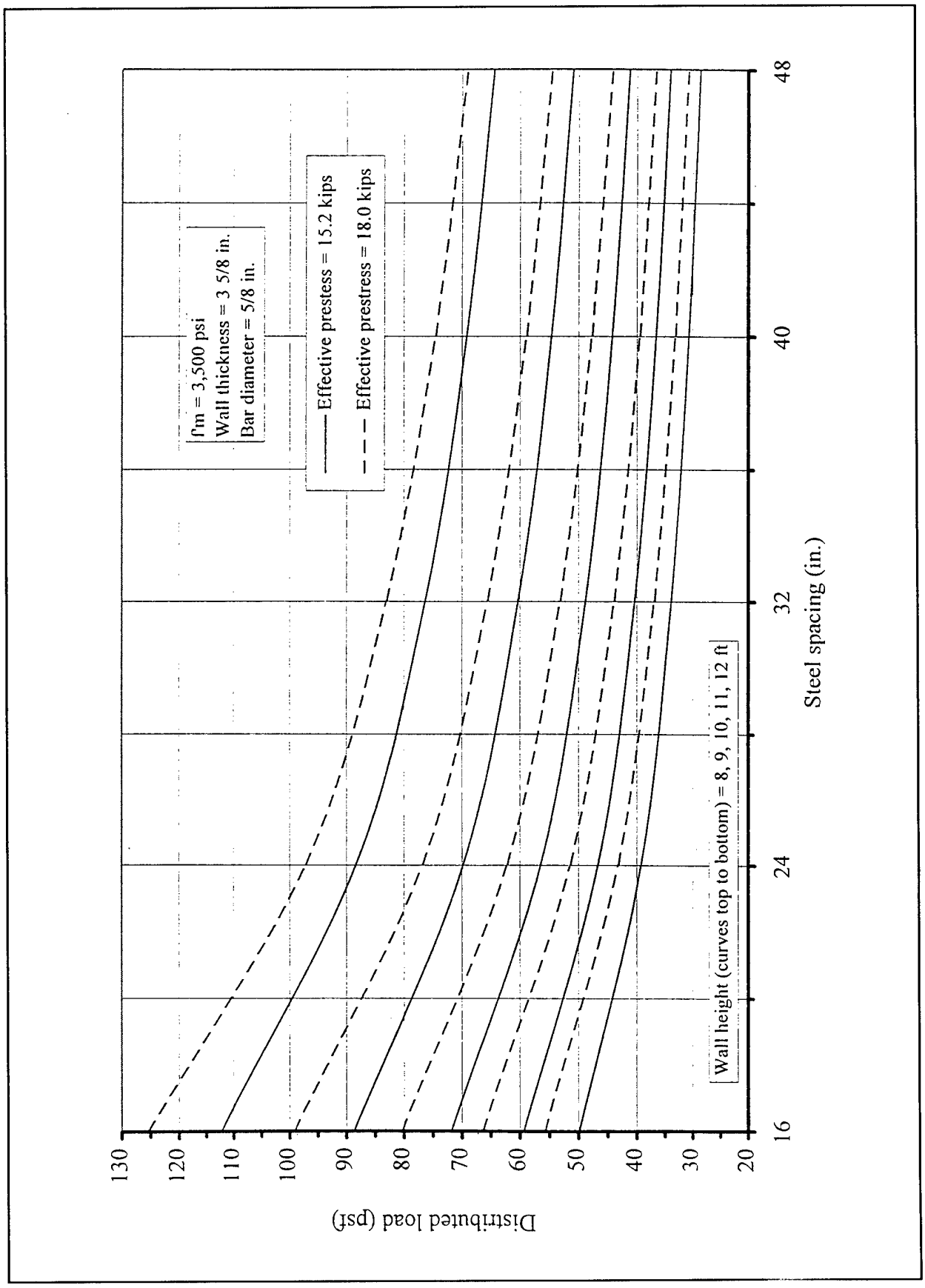

Figure 5.12. Wall capacity at cracking vs. steel spacing.

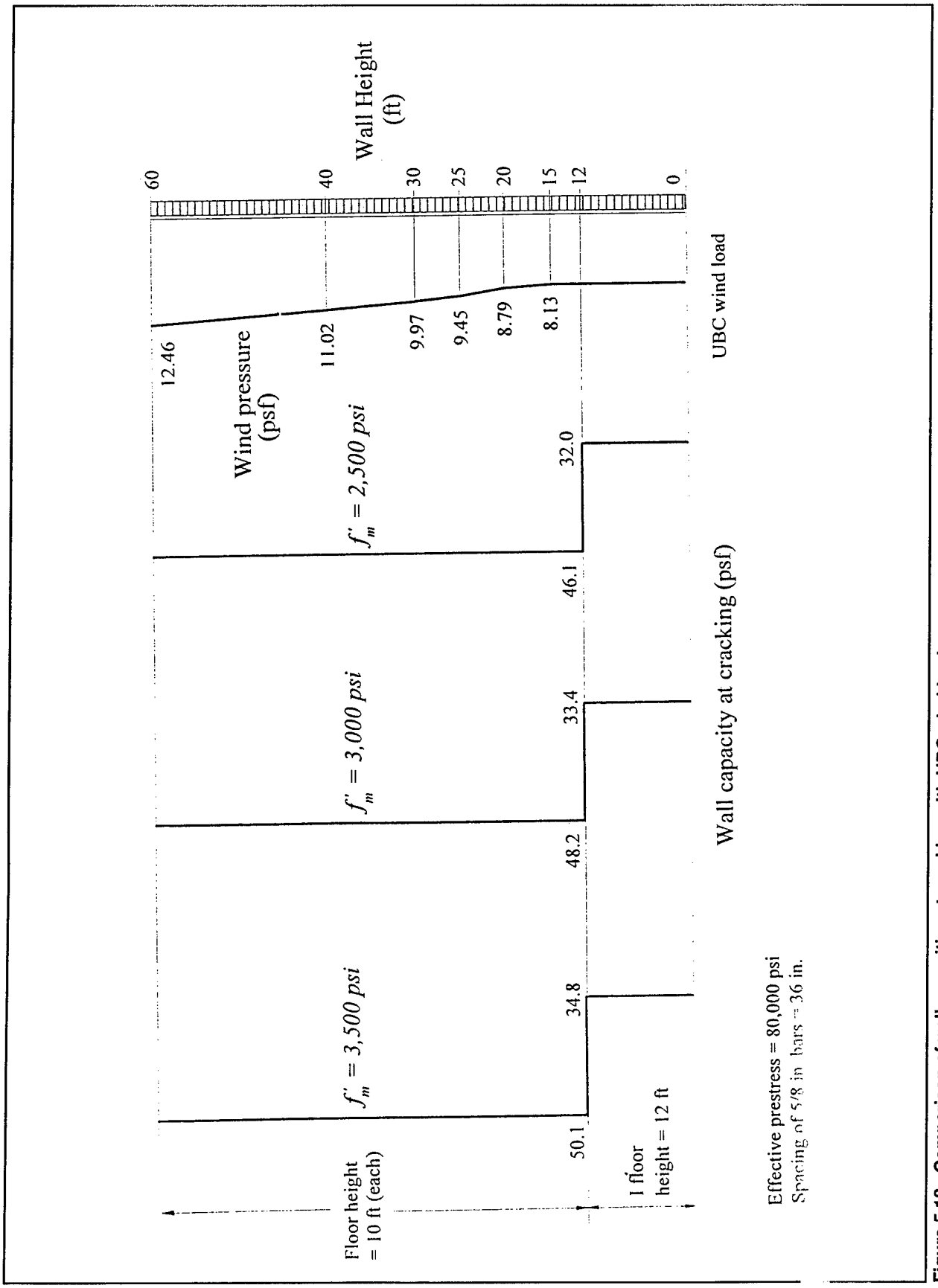

Figure 5.13. Comparison of wall capacities at cracking with UBC wind load.

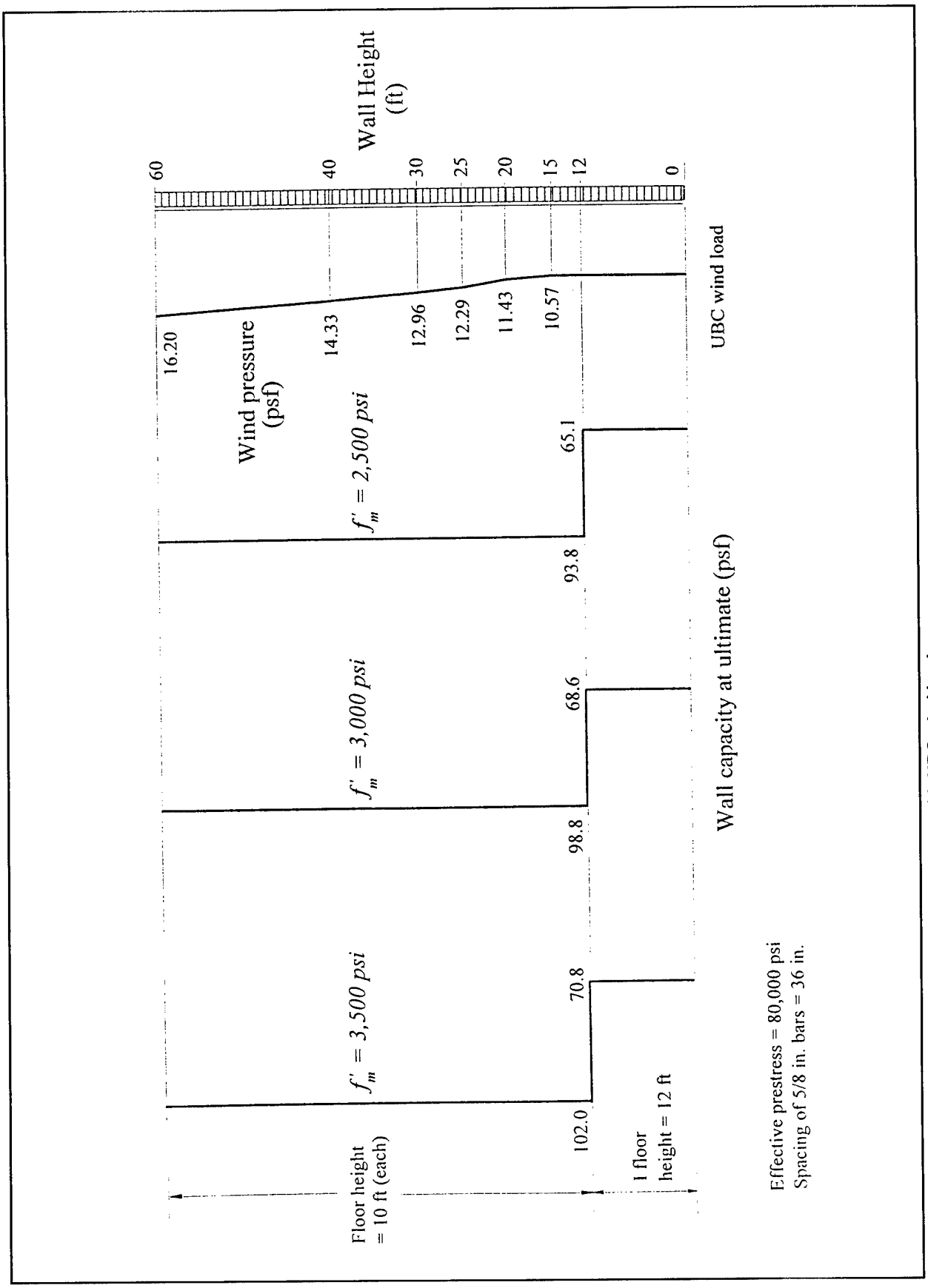

Figure 5.14. Comparison of wall capacities at ultimate with UBC wind load.

Table 5.2. Strain distribution in masonry measured with time.

Wall Designation	Stage (Age After Construction)	Strain Measured from Demec Gage at Different Locations			
		1	2	3	4
	Post-tensioning (9 days)	0.000112	0.000104	0.000032	0.000072
PLP-1	(40 days)	0.000268	0.000224	0.000168	0.000088
	(187 days)	0.000360	0.000312	0.000224	0.000112
	Post-tensioning (7 days)	0.000256	0.000104	0.000056	-0.000008
PLP2	Exposed to outside (40 days)	0.000840	0.000592	0.000524	0.000456
	(187 days)	0.000720	[3]	0.000416	0.000256
	Post-tensioning (8 days)	0.000376	0.000160	0.000088	0.000024
PLA-1	(40 days)	0.000956	0.000648	0.000588	0.000476
	(187 days)	0.001112	0.000728	0.000632	0.000456
	Post-tensioning (7 days)	0.000248	0.000088	0.000024	-0.000024
PLA-2	Exposed to outside (40 days)	0.000808	0.000660	0.000608	0.000480
	(187 days)	0.000704	0.000632	0.000568	0.000696
	Post-tensioning (8 days)	0.000400	0.000176	0.000120	0.000016
PLA-3	(40 days)	0.000928	0.000656	0.000616	0.000448
	(187 days)	0.000968	0.000696	0.000624	0.000456
	Post-tensioning (9 days)	0.000232	0.000096	0.000048	0.000032
PLA-4	Exposed to outside (40 days)	0.000336	0.000220	0.000156	0.000012
	(187 days)	0.000264	0.000176	0.000056	-0.000216
	Post-tensioning (9 days)	[1]	0.000080	0.000040	0.000012[2]
PLA-5	(40 days)	[1]	[3]	0.000128	0.000030[2]
	(187 days)	[1]	[3]	0.000160	-0.000024[2]
	Post-tensioning (9 days)	[1]	0.000100[2]	[1]	0.000008[2]
PLA-6	(40 days)	[1]	0.000216[2]	[1]	0.000052[2]
	(187 days)	[1]	0.000320[2]	[1]	0.000064[2]

[1] not measured at this location
[2] average of two readings
[3] Demec point detached from masonry

Table 5.3. Stress distribution in masonry during post-tensioning.

Number of panels (average)	Initial Prestressing Force (lb)	Theoretical Stress (psi)	Stress Calculated from Strains Measured at Different Locations (psi)			
			1	2	3	4
5	19,000	145.6	674.2	306.1	154.9	38.7
3	16,000	122.6	561.8	222.8	106.6	42.0

Table 5.4. Deformation coefficients at different ages.

Wall Designation	Stage (Age After Construction)	Strain Coefficients at Different Locations			
		1	2	3	4
	Post-tensioning (9 days)	1.00	1.00	1.00	1.00
PLP-1	(40 days)	2.39	2.15	5.25	1.22
	(187 days)	3.21	3.00	7.00	1.55
	Post-tensioning (7 days)	1.00	1.00	1.00	1.00
PLP2	Exposed to outside (40 days)	3.28	5.69	9.35	58.00
	(187 days)	2.81	[2]	7.43	33.13
	Post-tensioning (8 days)	1.00	1.00	1.00	1.00
PLA-1	(40 days)	2.54	4.05	6.68	19.83
	(187 days)	2.96	4.55	7.18	19.00
	Post-tensioning (7 days)	1.00	1.00	1.00	1.00
PLA-2	Exposed to outside (40 days)	3.25	7.50	25.33	21.00
	(187 days)	2.84	7.18	23.67	30.00
	Post-tensioning (8 days)	1.00	1.00	1.00	1.00
PLA-3	(40 days)	2.32	3.73	5.13	28.00
	(187 days)	2.42	3.95	5.20	28.50
	Post-tensioning (9 days)	1.00	1.00	1.00	1.00
PLA-4	Exposed to outside (40 days)	1.45	2.29	3.25	0.38
	(187 days)	1.138	1.83	1.17	-7.75
	Post-tensioning (9 days)	[1]	[1]	1.00	1.00
PLA-5	(40 days)	[1]	[1]	3.20	2.50
	(187 days)	[1]	[1]	4.00	-3.00
	Post-tensioning (9 days)	[1]	1.00	[1]	1.00
PLA-6	(40 days)	[1]	2.16	[1]	1.23
	(187 days)	[1]	3.20	[1]	8.00

[1] not measured at this location
[2] Demec point detached from masonry

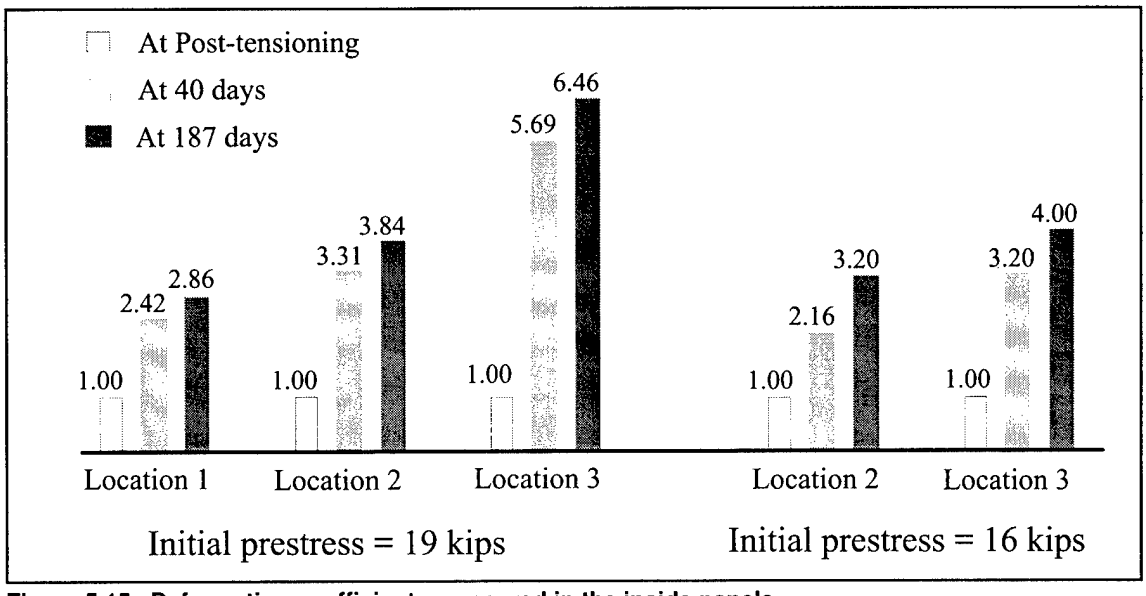

Figure 5.15. Deformation coefficients measured in the inside panels.

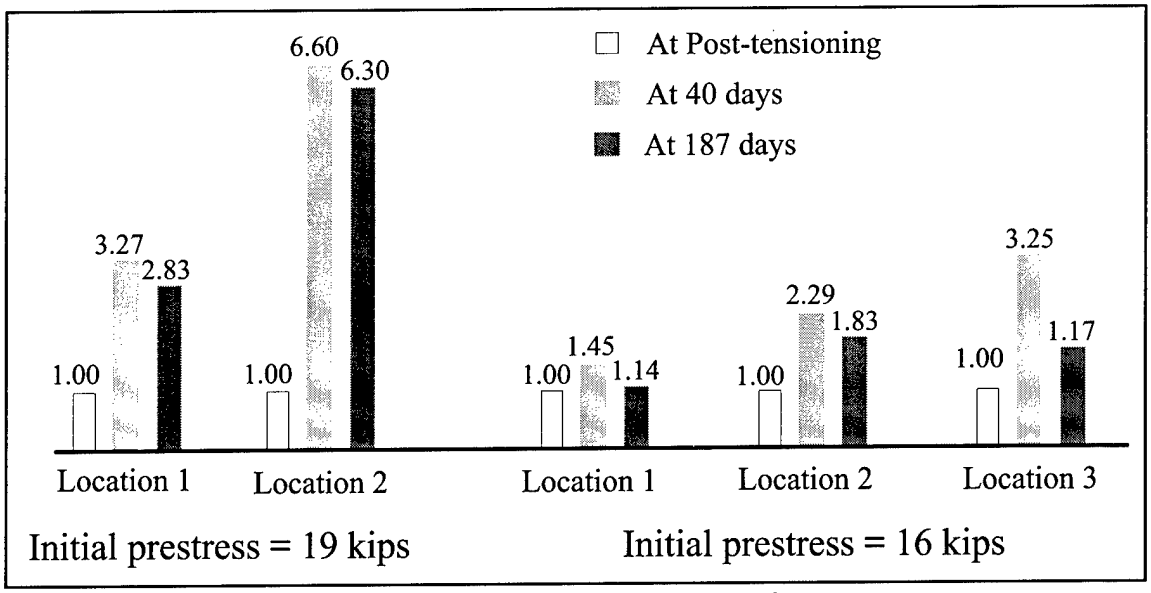

Figure 5.16. Deformation coefficients measured in the outside panels.

Table 5.5. Stress change in prestressing steel.

Wall Designation	Change in Stress Recorded from Strain Gages (%)
PLP-1	-6.03
PLP-2	+15.01
PLA-1	[1]
PLA-2	-5.96
PLA-3	-8.76
PLA-4	-5.20
PLA-5	-8.40
PLA-6	-6.16

Note: +ve indicates gain, and -ve indicates loss
[1] ignored due to abrupt values

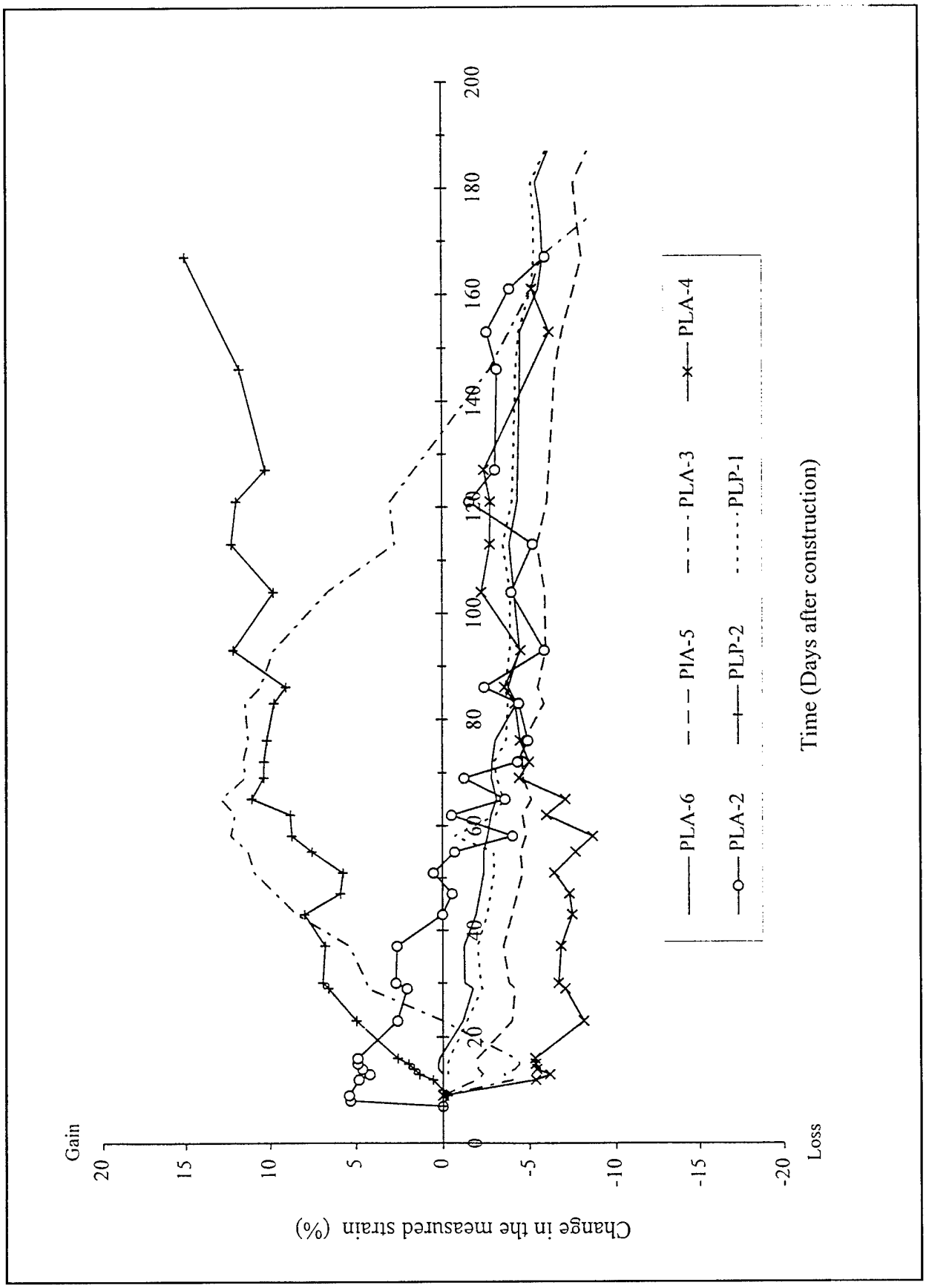

Figure 5.17. Change in steel strain with time.

6 Design Guidelines and Details

Design issues such as the allowable stresses in masonry and steel are discussed in this chapter based on the results of this research. The results discussed here may not be generalized to all prestressed masonry applications. Since there has been a lack of experimental research available on prestressed clay brick masonry, the comparisons are made with codes and standards. The provisions of the MSJC Code [Prestressed 1995], BS 5628 [Code 1985], and ACI 530/ASCE 5/TMS/402 [Building 1992] are compared wherever applicable. A summary of prestress loss results is given with recommendations. A detailed analysis of bonded and unbonded wall panels is included in Appendix B.

6.1 Permissible Stresses

The allowable compressive, flexural tension, and bearing stresses are covered in this section. The steel stresses encountered at transfer and service are discussed. At present only the MSJC Code [Prestressed 1995] addresses the provisions for prestressed masonry design. The results are compared with other previous studies and code provisions.

6.1.1 Masonry

6.1.1.1 ***Flexural Tension.*** The tensile stresses obtained from the test specimens of Stage I and II were $2.66\sqrt{f'_m}$ and $2.87\sqrt{f'_m}$ respectively, which corresponds to 143 psi (0.98 MPa) and 168 psi (1.2 MPa). These experimental values were approximately 5 percent of their compressive strengths, and are higher than the UBC's allowable stress limitation of $2.5\sqrt{f'_m}$ [UBC 1994]. The ACI 530/ASCE 5/TMS 402 [Building 1992] standard allows a value of 30 psi (0.21 MPa).

The British Code BS 5628 [1985] allows cracking of prestressed masonry members under service loads. This is a reasonable provision considering that prestressed masonry has a tendency to close cracks upon the removal of external loads. The testing of panels yielded a smooth load-deflection behavior without any significant loss of stiffness after cracking. Based on these experimental studies, it is suggested to restrict the flexural tension to its modulus of rupture under service loading for the application of a veneer wall subjected to wind loads. This will help safeguard

against water getting into the masonry through cracks which could lead to corrosion.

6.1.1.2 ***Compression Stress at Prestress Transfer.*** When prestressing the walls, care must be taken to avoid local crushing of the masonry. To avoid crushing, limits are placed on the maximum compression that can be applied to the masonry during prestressing. This stage is considered to be the most severe loading in the life span of a prestressed member. Pure compressive stresses are discussed here based on the stresses that occurred during the post-tensioning operation. The stress distribution showed that the prestress did not induce a completely uniformly distributed stress in the cross-section. The maximum stress recorded below the anchorage was 674.2 psi (4.65 MPa) which was nearly 23 percent of the strength of masonry at transfer. This stress was induced at the age of one day to the wall specimens, and no cracks were noticed surrounding the highly stressed area.

The maximum allowable stress by the BS 5628 [Code 1985] at transfer is limited to $0.4\,f'_m$. Schultz and Scolforo [1992] recommended a conservative limit of $0.3\,f'_m$ based on the research to date, and suggested to increase the limit to $0.33\,f'_m$ in the future. The ACI 530/ASCE 5/TMS 402 [Building 1992] limitations to reinforced masonry is approximately $0.25\,f'_m$ without the slenderness effects. The UBC [1994] allows a maximum of 25 percent of the compressive strength plus slenderness effects if any. The allowable compression limits can be increased after all losses have occurred in the member. This can be attributed to the increase in masonry strength over time and a decreased prestressing force due to long-term losses. The results of the panel tests indicate that the $0.25\,f'_m$ limit works well for prestressed clay brick masonry also.

6.1.1.3 ***Bearing Stresses.*** In the design of post-tensioned masonry members, consideration should be given to anchorage zone stresses that develop beneath the bearing plate. Underestimation of these stresses could lead to localized crushing and spalling of masonry. The ACI 530/ASCE 5/TMS 402 [Building 1992] standard requires the bearing stress, F_{br}, to be less than $0.25\,f'_m$. The supporting area is to be calculated assuming an 45° sloping surface. The limitation is very close to the UBC limit of $0.26\,f'_m$ or $0.38\,f'_m$ depending on the area being loaded. In the test panels, the bearing plates were 1/3 the width of panel, and thus the $0.38\,f'_m$ limitation controls, but in the panels where shelf angles were used, which spanned all across the width of the panel, it is limited to $0.25\,f'_m$.

The stress concentrations experienced by the test specimens beneath the anchorage were nearly 4.63 times the average theoretical value (see Table 5.3). It corresponds to $0.2\,f_{mi}$ and did not cause any distress or crushing in the bearing zone. The prestress was reduced as it was farther from the anchorage zone. Based on these

tests, it appears that the 20 percent of compressive strength limit at transfer works well for prestressed clay brick masonry also.

6.1.2 Prestressing Steel Stresses

In the case of post-tensioned applications, the stress at jacking will be the same as the stress at initial prestress transfer. This is due to the fact that the elastic shortening of the masonry occurs simultaneously with the application of the prestress. The MSJC Code [Prestressed 1995] specifications allow a maximum stress in the steel of 0.82 f_{py} or 0.74 f_{pu} whichever is smaller. The high-strength prestressing bars used for post-tensioning in this research had a yield strength of 0.75 f_{pu}. Hence the limitation would be 0.82 (0.75) f_{pu} = 0.62 f_{pu} which corresponds to 80,200 psi (553 MPa).

BS 5628 [Code 1985] uses a value of 0.70 f_{pu} for maximum allowable jacking force with a quality control factor of 1.0 for serviceability and 1.15 for ultimate strength. Schultz and Scolforo [1992] recommended the ACI 318 [1989] limits of prestressed concrete for prestressed masonry. The allowable limit for the bar tendons at transfer is 0.70 f_{pu} immediately after anchorage. The different initial prestress applied to the panels were 19 kips (84.5 kN) and 16 kips (71.2 kN). These correspond to 0.65 f_{pu} and 0.55 f_{pu} and in the former case, the code limit was exceeded by 5 percent. It should be noted that the code does not include steel grades lower than 150 ksi (1035 MPa). Based on the experimental test results, these limits on stresses in steel seem to work well in prestressed clay brick applications.

Two different cases of test specimens with bonded and unbonded tendons were tested in Stage I of the experimental work. In the case of bonded beams, the stress in the steel at ultimate flexure was calculated by strain compatibility analysis. Based on the theoretical calculations using actual material properties, the steel stress at nominal strength was equal to 0.9 f_{pu}, in Stage I and 0.92 f_{pu} in Stage II panels. The average ultimate stresses measured from strain gages of the test specimens were equal to 0.81 f_{pu} from Stage I and 0.78 f_{pu} from Stage II. These results indicate that the steel did not develop to its ultimate capacity at nominal strength. These values were in agreement with the measured and theoretical values of ultimate moment shown in Chapter 5.

To calculate the stress in steel at nominal moment of unbonded specimens (Stage I), the following MSJC Code [1995] equation was used:

$$f_{ps} = f_{se} + (100{,}000)\left(\frac{d}{l}\right)\left[1 - 1.4\left(\frac{f_{pu}A_{ps}}{bdf'm}\right)\right] \qquad \text{[Eq 6-1]}$$

Using Equation 6-1, the stress in the steel was calculated to be 80,557 psi (555.6 MPa). The second term on the right hand side of the equation yielded a negligible stress increase (1.15 percent) to the effective prestress (see Appendix B). But the experimental stress values (recorded from strain gages) showed an average increase of 21 percent of the effective prestress. From this comparison, it is clear that the equation (6-1) did not accurately reflect the measured behavior of the test specimens.

6.2 Prestress Losses

The analysis of prestress losses has been discussed in detail in Chapter 5. In this section, the results obtained for the tests are discussed. There was no prestress loss due to the elastic deformation of masonry as it occurred simultaneously during post-tensioning. The masonry deformation was monitored in each panel at different locations. The recorded deformation values represented the cumulative effects for all the above mentioned causes. The steel strains were monitored through strain gages which included relaxation loss plus the deformations occurring in masonry. Loss due to stress relaxation could not be differentiated since the steel bars were grouted.

The total loss of steel stress as recorded from the strain gages for the inside panels, ranged from 6.03 percent to 8.76 percent. Among the three outside panels, one experienced a gain of 15.01 percent and the other two showed a loss of 15.2 percent and 5.96 percent. The masonry strains recorded showed an increase in the compressive strains in the inside panels. Nearly 85 percent of the total compression deformation occurred in the first 40 days in the panels with an initial prestress of 19 kips (84.5 kN). The strains decreased (due to masonry expansion) in the three specimens that were exposed to outdoor temperature and humidity.

Appendix C gives the calculation of prestress losses based on the MSJC Code [Prestressed 1995] provisions. The test results compare well with the prestress gain of 0.4 percent calculated using the MSJC Code. It showed that the procedure used in the MSJC Code to calculate prestress losses also worked reasonably well for pre-stressed clay brick masonry.

6.3 System Details

6.3.1 Construction

During the construction of the panels, a sponge connected to a wire was used to keep the void in the brick clear of any mortar, so that the prestressing bar could

readily be placed after the wall was constructed (see Chapter 4, Figure 4.13). Although this requires considerable care by the mason, it is a common practice for standard (not prestressed) reinforced clay masonry construction, and therefore does not represent a significant change in practice.

6.3.2 Design

The most significant change as a result of this construction was the elimination of wall ties and the inclusion of an angle section at each story height (in addition to the typical shelf angle). The angle sections act as supports for the vertical and horizontal loads and transfer these loads into the structural system, as well as bearing plates for the post tensioning system. Two angles are used to uncouple the system from one story height to the next and facilitate prefabrication as well. Standard details for this type of construction are shown in Figures 6.1 and 6.2 for connections at the foundation level, and at the top of each wall respectively.

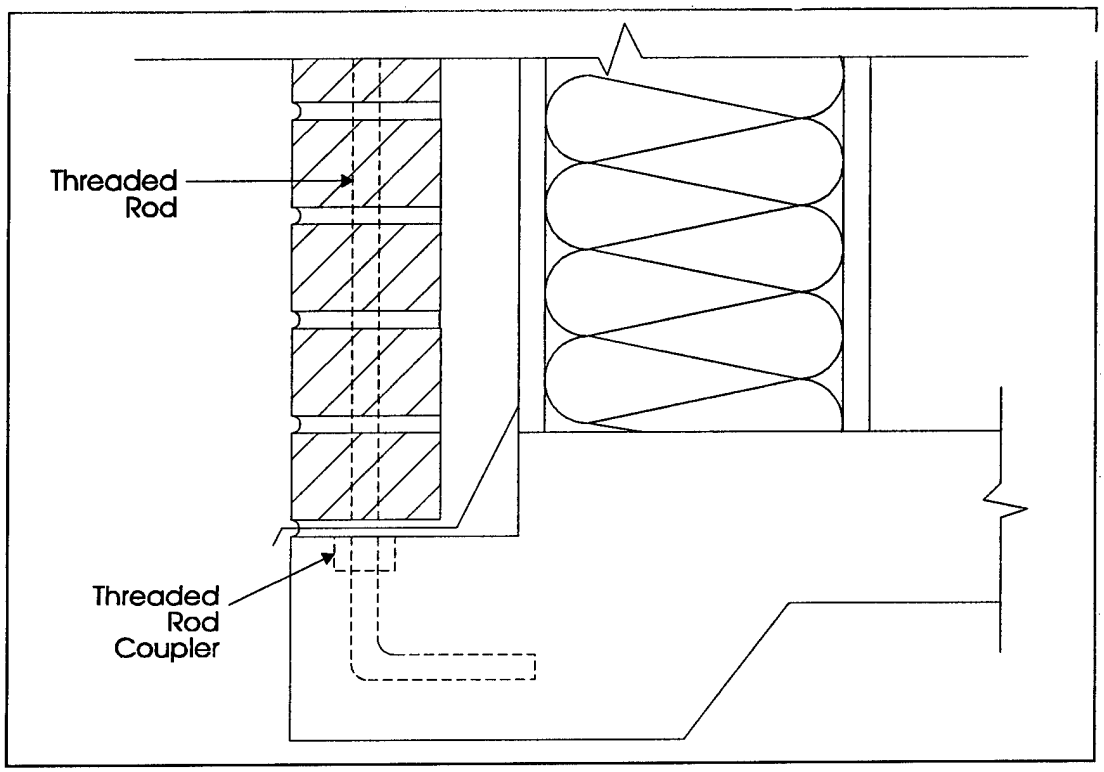

Figure 6.1. Detail of prestressing bar at foundation.

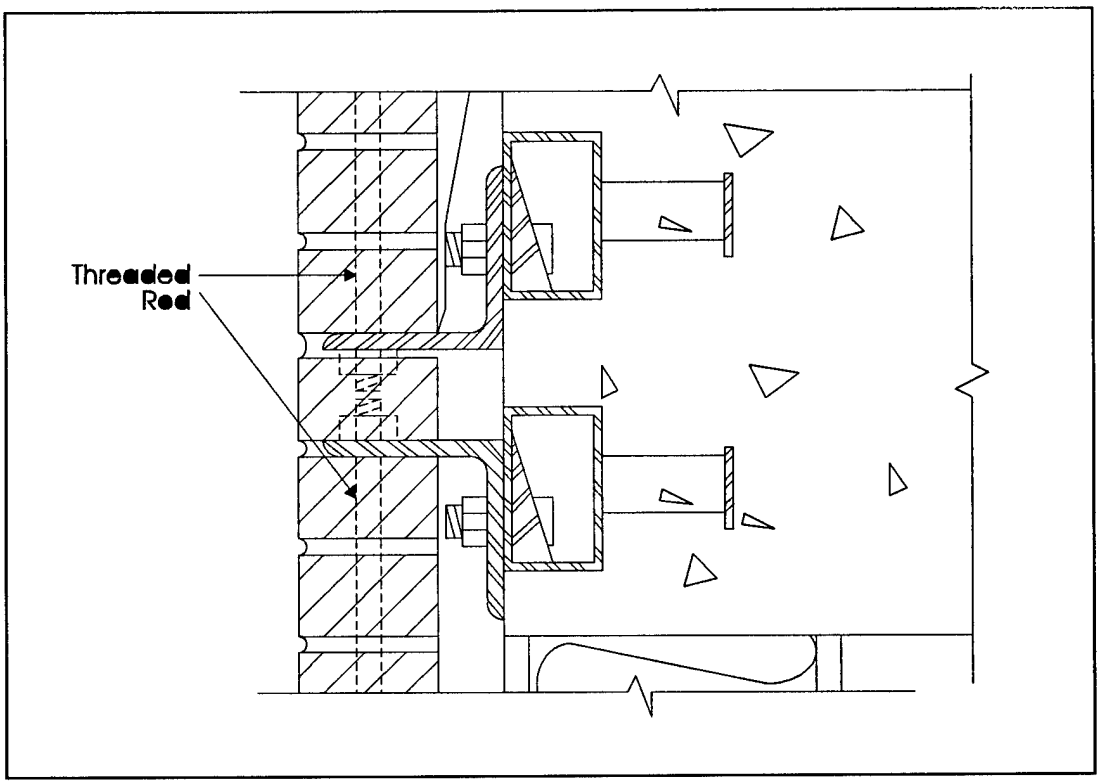

Figure 6.2. Detail of connection at top of wall.

7 Conclusions, Recommendations, and Commercialization

A new post-tensioned clay brick masonry wall system has been developed. A total of 14 wall panels were tested to study the out-of-plane loading behavior. Eight panels were monitored for 180 days to investigate the prestress losses. The test results were compared with the design wind loads of the UBC. A load-deflection analysis was conducted and the results were compared with experimental results. Based on the results of this research study, the following conclusions can be drawn.

7.1 Conclusions

Prestressed clay brick masonry walls provide significant overall performance improvement compared to standard clay brick construction. Using a standard design approach and modified structural detailing, simple prestressed clay brick walls can be constructed in the field. With the exception of the custom-designed masonry unit, which allows for the insertion of prestressing tendons, the system documented here can be constructed using common commercially available materials. The masonry unit presented varies in shape only; it is made from standard materials and processes and can be manufactured by most modern brick producing plants. The system is documented and ready for adoption by construction specifiers and engineers. If used appropriately and within the guidelines and limitations stated in this report, the system will provide overall construction and performance benefits over standard brick masonry configurations, and it advances technology in this sector of the masonry construction industry.

7.1.1 Technique

The masonry post-tensioning system proposed in this research uses DTI washers to measure the prestressing force. The system uses high-strength threaded bars

with the prestressing force being applied by turning the nut. It is concluded that the technique is simple and reliable, and that it offers the following advantages:

1. Prestressed clay brick masonry walls are feasible, potentially simple to build on job sites, and could be adopted as an alternative to the current system of veneer construction.
2. The system eliminates the need for wall ties.
3. Standard construction materials can be used for the prestressed masonry system with only minor changes in the brick shape and construction technique.
4. The use of the DTI washers is a reliable way to measure prestressing force.
5. The use of a shelf angle instead of a plate at the anchorage does not cause any significant difference in ultimate strength or deflection.
6. The proposed method will be suitable for different wall thickness.
7. Post-tensioning can be applied as soon as one day after the construction of the walls, with the limitation on compressive stress of 0.25 f'_m, without any negative effects.

7.1.2 Material Properties

Because masonry strengths varied greatly even though the same materials were used in all specimens, it is concluded that a large number of prism specimens is required to accurately determine the strength of the masonry.

7.1.3 Wall Strength

Based on the out-of-plane load tests, which were conducted in two stages, it is concluded that prestress significantly improves wall performance both at service and ultimate loads. It also is concluded that:

1. Ungrouted wall panels are not recommended due to their lower capacity and sudden brittle failure.
2. Veneer wall panels designed using the new system can easily withstand the UBC design level wind pressure without cracking.
3. The load-deflection curves show that the walls are capable of resisting loads even after cracking without significant loss of stiffness.
4. The wall panels regain nearly 50–60 percent of the deflection upon the removal of the applied load.
5. A single crack formed in the ungrouted specimens, whereas in grouted specimens, several cracks developed in the middle third span.
6. The behavior of the panels follows the theoretical behavior very closely, indicating that prestressed clay brick masonry can be analyzed accurately by current methods.

7.1.4 *Prestress Losses*

Eight walls were monitored for the prestress loss study for a period of 187 days. Three of these specimens were subjected to outside weather conditions from the age of 40 days. Comparison studies were made in Chapter 6 between outside and inside panels and panels with two different initial prestressing forces. The proposed system of post-tensioning of masonry showed a lower prestress loss compared to the standard methods adopted for concrete members. Based on the experimental results, it is concluded that:

1. Walls exposed to outside weather conditions experience a gain (15.01 percent maximum in this study) in prestress due to the moisture expansion of clay masonry while inside panels experience a prestress loss (8.76 percent maximum in this study at 180 days).
2. Loss and gain values are well within the bounds reported by other previous research studies.
3. The MSJC Code equations for predicting prestress losses are applicable to prestressed clay brick walls.
4. The results of this loss study should be considered preliminary until further research into the separate causes of the loss/gain can be performed.

7.2 Recommendations

Based on this research and work by others cited in this report, it is recommended that prestressed clay brick walls be used for clay brick veneers as appropriate under the limitations detailed within this report. Particular attention and consideration should be given to the following issues when designing prestressed masonry wall systems:

1. post-cracking behavior of prestressed masonry, which is nonlinear and complex in nature
2. practical connection detail for the ends of panels
3. the effect of slenderness on the strength of taller walls (i.e., higher than 15 ft)
4. the long-term loss of prestress.

7.3 Technology Transfer and Commercialization

The innovative two-cored clay brick design produced in this project conforms to ASTM C 216-87, *Standard Specification for Facing Brick*. Fabrication of the two-cored brick requires no specialized technology, so the unit can be manufactured by

any modern brick-manufacturing plant. The design details documented in the current report are complete and ready for adoption by manufacturers.

The Masonry Structures Joint Committee, comprising representatives of interested technical and professional societies including the American Concrete Institute, the American Society of Civil Engineers, and The Masonry Society, is currently developing a limit-states design code that will become the national standard masonry design code. The results of the current research have been provided to the Joint Committee for inclusion in this limit-states design code.

When the Joint Committee completes the limit-states design code, it is anticipated Army Technical Manual (TM) 5-809-3, *Masonry Structural Design,* will be discontinued as part of the effort to use national standards in military construction. If specific recommendations for the use of prestressed clay brick construction are not adopted in the upcoming national standard, recommendations for incorporating design procedures for this system will, in compliance with the new limit-states code, be proposed for inclusion into Army engineering instructions.

Results of this research were presented to and published for industry professionals at The 10th International Brick/Block Masonry Conference (University of Calgary, Alberta, July 1994) in the paper "Experimental Investigation on the Flexural Behavior of Prestressed Masonry," by Devalapura, Krause, and Tadros.

Manufacturing details for the prestressing system developed in this work were developed through the University of Nebraska, and are available from the University of Nebraska (Omaha) Center for Infrastructure Research.

References

American Society for Testing and Materials (ASTM) C67 - 87, *Standard Method of Sampling and Testing Brick and Structural Clay Tile* (ASTM, Philadelphia, PA, 1987).

ASTM F 959-93a, *Standard Specification for Compressible-Washer-Type Direct Tension Indicators for Use with Structural Fasteners* (ASTM, Philadelphia, PA, 1993).

ASTM C 216-87, *Standard Specification for Facing Brick* (ASTM, Philadelphia, PA, 1987).

ASTM C 270 - 87a, *Standard Specification for Mortar for Unit Masonry* (ASTM, Philadelphia, PA, 1987).

ASTM E 447 - 84, *Standard Test Methods for Compressive Strength of Masonry Prisms* (ASTM, Philadelphia, PA, 1984).

Al-Manaseer, A.A., and Neis, V.V., "Load Tests on Post-tensioned Masonry Wall Al-Manaseer, A.A., and Neis, V.V., "Load Tests on Post-tensioned Masonry Wall Panels," *ACI Structural Journal*, vol 84, no. 6 (November-December 1987), pp 467-472.

Amrhein, J.E., W.M. Simpson, L.G. Selna, and R.E. Tobin, "Slender Masonry Wall Test," *Proceedings of the Third Canadian Masonry Symposium* (University of Edmonton, Edmonton, Alberta, 1983), pp 11-1–11-15.

Anderegg, F.O., and C.L. Dalzell, "Pre-Stressed Ceramic Members," *Proceedings of the American Society for Testing and Materials (American Society for Civil Engineers [ASCE]*, vol 35, pt. 2, 1935), pp 447-456.

Arora, S.K., "Review of BRE Research Into Performance of Masonry Walls Under Concentrated Load," *Proceedings of the 8th International Brick and Block Masonry Conference* (Dublin, Republic of Ireland, September 1988), vol 1, pp 446-457.

Bexten, K.A., M.K. Tadros, and R.T. Horton, "Compression Strength of Masonry," *Proceedings of the 5th Canadian Masonry Symposium* (University of British Columbia, Vancouver, British Columbia, June 1989), pp 629-639.

Bradshaw, R.E., J.P. Drinkwater, and S.E. Bell, "A Multi-Purpose Farm Building Incorporating Pre-stressed Brickwork Diaphragm Walling," *Proceedings of the British Ceramic Society, Load-Bearing Brickwork (7)*, vol 30 (September 1982), pp 308-315.

Brick Veneer, Steel Stud Panel Walls, Technical Notes on Brick Construction (Brick Institute of America [BIA], No. 28B Revised II, Reston, VA, February 1987).

Brochelt, G.B., "History of Masonry Veneer," *Proceedings of the Eighth International Brick and Block Masonry Conference* (Dublin, Republic of Ireland, September 1988), pp 1496-1506.

Brooks, J.J., and P.R. Bingel, "Stress Relaxation Due to Creep and Moisture Movement in Single-Leaf Masonry Walls," *Proceedings of the 10th International Brick/Block Masonry Conference* (University of Calgary, Calgary, Alberta, July 1994), vol 3, pp 1623-1633.

Building Code Requirements for Reinforced Concrete (ACI 318-89) (American Concrete Institute [ACI], Detroit, MI), pp 353.

Building Code Requirements for Masonry Structures (ACI 530-92/ASCE 5-92/TMS 402-92) (ACI, American Society for Civil Engineers [ASCE], and The Masonry Society [TMS], 1992).

Code of Practice for Use of Masonry: Parts 1, 2, and 3, BS 5628 (British Standards Institution, London, 1985).

"Corrosion Problems in Masonry Veneer Over Metal Stud Wall System," *Concrete Technology Today* (Portland Cement Association, Skokie, IL, vol 4, no 3, September 1983), pp 4.

Cowie, J.W., "The Failure of Steel Studs," *The Magazine of Masonry Construction*, vol 3, no. 2 (February 1990), pp 82-84.

Curtin, W.G., "An Investigation of the Structural Behavior of Post-Tensioned Brick Diaphragm walls," *The Structural Engineer*, 64B, no 4 (December 1986), pp 77-84.

Curtin, W.G., "Development, Application and Potential of Reinforced and Prestressed Masonry," Reinforced and Prestressed Masonry (Telford Ltd, London, May 1982), pp 1-12..

Curtin, W.G., "Post-Tensioning Opens Brickwork Frontiers," *Contract Journal*, vol 333, no 558 (1986), pp 26-27.

Curtin, W.G., "Site Testing and Lab Research for the Design Development of Prestressed Brickwork," *Practical Design of Masonry Structures* (Thomas Telford Ltd., London, 1987), pp 237-254.

Curtin, W.G., S. Adams, and M. Sloan, "The Use of Post-Tensioned Brickwork in the SCD System," *Proceedings of the British Ceramic Society, Load-Bearing Brickwork(5),* no. 24 (September 1975), pp 233-245.

Curtin, W.G., and J.K. Beck, 'The Structural Design of a Concrete Blockwork Retaining Wall," *Concrete*, vol 20, no. 7 (1986), pp 19-21.

Curtin, W.G., and J. Howard, "Lateral Loading on Tall Post-Tensioned Brick Diaphragm Walls," *Proceedings of the 8th International Brick and Block Masonry Conference* (Dublin, Republic of Ireland, September 1988), pp 595-605.

Curtin, W.G., G. Shaw, and J. Howard, "Structural Testing of a Post-Tensioned Brick Fin Wall," *Proceedings of the 9th International Brick/Block Masonry Conference (IBMAC)* (Berlin, Germany, October 1991), pp 333-341.

Curtin, W.G., G. Shaw, J.K. Beck, and W.A. Bray, "Modern Philosophy of Structural Brickwork Design and a Change of Outlook for the Brick Industry," *Proceedings of the 6th International Masonry Conference, ANDIL*, Rome (1982), pp 939-948.

Curtin, W.G., G. Shaw, J.K. Beck, and W.A. Bray, *Structural Masonry Designers' Manual*, Second Edition (BSP Professional Books, Oxford, England, 1987), pp 448.

Curtin, W.G., G. Shaw, J.K. Beck, and L.S. Pope, "Post-Tensioned Free Cantilever Diaphragm Wall Project," *Reinforced and Prestressed Masonry* (The Institution of Civil Engineers, Thomas Telford, Ltd., London, 1982), pp 79-88.

Dawe, J.L., and G.G. Aridru, "Post-Tensioned Concrete Masonry Walls Subjected to Uniform Lateral Loading," *Proceedings of the 6th Canadian Masonry Symposium* (University of Saskatchewan, Saskatoon, Saskatchewan, June 1992), pp 201-212.

Devalapura, R.K., G.L. Krause, and M.K. Tadros, "Experimental Investigation on the Flexural Behavior of Prestressed Masonry," *Proceedings of the 10th International Brick/Block Masonry Conference* (University of Calgary, Calgary, Alberta, July 1994).

Differential Movement, Technical Notes on Brick Construction (Brick Institute of America [BIA], No. 18, 18A, and 18B, Reston, VA, Revised 1991, 1986, and 1988).

Dikkers, R.D., and F.Y. Yokel, "Strength of Brick Walls Subject to Axial Compression and Bending," *Proceedings of the 2nd International Brick Masonry Conference* (England, April 1970), pp 125-132.

Donida, G., A.M.L. Piemontese, and M. Tamburri, "Numerical Experimental Analysis of Prestressed Masonry Walls," *Proceedings of the 9th International Brick/Block Masonry Conference* (Berlin, Germany, October 1991), pp 823-830.

Drinkwater, J.P., and R.E. Bradshaw, "Reinforced and Prestressed Masonry in Agriculture," *Reinforced and Prestressed Masonry* (Thomas Telford Ltd., London, England, 1982), pp 89-96.

Essawy, A., and R.G. Drysdale, "Capacity of Block Masonry Under Uniformly Distributed Loading Normal to the Surface of the Wall," *Proeedings of the 3rd Canadian Masonry Symposium* (University of Edmonton, Edmonton, Alberta, 1983), pp 39-1–39-16.

Foster, D., "Design and Construction of a Prestressed Brickwork Water Tank, *Proceedings of the 2nd International Brick Masonry Conference (SIBMAC)* (Stoke-on-Trent, England, April 1970), pp 287-294.

Ganz, H.R., "New Post-Tensioning System for Masonry," *Proceedings of the 5th Canadian Masonry Symposium* (University of British Columbia, Vancouver, British Columbia, June 1989), pp 165-176.

Ganz, H.R., "Strengthening of Masonry Structures With Post-Tensioning," *Proceedings of the 6th North American Masonry Conference* (Drexel University, Philadelphia, June 1993), pp 645-655.

Garrity, S.W., and M.E. Phipps, "An Experimental Study of the Influence of Vertical Prestress on the Horizontal Flexural Strength of Clay Brickwork," *Proceedings of the 8th International Brick and Block Masonry Conference* (Dublin, Republic of Ireland, September 1988), vol 2, pp 642-652.

Garrity, S.W., and M.E. Phipps, "A Study of the Effect of Vertical Prestress on the Horizontal Flexural Strength of Clay Brickwork," *Proceedings of the 4th North Americam Masonry Conference* (Los Angeles, California, June 1987), pp 28.1–28.14.

Gero, J.S., "Prestressed Masonry - Reinforced Concrete Space Structure," *Proceedings of the International Conference on Masonry Structural Systems*, Austin, Texas, 1967, F.B. Johnson, Editor (Gulf Publishing Co., 1969) pp 210-215.

Geschwindner, L.F., and W.P. Ostag, "Post-Tensioned Single-Wythe Concrete Masonry Walls," *Proceedings of the 5th North American Masonry Conference* (University of Illinois at Urbana-Champaign, Champaign, IL, June 1990), pp 1123-1134.

Goyal, A., M.A. Hatzinikolas, and J. Warwaruk, "Differential Movement in Cavity Walls and Veneer Walls Due to Material and Environmental Effects" (A Research Report by Canadian Masonry Research Institute, August 1992), pp 23.

Graham, K.J., and A.W. Page, "An Experimental Study of the Flexural Behavior of Post-Tensioned Hollow Clay Masonry," *Proceedings of the 10th International Brick / Block Masonry Conference* (University of Calgary, Calgary, Alberta, July 1994), vol 2, pp 639-648.

Grimm, C.T., "Brick Veneer: A Second Opinion," *The Construction Specifier*, Alexandria, VA, April 1984.

Grimm, C.T., "Design for Differential Movement in Brick Walls," *Journal of the Structural Division*, American Society of Civil Engineers, vol 101, no ST 11 (November 1975), pp 2385-2403.

Grimm, C.T., "What is Wrong With Brick Masonry Veneer Over Steel studs?," *The Masonry Society Journal*, vol 10, no 2 (February 1992), pp 9-14.

Hamid, A.A., B.E. Abboud, M. Farah, and H.G. Harris, "Flexural Behavior of Vertically Spanned Reinforced Concrete Block Masonry Walls," *Proceedings of the 5th Canadian Masonry Symposium* (University of British Columbia, Vancouver, British Columbia, June 1989), vol 1, pp 209-218.

Hamid, A.A., and H.G. Harris, "State-of-the-Art Report: Nonlinear Behavior of Reinforced Masonry Walls Under Out-of-Plane Lateral Loading," *Proceedings of the International Symposium on Reinforced and Prestressed Masonry* (University of Edinburgh, Edinburgh, Scotland, August 1984), pp 302-321.

Hanlon, J.R.G., "Concrete Masonry in New Zealand: Prestressed Concrete Masonry," *Concrete*, The Concrete Society (England), vol 4, no. 9 (September 1970), pp 356-358.

Harton, R.T., and M.K. Tadros, "Deflection of Reinforced Masonry Members," *ACI Structural Journal*, vol 87, no. 4 (July-August 1990), pp 453-463.

Haseltine, B.A., "A Design Guide for Reinforced and Prestressed Brickwork," *Proceedings of the North American Masonry Conference* (University of Colorado, Boulder, CO, August 1978), pp 30-1–30-14.

Haseltine, B.A., "Codification of Reinforced and Prestressed Masonry Design and Construction," *Proceedings of the Institution of Civil Engineers*, Reinforced and Prestressed Masonry (Thomas Telford Ltd., London, England, May 1982), pp 115-121.

Heat Transmission Coefficients of Brick Masonry Walls, Technical Notes on Brick Construction (Brick Institute of American [BIA], no. 4 Revised, Reston, VA, January 1982).

Hendry, A.W., "Concentrated Loading on Brick Masonry With Precompression," *Proceedings of the 8th International Brick and Block Masonry Conference*, Dublin, Republic of Ireland, September 1988, vol 1, pp 458-466.

Hinkley, A.T., "Tests of One-Story Prestressed Brickwork Shear Walls," *New Zealand Engineering*, vol 21, no. 6 (June 1966), pp 245-252.

Hosny, A.H., M.I. Soliman, and K.A. Hamdy, "Behavior of Block Masonry Walls Under Concentrated Loads," *Proceedings of the 8th International Brick and Block Masonry Conference* (Dublin, Republic of Ireland, September 1988), vol 1, pp 467-478.

Huizer, A., and R.E. Loov, "Post-Tensioning of a Single-Wythe Clay Brick Masonry Wall," *Proceedings of the 7th International Brick Masonry Conference* (Melbourne, Australia, vol 2, February 1985), pp 993-1000.

Huizer, A., and N.G. Shrive, "Analysis of a Post-Tensioned Masonry Wall With Vertical Eccentricity," *Proceedings of the 3rd North American Masonry Conference* (Arlington, TX, June 1985), pp 78.1-78.9.

Huizer, A., and N.G. Shrive, "Loss of Prestress in a Post-Tensioned Masonry Wall," *Proceedings of the International Symposium on Reinforced and Prestressed Masonry* (University of Edinburgh, Scotland, August 1984), pp 381-391.

Huizer, A., and N.G. Shrive, "Performance of a Post-Tensioned, Single-Wythe, Clay Brick Masonry Wall Tested in Shear," *Proceedings of the 4th Canadian Masonry Symposium* (University of New Brunswick, Fredericton, New Brunswick,vol 2, June 1986), pp 609-619.

Kingsley, G.R., and R.H. Atkinson, "Comparison of the Behavior of Clay and Concrete Masonry in Compression," *Proceedings of the 4th Canadian Masonry Symposium* (University of New Brunswick, Fredericton, New Brunswick, vol 1, June 1986), pp 278-689.

Kingsley, G.R., J.L. Noland, and M.P. Schuller, "The Effect of Slenderness and End Restraint on the Behavior of Masonry Prisms: A Literature Review," *The Masonry Society Journal* (February 1992), pp 65-74.

Lawrence, S.J., and H.T. Cao, "Cracking of Non-loadbearing Masonry Walls Under Lateral Forces," *Proceedings of the 8th International Brick and Block Masonry Conference* (Dublin, Republic of Ireland, September 1988), vol 2, pp 1184-1194.

Lenczner, D., "Creep in Concrete Blockwork Piers," *The Structural Engineer* (Institution of Structural Engineers, London, vol 52, no. 3, March 1974), pp 97-101.

Lenczner, D., "Creep and Prestress Losses in Brick Masonry," *The Structural Engineer* (Institution of Structural Engineers, London, vol 64B, no. 3, September 1986), pp 57-62.

Lenczner, D., and P. Davis, "Loss of Prestress in Post-Tensioned Brickwork Walls and Columns," *Proceedings of the International Symposium on Reinforced and Prestressed Masonry* (Edinburgh, Scotland, August 1984), pp 76-89.

Lenczner, D., and R.J. Harvey, "Creep and Loss of Prestress in Concrete Block Masonry," *Proceedings of the 9th International Brick / Block Masonry Conference* (Berlin, Germany, October 1991), pp 1068-1078.

Levy, M., and E. Spira, "Prestressed Concrete Hollow-Block Masonry," *Building Science*, vol 8, no. 2 (Great Britain, February 1973), pp 187-199.

Liaw, S., and R.G. Drysdale, "Reinforced Masonry Veneer Walls," *Proceedings of the 6th Canadian Masonry Symposium* (University of Saskatchewan, Saskatoon, Saskatchewan, June 1992), vol 1, pp 35-46.

Lin, T.Y., and N.H. Burns, *Design of Prestressed Concrete Structures* (John Wiley & Sons, Third Edition, 1981), pp 646.

Mallagh, T.J.S., "Prestressed Blockwork Silos," *Reinforced and Prestressed Masonry*, The Institution of Civil Engineers (Thomas Telford Ltd., London, England, 1982), pp 97-102.

Masonry Structures Joint Committee (MSJC), *Prestressed Masonry Design Criteria-Draft no. 2* (September 1993).

Maurenbrecher, A.H.P., "Masonry Research in Canada," Proceedings of the 6th Canadian Masonry Symposium (University of Saskatchewan, Saskatoon, Saskatchewan, June 1992), pp 181-190.

McGinley, W.M., J. Warwaruk, J. Longworth, and M. Hatzinikolas, "Masonry Veneer and Steel Stud Curtain Walls," *Proceedings of the 4th Canadian Masonry Symposium* (University of New Brunswick, Fredericton, New Brunswick, vol 2, June 1986), pp 730-743.

Mehta, K.C., and D. Fincher, "Structural Behavior of Pre-Tensioned Prestressed Masonry Beams," *Proceedings of the 2nd International Brick Masonry Conference (SIBMAC)* (Stoke-on-Trent, England, April 1970), pp 215-219.

Mirmiran, A., and A.M. Wolde-Tinsae, "Prestressed Masonry Structures," *Proceedings of the 5th Canadian Masonry Symposium* (University of British Columbia, Vancouver, British Columbia, June 1989), pp 187-196.

Montague, T.I., and M.E. Phipps, "Prestressed Concrete Blockwork Diaphragm Walls," *Proceedings of the 3rd North American Masonry Conference* (Arlington, TX, June 1985), pp 79.1-79.15.

Montague, T.I., and M.E. Phipps, "The Behavior of Post-tensioned Masonry in Flexure and Shear," *Proceedings of the International Symposium on Reinforced and Prestressed Masonry* (Edinburgh, Scotland, August 1984), pp 427-447.

National Concrete Masonry Association (NCMA), *A Critical Evaluation of Metal Stud Backup for Masonry Veneer* (Herdon, VA, 1981).

Nawy, E.G., *Prestressed Concrete, A Fundamental Approach* (Prentice Hall, Englewood Cliffs, NJ, 1989).

Ostag, W.P., "Post-Tensioned Single-Wythe Concrete Masonry Walls," *A Thesis Submitted in Partial Fulfillment of the Requirements for the Degree of Master of Science* (Department of Architectural Engineering, The Pennsylvania State University, May 1986).

Page, A.W., and A. Huizer, "Racking Tests on Reinforced and Prestressed Hollow Clay Masonry Walls," *Proceedings of the 8th International Brick / Block Masonry Conference* (Dublin, Republic of Ireland, vol 2, September 1988), pp 538-547.

Page, A.W., A.W. Hendry, "Design Loads for Concentrated Loads on Masonry," *The Concrete International*, vol 66, no. 17 (September 1988), pp 273-281.

Papanikolas, P.K., M.A. Hatzinikolas, and J. Warwaruk, "Stresses on Shear Connectors in Cavity Walls Due to Climatic Conditions and Material Properties," *Proceedings of the 5th Canadian Masonry Symposium* (University of British Columbia, Vancouver, British Columbia, June 1989), pp 557-567.

Pedreschi, R.F., and B.P. Sinha, "Deformation and Cracking of Post-Tensioned Brickwork Beams," *The Structural Engineer*, The Institution of Structural Engineers (England), vol 63B, no. 4 (December 1985), pp 93-99.

Pedreschi, R.F., and B.P. Sinha, "Development and Investigation of the Ultimate Load Behavior of Post-Tensioned· Brickwork Beams," *The Structural Engineer*, Institution of Structural Engineers (England), vol 60B, no. 3 (September 1982), pp 63-67.

Pedreschi, R.F., and B.P. Sinha, "The Shear Strength of Prestresssed Brickwork Beams," *Proceedings of the British Masonry Society*, no. 1 (1986), pp 114-116.

Phipps, M.E., and T.I. Montague, "Concrete Blockwork Diaphragm Walls - Prestressed and Unprestressed," *Practical Design of Masonry Structures* (Thomas Telford Ltd., London, 1987), pp 265-276.

Phipps, M.E., "Codification of Prestressed Masonry Design," *Proceedings of the 6th Canadian Masonry Symposium* (University of Saskatchewan, Saskatoon, Saskatchewan, June 1992), pp 563-572.

Phipps, M.E., "The Principles of Post-Tensioned Masonry Design," *Proceedings of the 6th North American Masonry Conference* (Philadelphia, PA, June 1993), vol 2, pp 621-632.

Phipps, M.E., "The Strength of Prestressed and Unprestressed Masonry Diaphragm Walls," *Proceedings of the 4th Canadian Masonry Symposium* (University of New Brunswick, Fredericton, New Brunswick, vol 2, June 1986), pp 854-867.

Phipps, M.E., and T.I. Montague, "The Testing of Plain and Prestressed Concrete Blockwork Beams and Walls of Geometric Cross Section," *Masonry International,* vol 1, no. 3 (1987), pp 96-99.

Plauk, G., "Wind-Load Tests on Story High Reinforced Masonry Wall Panels," *Proceedings of the 5th Canadian Masonry Symposium* (University of British Columbia, Vancouver, British Columbia, June 1989), vol 1, pp 241-250.

Prestressed Masonry Design Criteria (Masonry Standards Joint Committee, Draft no. 6, April 1995).

Ramaswamy, G.S., "Prestressing and Assembly of Stone Blocks by Post-Tensioning," *Indian Concrete Journal*, vol 27, no. 12 (1953), pp 450-451.

Reinforced and Prestressed Masonry, Cement and Concrete Association and Brick Development Association, *Proceedings of the Institution of Civil Engineers* (Thomas Telford Ltd., London, May 1982).

Rodriguez, R., A.A. Hamid, and J. Larralde, "Flexural Behavior of Post-Tensioned Masonry Walls Subjected to Out-of-Plane Loads: Preliminary Results," *Proceedings of the 10th International Brick/Block Masonry Conference* (University of Calgary, Calgary, Alberta, July 1994), vol 2, pp 597-607.

Rosenhaupt, S., F.D. Beresford, and F.A. Blakey, "Test of a Post-Tensioned Concrete Masonry Wall," *ACI Journal Proceedings*, vol 64, no. 12 (December 1967), pp 829-837.

Roumani, N., and M.E. Phipps, "The Shear Strength of Prestressed Brickwork I and T Sections," *Proceedings of the 7th International Brick Masonry Conference* (Melbourne, Australia, vol 2, February 1985), pp 1001-1014.

Roumani, N., and M.E. Phipps, "The Shear Strength of Prestressed Brickwork I Sections," *Proceedings of the British Masonry Society*, vol 1 (1986), pp 110-113.

Sakr, S.K., and V.V. Neis, "Full Scale Testing of Masonry Cavity Walls Subjected to Lateral Loading," *Proceedings of the 10th International Brick/Block Masonry Conference* (University of Calgary, Calgary, Alberta, July 1994), vol 2, pp 629-638.

Samuely, F.J., "Note in Addition to Blackwell Secondary Modern School," *Journal of Royal Institute of British Architects*, vol 60, no. 12 (1953), pp 476-477.

Schultz, A.E., and M.J. Scolforo, "An Overview of Prestressed Masonry," *The Masonry Society Journal*, vol 10, no. 1 (August 1991), pp 6-21.

Schultz, A.E., and M.J. Scolforo, "Engineering Design Provisions for Prestressed Masonry Part 1: Masonry Stresses," *The Masonry Society Journal*, vol 10, no. 2 (February 1992), pp 29-47.

Schultz, A.E., and M.J. Scolforo, "Engineering Design Provisions for Prestressed Masonry Part 2: Steel Stresses and Other Considerations," *The Masonry Society Journal*, vol 10, no. 2 (February 1992), pp 48-64.

Scolforo, M.J., and A.E. Schultz, "Towards the Development of Prestressed Masonry Design in the U.S.A.," Research Report (Department of Civil Engineering, North Carolina State University, Raleigh, NC, May 1991).

Shaw, G., "Post-Tensioned Brickwork Diaphragm Subject to Severe Mining Settlement," *Reinforced and Prestressed Masonry* (The Institution of Civil Engineers, Thomas Telford Ltd., London, May 1982), pp 103-114.

Shiv Kumar, S., and R.H. Heidersbach, "Corrosion of Steel-Stud Masonry Buildings," *Proceedings of the 4th Canadial Masonry Symposium* (University of New Brunswick, Fredericton, New Brunswick, vol 2, 1986), pp 815-825.

Shrive, N.G., "Effects of Time Dependent Movements in Composite and Post-Tensioned Masonry," *Masonry International* (The British Masonry Society, vol 2, no. 1, Spring 1988), pp 25-29.

Shrive, N.G., "Post-Tensioned Masonry - Status & Prospects," *Proceedings of the Annual Conference* (Canadian Society for Civil Engineers, Calgary, Alberta, May 1988), pp 679-696.

Sinha, B.P., "Shear Strength of Prestressed Brickwork Beams," *Proceedings of the 8th International Symposium on Load Bearing Brickwork*, 1983.

Sinha, B.P., and C. Liang Ng, "Behavior of Brickwork Panels Under Lateral Pressure," *Proceedings of the 10th International Brick/Block Masonry Conference* (University of Calgary, Calgary, Alberta, July 1994), vol 2, pp 649-658.

Sinha, B.P., and J. Udehi, "Comparative Study of Prestressed Beams of Brickwork and Concrete," *Proceedings of the 1st International Synposium of British Masonry Society*, no. 2 (1986).

Sinha, B.P., and P. Walker, "Comparative Study of Reinforced, Fully and Partially Prestressed Brickwork Beams," *CIB Congress* (Washington, 1986), pp 2661-2671.

Sinha, B.P., R.F. Pedreschi, and R.C. DeVekey, "Investigation of the Ultimate Load Behavior of Prestressed Brickwork Beams Built with Perforated Bricks," *Proceedings of the International Symposium of Reinforced and Prestressed Masonry* (Edinburgh, Scotland, August 1984), pp 392-410.

Smith, B.S., and C. Carter, "Distribution of Stresses in Masonry Walls Subjected to Vertical Loading," *Proceedings of the 2nd International Brick Masonry Conference* (England, April 1978), pp 119-124.

Suter, G.T., E.M.F. Naguib, and W.H. Bowes, "Stress Analysis of Masonry Walls Subjected to Concentrated Amounts of Prestressing," *Proceedings of the 3rd Canadian Masonry Symposium* (University of Alberta, Edmonton, Alberta, 1983), pp 16.1-16.18.

Taneja, R., N.G. Shrive, and A. Huizer, "Loss of Prestress in Post-Tensioned Hollow Masonry Walls," *Proceedings of the Symposium on Advances in Analysis of Structural Masonry* (American Society of Civil Engineers [ASCE], 1986), pp 76-93.

Tasta, E., O. Yishai, and M. Levy, "Loss of Steel Stresses in Prestressed Concrete Blockwork Walls," *The Structural Engineer*, vol 51, no. 5 (London, May 1973), pp 177-182.

Taylor, J.B., "Prestressed Granite Masonry for a Retaining Wall," *Proceedings of the American Society of Civil Engineers*, vol 31, no. 1 (January 1961), pp 33-34.

Thomas, K., "Current Post-Tensioned and Prestressed Brickwork and Ceramics in Great Britain," *Proceedings of the International Conference on Masonry Structural Systems*, F.B. Johnson, Editor (Gulf Publishing Co., 1969), pp 285-301.

Ungstad, D.G., M.A. Hatzinikolas, and J. Warwaruk, "Prestressed Concrete Masonry Walls," *Proceedings of the 5th North American Masonry Conference* (University of Illinois at Urbana-Champaign, Champaign, IL, June 1990), pp 1147-1161.

Uniform Building Code, International Conference of Building Officials, Whittier, California, 1994 Edition.

Warren, D., and D. Lenczner, "Measurement of the Creep Strain Distribution in an Axially Loaded Brickwork Wall," *Proceedings of the 2nd North American Masonry Conference* (University of Maryland, College Park, MA, August 1982), pp 5-1 - 5-19.

Wolde-Tinsae, A.M., R.H. Atkinson, and A.A. Hamid, "State-of-the-Art Modulus of Elasticity of Masonry," *Proceedings of the 6th North American Masonry Conference* (Philadelphia, PA, June 1993), vol 2, pp 1209-1220.

Wyatt, K.J., "Dimensional Change and Its Control in Clay Masonry Construction," *Proceedings of the North American Masonry Conference* (University of Colarado, Boulder, CO, August 1978), pp 89-1–89-11.

Xingzhi, C., and L. Yue, "The Influence of the Precompressed Stress at Early Age on Brickwork," *Proceedings of the 9th International Brick/Block Masonry Conference* (Berlin, Germany, October 1991), pp 252-259.

Acronyms

ACI	American Concrete Institute
ASCE	American Society of Civil Engineers
ASTM	American Society for Testing and Materials
BIA	Brick Institute of America
CPAR	Construction Productivity Advancement Research
DTI	direct tension indicator
IBMAC	International Brick Block Masonry Conference
kips	kilopounds
kN	kilonewtons
kN/m2	kilonewtons per square meter
kPa	kilopascals
MPa	megapascals
MSJC	Masonry Structures Joint Commission
NCMA	National Concrete Masonry Association
psf	pounds per square foot
psi	pounds per square inch
SIBMAC	Second International Brick Masonry Conference
SIDL	Self-weight and superimposed dead load
TMS	The Masonry Society
UBC	Uniform Building Code

Appendix A: Load-deflection Calculations

General

The calculations of load-deflection curves for the analysis of post-tensioned panels is given this appendix. The theoretical relations for three methods considered are explained in Chapter 4. The relations are derived for a prestressing force of 19 kips. The data used in the analysis is based on actual measured material properties, and the assumptions as given in Chapter 4. The following example shows the calculation only for initial prestressing force of 19 kip. Table A.2 includes the load and deflection values calculated by the three different methods.

Moment-Curvature Method

Moment-curvature relations were converted to load-deflection curves and are plotted in Fig. A.1.

Specimen and Material Data:

Width, $b = 36$ in.

Overall depth, $h = 3.625$ in.

Effective depth, $d = 1.81$ in.

Characteristic compressive strength of masonry, $f'_m = 2{,}845$ psi

Modulus of elasticity of masonry, $E_m = 2{,}160{,}000$ psi

Effective area of prestressing steel, $A_{ps} = 0.226$ in^2

Initial prestressing force, P_i = 19,000 lb

Modulus of elasticity of prestressing steel, E_{ps} = 26,500 ksi

Section Properties:

Cross sectional area of masonry, $A_m = b \times h = 130.5$ in^2

Section modulus, $S = \frac{bh^2}{6} = 78.84$ in^3

Gross moment of Inertia, $I_g = \frac{bh^3}{12} = 142.9$ in^4

Modulus of repute of masonry, $f_r = 2.66\sqrt{f'_m} = 2.66\ \sqrt{2{,}845} = 142$ psi

Effective prestress, f_{se} = 18,000 lb = 79.64 ksi

Reinforcement ratio, $\rho = 0.00346$

(a) Initial post-tensioning of masonry:

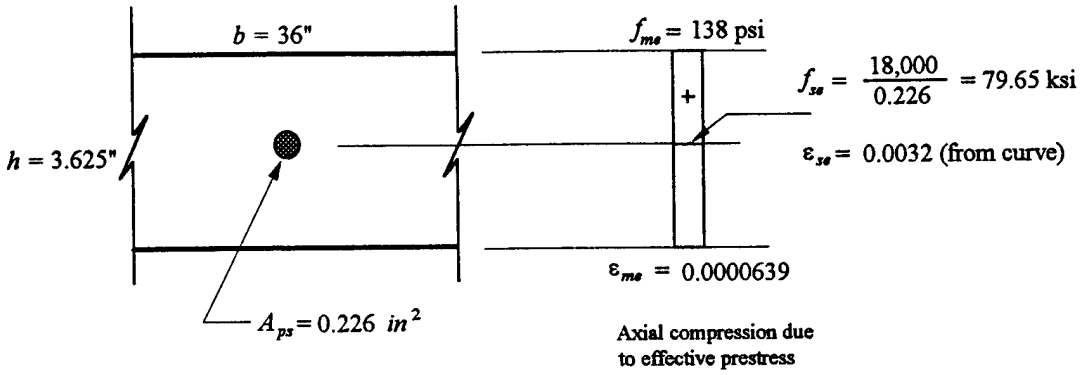

Moment, M = 0 k-in

Curvature, ϕ = 0 rad/in.

Effective prestressing force in the prestressing steel is taken to be equal to 95% of the initial prestress (assuming 5% losses). The force is assumed to distribute uniformly along the entire cross-section in the middle-third zone of the span.

(b) Self-weight and superimposed dead load (SIDL):

The self weight of the panel is calculated based on the unit weight of brick masonry, equal to 10 lbs /ft^2/inch thickness. The weight of the panel is equal to 109 lb/ft. The superimposed dead load placed on the test panel (loading frame) was approximately 250 lbs. The total moment calculated from these two dead loads was = 8.87 k-in.

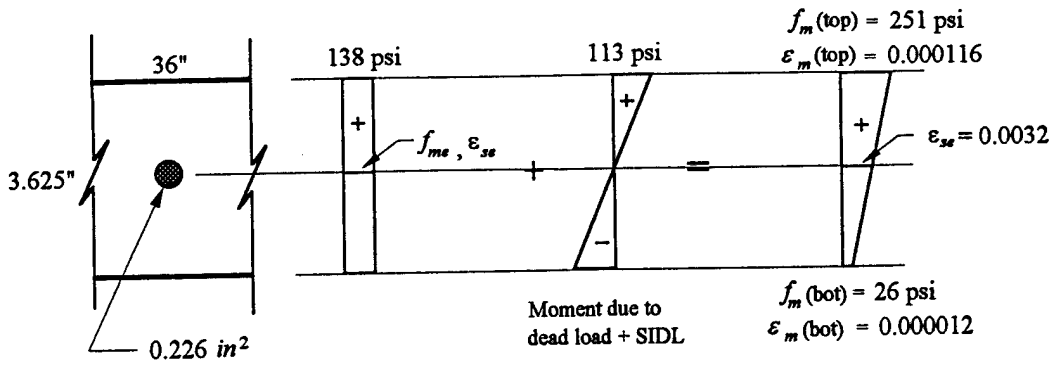

Moment, M = 8.87 k-in.

Curvature, ϕ = $\frac{0.0001162 - 0.00001204}{3.625}$ = 0.00002873 rad/in.

(c) At cracking moment stage:

The masonry is assumed to be cracked when the bottom fiber reaches its modulus of rupture value. From panel load-deflection curves, it was determined to be at $f_r = 2.66\sqrt{f'_m}$. The additional moment required to cause the section to crack and the total moment and curvatures are calculated at that stage.

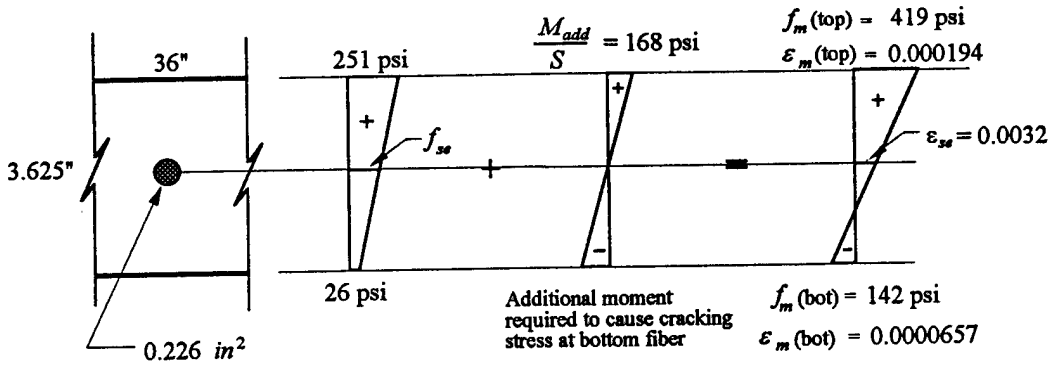

Moment, M = 13.25 k-in.

Curvature, ϕ = $\frac{0.000194 - 0.00006574}{3.625}$ = 0.00007165 rad/in.

(d) At different strain increments at top fiber of masonry after cracking:

After cracking until the ultimate stage, the masonry strain at the compression fiber is incrementally assumed to get intermediate points. The neutral axis depth at each point is assumed, and checked to have compression and tension forces equal. The equilibrium condition is calculated from statics. For example, the strain in masonry top fiber is assumed to be 0.0005 in this stage.

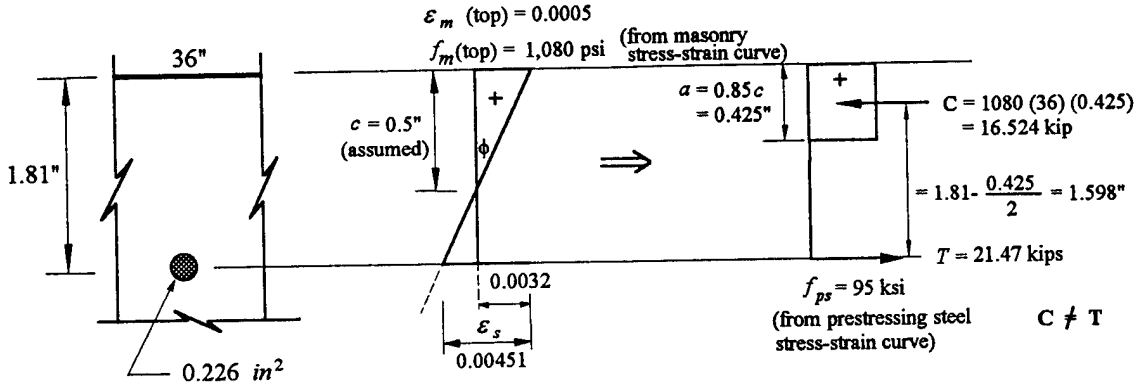

Since compression is not equal to the tension force from steel, a new neutral axis depth is chosen (0.625 in.). The above procedure is repeated to determine the forces. The forces are found to be in equilibrium, and hence the moment is calculated by taking moment of tension force at the level of compression force.

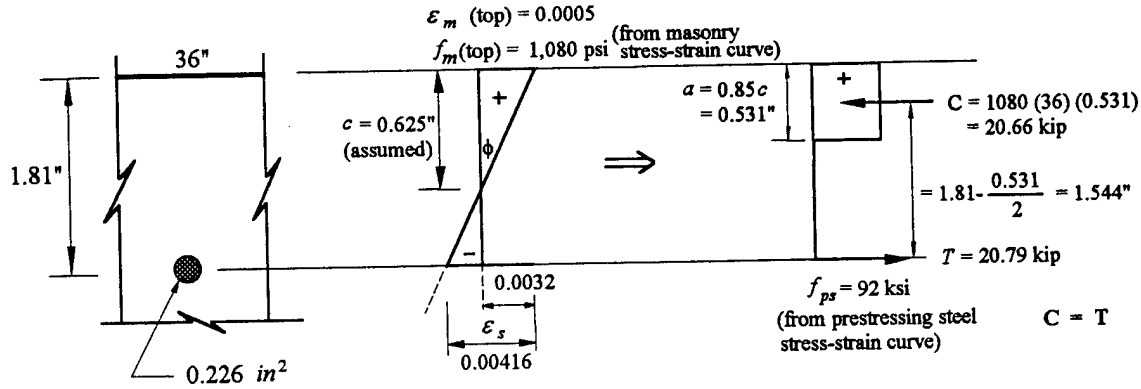

Moment, M = 32.0 k-in.

Curvature, $\phi = \frac{0.0005}{0.625} = 0.0008$ rad/in.

(e) At ultimate moment capacity:

The ultimate moment capacity of the panel was assumed at an masonry compressive strain of 0.0019 at which the stress corresponds to f'_m = 2,845 psi.

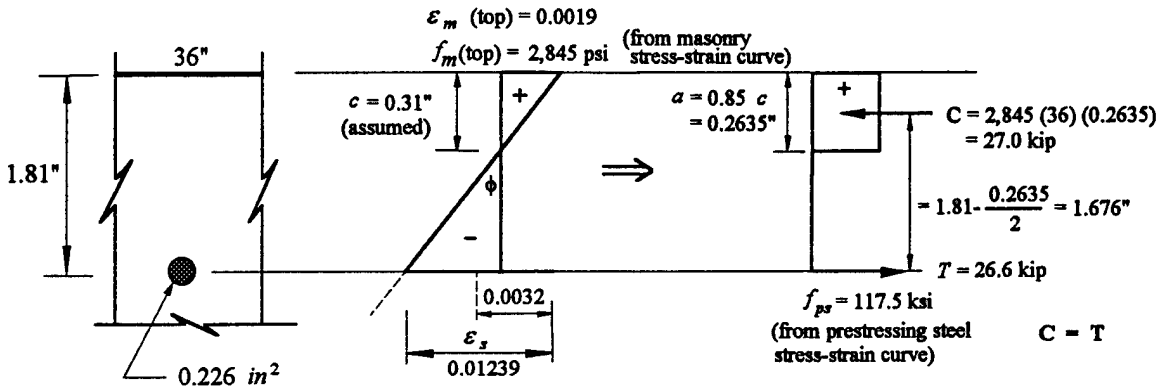

Moment, M = 44.56 k-in.

Curvature, $\phi = \frac{0.0019}{0.31} = 0.006129$ rad/in.

The moment values were converted to applied loads using the relation derived for the third-point loading. The calculated rotation of the panel was converted to mid-span deflection for simply supported beams using the following equation (Nawy, 1989). The load and deflection values calculated from these equations are shown in Table A.1.

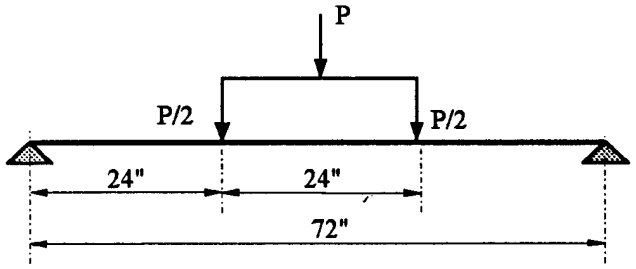

Moment, $M = \frac{Pl}{6}$

Mid-span deflection, $\delta_c = \frac{\phi l^2}{8}$

where, M = moment

P = total applied load

l = span length

δ_c = deflection at mid-span

Table A.1 Moment-curvature values at different loading stages

Loading stage or strain in extreme compression fiber of masonry	Moment, M (kip-in)	Curvature, ϕ (rad/in.)
Initial post-tensioning	0	0
Self weight + SIDL	8.87	0.00002873
Cracking	13.25	0.00007165
$\varepsilon_m = 0.0002$	21.83	0.0001509
$\varepsilon_m = 0.00021$	22.47	0.0001647
$\varepsilon_m = 0.00025$	24.40	0.0002273
$\varepsilon_m = 0.0005$	31.92	0.0008065
$\varepsilon_m = 0.001$	39.31	0.002500
$\varepsilon_m = 0.0015$	42.93	0.004615
$\varepsilon_m = 0.0019$ (Ultimate)	44.89	0.006129

Bilinear Behavior Method

The theoretical equations for this method are given in Section 4.2. The calculations are shown below along with the panel data considered. The cracking moment of inertia was calculated using working stress design equations.

Calculation Steps

When applied moment, M_{ser} is less than the Cracking moment, M_{cr}, the deflection is given by:

$$\Delta_s = \frac{5M_s h^2}{48E_m I_g}$$

(a) Deflection due to self wt and super imposed dead loads:

$$\Delta_s = \frac{5(8872.5)(72)^2}{48(2160000)(142.9)} = 0.015522\ in.$$

(b) Cracking load deflection

$$\Delta_s = \frac{5(13250)(72)^2}{48(2160000)(142.9)} = 0.02318\ in.$$

After cracking, the deflection is given by the following equation:

$$\Delta_s = \frac{5M_s h^2}{48E_m I_g} + \frac{5(M_{ser} - M_{cr})h^2}{48\,E_m I_{cr}}$$

where, I_{cr} is given by

$$I_{cr} = \frac{b(kd)^3}{3} + n\rho bd(d - kd)^2$$

$$n = \frac{E_{ps}}{E_m} = \frac{26{,}500{,}000}{2{,}160{,}000} = 12.27$$

$$\rho = \frac{A_{ps}}{bd} = \frac{0.226}{36(1.815)} = 0.003464$$

$$k = \sqrt{2\rho n + (\rho n)^2} - \rho n \quad = \quad 0.252\ in.$$

Substituting all the values in to the cracking moment equation,

$$I_{cr} \quad = \quad \frac{36(0.0425)^3}{3} \quad + \quad 0.0425(36)\,(1.8125)(1.8125 - 0.4563)^2 \quad = \quad 6.2398\ in^4$$

The deflection values are calculated after cracking to an applied moment corresponding to a compressive masonry strain of 0.0019. A sample calculation is shown below. The calculated values are tabulated in the Table A.2.

$$\Delta_s \ = 0.02318 + \frac{5\,(24400 - 13250)\,(72)^2}{48\,(2160000)(6.2398)} \quad = \quad 0.469908\ in.$$

Harton and Tadros Method

The procedure of Horton and Tadros method was described in Section 4.3 with the theoretical equations. In this section, a sample calculation is shown to explain how the method can be applied.

Consider an applied moment, M_a = 24400 lb-in.

Cracked Moment of Inertia, I_{cr} = 6.2398 in^4

Gross Moment of Inertia, I_g = 142.9 in^4

Cracking Moment, M_{cr} = 13,250 lb-in.

$$\Delta_{cr} = \frac{5L^2 M_a}{48 E_m I_{cr}} = \frac{5(72)^2(24400)}{48(2160000)(6.2398)} = 0.9776\,in.$$

$$\Delta = \Delta_{cr}\left(\frac{I_{cr}}{I_g}\right) = 0.9776\left(\frac{6.2398}{142.9}\right) = 0.04268\,in.$$

Coefficient, $\alpha = \left(\frac{M_{cr}}{M_a}\right)^2\left(2 - \frac{M_{cr}}{M_a}\right)\left(1 - \frac{I_{cra}}{I_g}\right)$

$$= \left(\frac{13250}{24400}\right)^2\left(2 - \frac{13250}{24400}\right)\left(1 - \frac{6.2398}{142.9}\right)$$

$$= 0.41088$$

Deflection, $\Delta = \Delta_{cr}(1-\alpha)$

Therefore, $\Delta = 0.9776\ (1-0.41088) = 0.596$ in.

Table A.2 Load-deflection values from different prediction methods

Loading Stage or Strain in Extreme Compression Fiber of Masonry	Load, P (lbs)	Deflection From Moment Curvature Method Δ (in.)	Deflection Form UBC Method Δ (in.)	Deflection Form Horton and Tadros Method Δ (in.)	Experimental Test Deflection Δ (in.)
Initial post-tensioning	0	0.0000	0.000	0.000	0.000
Self weight + SIDL	739	0.0186	0.0156	0.016	0.015
Cracking	1,104	0.0464	0.023	0.023	0.025
$\varepsilon_m = 0.00020$	1,819	0.0978	0.367	0.490	0.100
$\varepsilon_m = 0.00021$	1,873	0.1067	0.393	0.522	0.125
$\varepsilon_m = 0.00025$	2,034	0.1473	0.470	0.596	0.150
$\varepsilon_m = 0.00050$	2,661	0.5226	0.771	0.946	0.400
$\varepsilon_m = 0.00100$	3,276	1.6200	1.067	1.292	0.863
$\varepsilon_m = 0.00150$	3,576	2.9910	1.212	1.462	1.475
$\varepsilon_m = 0.00190$ (Ultimate)	3,714	3.9720	1.291	1.548	-

* averaged from three specimens

Appendix B: Ultimate Moment Capacity of Wall Panels

The theoretical nominal moment capacities of the Stage II and II test specimens are calculated in this appendix. The material properties of masonry and steel were determined form the laboratory tests (Chapter 3). The ungrouted specimens were analyzed using MSJC Code [Prestressed, 1995] provisions. Strain compatibility equations were used for the grouted specimen analysis. The following assumptions were made during the theoretical analysis of panels.

1. The ultimate moment capacity is assumed to occur at the midspan.
2. Prestress was assumed to be uniformly distributed over the entire cross-section of the member.
3. Maximum strain in the masonry was limited to 0.003.
4. The strain is linearly varying along the cross-section.
5. In the case of ungrouted specimen, effective depth is calculated assuming that the prestressing steel was touching the masonry surface in the core at midspan section.

Material and Sectional Properties:

Width, $b = 36$ in.

Overall depth, $h = 3.625$ in.

Effective depth, $d = 1.8125+0.625/2 = 1.0625$ in.

Characteristic compressive strength of masonry, $f'_m = 2{,}845$ psi

Modulus of elasticity of masonry, $E_m = 2{,}160{,}000$ psi

Effective area of prestressing steel, $A_{ps} = 0.226$ in^2

Effective prestressing force, P_e = 18,000 lb

Modulus of elasticity of prestressing steel, E_{ps} = 26,500 ksi

Ultimate tensile strength of prestressing steel, f_{pu} = 131 ksi

Ungrouted Specimen (Stage I)

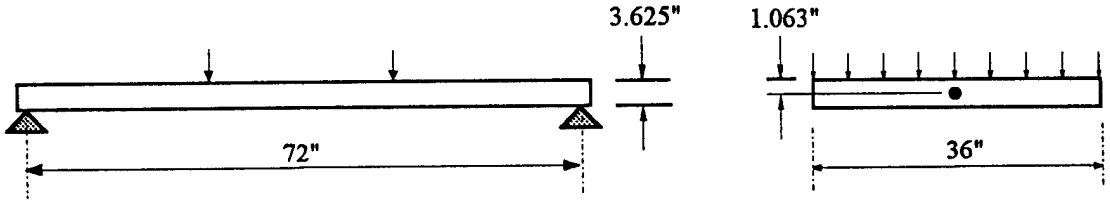

Elevation Side view

Stress in prestressing tendon at nominal strength in members with unbonded tendons, given by the following MSJC Code [prestressed, 1995] formula:

$$f_{ps} = f_{se} + 100{,}000\left(\frac{d}{l}\right)\left[1 - 1.4\left(\frac{f_{pu}A_{ps}}{bdf_m'}\right)\right]$$

$$= 79{,}645 + 100{,}000\left(\frac{1.0625}{72}\right)\left[1 - 1.4\left(\frac{131.5(0.226)}{36(1.0625)(2{,}845)}\right)\right]$$

$$= \ 80{,}557 \ psi$$

The depth of equivalent compression zone, x, is given by:

$$x = \frac{f_{pu}A_{ps}}{0.85bf_m'}$$

$$x = \frac{80{,}557\,(0.226)}{0.85\,(2845)(36)} = 0.209\ in.$$

The ratio x/d is less than 0.425 (0.197). Hence the nominal moment strength, M_n, is calculated based on the compression portion of the moment couple.

$$\begin{aligned} M_n &= 0.85 f_m' b x \left(d - \frac{x}{2}\right) \\ &= 0.85\,(2{,}845)(36)(0.209)\left(1.0625 - \frac{0.209}{2}\right) \\ &= 17{,}430\ lb - in. \\ &= 1{,}453\ lb - ft \end{aligned}$$

Grouted Specimen (Stage II)

The analysis is carried out using the strain compatibility method similar to prestressed concrete. All data remains same as ungrouted specimen except characteristic compressive strength of masonry, f_m' = 3,430 psi

Assuming the stress in prestressing steel to be equal to its ultimate strength. i.e.

f_{ps} = 115 ksi

Total tensile force, $T = A_{ps}\, f_{ps} = 0.226(115) = 26.0\ kips$

The equivalent compression block depth, $a = \frac{T}{0.85 f_m' b} = \frac{26{,}000}{0.85(3{,}430)(36)} = 0.248\ in.$

The neutral axis depth, $c = \frac{a}{0.85} = \frac{0.248}{0.85} = 0.292\ in.$

Assuming a strain of 0.003 at the extreme compression fiber in the masonry, and using similar triangles, the strain in the prestressing steel is given by:

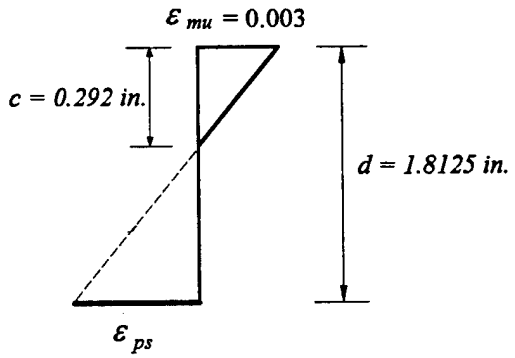

$$\frac{\varepsilon_{ps} + 0.003}{d} = \frac{0.003}{c}$$

Therefore, strain in the prestressing steel, $\varepsilon_{ps} = \frac{1.8125(0.003)}{0.292} - 0.003 = 0.0157$

From the stress-strain diagram (Fig. 3.9), f_{ps} = 122 ksi

Therefore, for the next iteration, T = 125 (0.226) = 27.57 kips

a = 0.263 in.

c = 0.309

ε_{ps} = 0.0146

f_{ps} = 120 ksi

The second iteration gives, T = 27.12 kips

and a = 0.258 in.

The nominal moment capacity, $M_n = A_{ps} f_{ps}\left(d - \frac{a}{2}\right)$

$$= 0.226(120)\left(1.8125 - \frac{0.258}{2}\right)$$
$$= 45.65\ kip - in.$$
$$= 3{,}805\ lb - ft$$

Appendix C: Prestress Loss Calculations

A step by step prestress loss calculation was carried out for the post-tensioned panels following the provisions of proposed MSJC Code [Prestressed, 1995]. Losses which are not applicable to the proposed system are also outlined. Prestress loss relations suggested by other codes and investigators are included. The following procedure outlines the example calculations for Stage I specimens with an initial prestressing force of 19 kips (84.5 kN).

(a) Anchorage seating loss

No loss due to the nature of post-tensioning technique (threaded bars and nuts).

(b) Elastic shortening of masonry

No loss due to elastic shortening of masonry since it occurs simultaneously during the application of prestress (compensates automatically).

(c) Creep of masonry

(i) ACI-530/ASCE-5/TMS-402 Standard [Building, 1992] specifies a constant specific creep, $k_c = 0.7 \times 10^{-7}$ per psi.

$$f_{cr} = k_c\left(\frac{P_i}{A_m}\right)E_{ps} = 0.7 \times 10^{-7}\left(\frac{19{,}000}{130.5}\right)(26{,}500) = 0.27\ ksi\ (1.86\ MPa) \qquad \text{(C-1)}$$

(ii) BS 5628 [Code, 1985] specifies a value of 1.5 for long term creep coefficient for clay masonry. The following equation (C-2) is typically used to calculate losses due to creep in masonry [Schultz and Scolforo, 1992].

$$\varepsilon_{mi} = \frac{f_{mi}}{E_m} = \frac{19{,}000 / 130.5}{2.486 \times 10^6} = 0.0000586 \quad \text{(C-2)}$$

$$C_c = 1.5\,(\varepsilon_{mi}) = 1.5\,(0.0000586) = 0.0000879 \quad \text{(C-3)}$$

$$f_{cr} = C_c\, E_{ps} = 0.0000879\,(26{,}500) = 2.33\ ksi\ (16.1\ \text{MPa}) \quad \text{(C-4)}$$

(iii) Lenczner [1986] proposed the following equation (C-5) to calculate creep coefficient for clay masonry walls based on his two decades of research.

$$C_c = 4.46 - 0.027\sqrt{f_b'} = 4.46 - 0.027\sqrt{9{,}360} = 1.85 \quad \text{(C-5)}$$

$$\varepsilon_c^{max} = C_c \varepsilon_{mi} = 1.85(0.0000586) = 0.000108 \quad \text{(C-6)}$$

Therefore, $f_{cr} = C_c\, E_{ps} = 0.000108\,(26{,}500) = 2.87\ ksi$ (19.8 MPa)

(d) Relaxation of tendon stress

(i) Stress relaxation loss in prestressing steel can be expressed using the formula suggested by Lin and Burns [1981]. Relaxation calculations are made using the actual material values and for a time interval assumed as 1000 hr. in Eq. (C-7).

$$\frac{f_p}{f_{pi}} = 1 - \frac{\log t}{10}\left(\frac{f_{pi}}{f_{py}} - 0.55\right) \quad \text{(C-7)}$$

$$\text{Change in the stress, } \Delta f_{pr} = f_{pi}\left[\frac{\log t}{10}\left(\frac{f_{pi}}{f_{py}} - 0.55\right)\right] \quad \text{(C-8)}$$

$$= \frac{19{,}000}{0.226}\left[\frac{\log(1000)}{10}\left(\frac{84{,}071}{99{,}900} - 0.55\right)\right] = 7.35 \text{ ksi (50.7 MPa)}$$

(ii) Curtin et al. [1987] suggests to use a relaxation loss of 7% decrease from the initial prestress, based on a 70% stress level. For the bars in question, it will result in a loss of 5.89 ksi (40.6 MPa).

(e) Moisture expansion of masonry

ACI-530/ASCE-5/TMS-402 [Building, 1992] standard recommends a coefficient value of 3×10^{-4} for clay masonry expansion which is a gain in the prestressing force:

$$f_{me} = k_e E_{ps} = 3 \times 10^{-4} (26{,}500) = -7.95 \text{ ksi } (54.8 \text{ MPa}) \quad \text{(C-9)}$$

The above calculations show a total time dependent loss of -0.33 ksi (2.27 MPa) (gain) of initial prestress, if the coefficients of ACI-530/ASCE-5/TMS-402 Standard are used. By using creep coefficients of other sources, results in a maximum loss of 2.27 ksi (15.7 MPa). If the moisture expansion of masonry is neglected it would result in a maximum loss of 10.22 ksi (70.5 MPa) to a minimum of 6.16 ksi (42.5 MPa) depending on methods considered.

USACERL DISTRIBUTION

Chief of Engineers
ATTN: CEHEC-IM-LH (2)
ATTN: CEHEC-IM-LP (2)
ATTN: CECC-R
ATTN: CEMP-ET
ATTN: CERD-L

US Army Engr District
ATTN: Library (40)

US Army Engr Division
ATTN: Library (11)

Defense Tech Info Center 22304
ATTN: DTIC-O (2)

60
9/96